

An Enthusiast's Guide to SICs in Low Dimensions

THESIS FOR THE GRADE OF MASTER IN SCIENCE

60 CREDITS

Author:
David Andersson

Supervisor:
Prof. Ingemar Bengtsson

January 13, 2015



*To Ewa Erixson-Carlqvist,
for making the world of science go around.*

Preface

This thesis was finished in June 2014 – some months before this preface was written in conjunction with the submission of the thesis. The relationship we propose in this thesis between the level of SICness and MUSness of a state, has since been systematically researched. In formalising this relationship the posed conjecture as to the maximum MUSness for any given SICness has since been proved. Furthermore the ideas of this thesis have proven successful for finding the MUB-balanced states introduced by Amburg et al. [5]. Using the methods presented in Chapter 6 we have provided circumstantial evidence that the MUB-balanced states found by these authors are the only ones that exist [7].

We have chosen not to include this research in this thesis since these ideas are still being developed. Also, in the spirit of keeping this thesis self-contained, this omission was necessary. However, the continued research will be presented in a future paper by D. Andersson, I. Bengtsson, H. B. Dang. and K. Blanchfield.

Abstract

In this thesis for the degree of Master of Science from Stockholm University we explore the ideas of Symmetric Informationally Complete Positive Valued Measures (SIC-POVMs; commonly just SICs). This is an emerging concept in quantum information theory with ambitious claims, such as being a candidate for standard measurements [23] and perhaps being of importance to error correcting universal quantum computing [32]. While the definition of a SIC is exceedingly simple they have proven notoriously hard to find. This thesis explores new approaches to finding SICs.

It is our ambition that this thesis shall provide the reader unfamiliar with SICs with a thorough introduction to the subject along with both the necessary quantum theory and group theory. We also hope to intrigue the reader already attuned to SICs by establishing a link between how close to a SIC a state is and how close to a MUS (Minimum Uncertainty State) it is. This is the main result of this thesis and we leave the reader with several open questions relating to this discovery to provoke further scrutiny of the matter.

The thesis is divided into two parts: the first part provides the necessary background and theory; while the second part presents our results. There are also three appendices attached to this thesis where we delve into a discussion about computing power and also present some of the code used. Being appendices these are not essential to the thesis per se – they are rather supplied as a reference for the curious reader who might be interested in recreating some of our results.

Sammanfattning

I det här examensarbetet i teoretisk fysik vid Stockholms Universitet undersöker vi konceptet Symmetriska Informationellt Kompletta Positiva Mått, som vi, lånat från engelskan, kommer att förkorta SIC eller SIC:ar. Det här är vissa uppsättningar av tillstånd som introducerades på 90-talet av G. Zauner [35] men som de senaste åren fått ökad uppmärksamhet eftersom de är kandidater till nya standardmätningar i kvantfysik [23] och de kan även vara av intresse för universella kvantdatorer [32]. Definitionen av en SIC är överväldigande enkel och bygger endast på elementär linjär algebra, det har däremot visat sig förrädiskt svårt att faktiskt finna SIC:ar.

Den här rapporten ger läsaren som inte är bekant med SIC:ar en bred introduction till dessa med utgångspunkt i både den nödvändiga fysiken och matematiken. Icke desto mindre är rapporten även riktad till den redan insatte läsaren. Förutom att rapporten sammanfattar viktiga delar av det arbete som gjorts på SIC:ar i låga dimensioner, etableras i rapportens slutskede en länk mellan så kallade Minimalt Osäkra Tillstånd (MUS:ar) och SIC:ar. Rapporten lämnar flera öppna frågor som relaterar till det här sambandet som var och en i sig själva rättfärdigar ytterligare studier.

Rapporten är indelad i två huvudsakliga delar. Den första delen redogör för den teoretiska bakgrund som behövs för att förstå SIC:ar och MUS:ar, medan den andra delen redogör för de faktiska resultaten som presterats i det här examensarbetet. Det läggs även tre appendix till den här rapporten om det omfattande datoranvändande som föreligger resultaten. Här presenteras såväl utdrag av kod som en diskussion om vilka begränsningar som sätts av beräkningskapacitet. Trots att det här avsnittet varken presenterar resultat eller bakomliggande teori, är det en bra referens för den som vill återskapa, eller ta vidare, delar av det här examensarbetet.

Contents

List of Abbreviations and Notation	iii
Why You Should Care About SICs	v
0 Introduction	vii
0.1 A sphere of states	vii
0.1.1 The physical approach	vii
0.1.2 The mathematical approach	x
0.2 The notion of a group	xii
0.3 Looking ahead	xv
I BACKGROUND	1
1 On the Geometry of Quantum States	2
1.1 Classification of states	2
1.2 The geometry of density matrices	5
1.3 Mutually unbiased bases	8
2 Exploring the Weyl-Heisenberg Group	12
2.1 Mathematical definitions	12
2.2 Orbits under the Weyl-Heisenberg group	19
2.3 A note on calculating MUBs	22
3 Getting to Know the SIC-POVM	24
3.1 Mathematical definition	24
3.2 The SICness function	26
3.3 Zauner subspaces	28
3.4 The MUS connection	29
II RESULTS	32
4 SICs in Low Dimensions	33
4.1 Two dimensions	33
4.2 Three dimensions	37
4.3 Four dimensions	39
4.3.1 The standard base	39

4.3.2	The Zauner subspace	39
4.4	Five dimensions	42
4.4.1	The standard base	42
4.4.2	The Zauner subspace	42
4.5	A note on the number of distinct inner products	45
5	MUSs and SICs in Seven Dimensions	48
5.1	Setting the scene	48
5.2	The special case	49
5.3	The general case	55
5.3.1	Gröbner bases	57
6	Connecting the MUSness and the SICness	59
6.1	Preamble	59
6.2	The naive approach	60
6.3	Further analysis	63
7	Epilogue	67
7.1	Concluding remarks	67
7.2	Open questions	68
7.3	Acknowledgements	68
III	Appendices	70
	Appendix A – Supplementary Code	71
	Appendix B – Computing power	77
	Appendix C – Exact Solutions to MUS in 7 Dimensions	79

List of Abbreviations and Conventions

Here we list the most crucial abbreviations, conventions, definitions and notation introduced in this thesis. We hope that it will prove a useful reference for the reader whenever he needs it. The order is such that relating concepts come in the order that they are introduced in the thesis.

POVM

Positive Operator Valued Measure; gives the most general notion of a measurement used in quantum mechanics (def. page 3).

MUBs

Mutually Unbiased Bases; a set of orthonormal bases where the inner product of any pair of basis vectors from separate bases has a fixed value (def. page 8).

MUS

Minimum Uncertainty State; a state which is situated in a similar way relative to all the bases in a complete set of MUBs (def. page 9).

SIC-POVM (SIC)

Symmetric Informationally Complete POVM; a set of vectors satisfying some simple relations for their inner and outer products (def. page 24).

G_{WH}

The Weyl-Heisenberg Group; a group which has played a major role in quantum mechanics since its introduction, we make extensive use of it throughout this whole thesis (def. page 13).

D_{ij}

The Displacement Operator; an operator representing some element $X^i Y^j$ in the Weyl-Heisenberg group (def. page 15).

G_C

The Clifford Group; the normaliser of the Weyl-Heisenberg group with respect to the group of unitary matrices (def. 17).

U

Clifford Group Element; a unitary matrix being an arbitrary element in the Clifford Group.

$SL(2, Z_N)$

The Special Linear Group of 2×2 matrices modulo N ; a group of all linear 2×2 matrices with unit determinant and with elements being integers modulo N (def. in unitary representation page 18).

ψ_0

SIC-Fiducial Vector; a vector generating a SIC as an orbit under the Weyl-Heisenberg group.

ψ_{ij}

A Shifted Vector; some vector ψ shifted by some displacement operator D_{ij} , such that $D_{ij}|\psi\rangle = |\psi_{ij}\rangle$.

f_{SIC}

The SICness Function; a function determining how much of a SIC some given state is (def. page 26).

f_{MUS}

The MUSness Function; a function determining how much of a MUS some given state is (def. page 59).

N

Dimension; the dimension of a space.

CP^N

The Complex Projective Space; the set of all straight lines passing through the origin in \mathbb{C}^{N+1} .

RP^N

The Real Projective Space; the set of all straight lines passing through the origin in \mathbb{R}^{N+1} .

ω

A primitive root of unity, $e^{\frac{2\pi i}{N}}$.

Why You Should Care About SICs

“When there is something that is really puzzling and cannot be understood, it usually deserves the closest attention because some time or other some big theory will emerge from it.”

– André Weil

The 20th century was a turbulent century from the point of view of physics with three paradigm shifts – the formulation of quantum mechanics, the theory of relativity and the revision of statistical mechanics – irreversibly changing how we understand the universe. Since its formulation, quantum mechanics has been the cause of many lively discussions, much due to its being fundamentally unintuitive. Ninety years after its formulation, we are still struggling to address fundamental issues such as the interpretation of the theory. There are also many seemingly basic mathematical questions yet to be answered, this thesis focuses on shedding some light on a few of these.

We start out from one of the pillars of quantum mechanics: the measurement. Traditionally we associate measurements in quantum mechanics with certain Hermitian* operators aptly called ‘observables’. This kind of measurements are referred to as ‘von Neumann measurements’. Broadly speaking there are two qualities to measurements in quantum mechanics; they are quantized and they may be incompatible. The topics discussed in this thesis relate to the latter of these.

When we write that two measurements are incompatible we mean that we cannot perform them at the same time. This is represented in the theory as two observables that are non-commuting – or perhaps more striking – that cannot be simultaneously diagonalised. Bohr was greatly intrigued by a certain class of incompatible observables known as ‘complementary observables’, being maximally incompatible[†]. Bohr’s insights led to the introduction of ‘the principle of complementarity’.

In finite dimension we regard maximally incompatible observables as two observables whose eigenvectors satisfy the following inner product: $|\langle e_i | f_j \rangle|^2 = \frac{1}{N}$, where N is the dimension. Notice that this captures exactly the complementarity that fascinated Bohr so long ago; if we know the outcome for a measurement in the $|e\rangle$ -eigenbasis then, $|\psi\rangle = |e_i\rangle$ for some i . But then the probability for every outcome in the $|f\rangle$ -eigenbase is $\frac{1}{N}$. Which means that we *know nothing* about the state in the $|f\rangle$ -eigenbase.

At this point a very relevant question arises: “*Can we always find a complete set of bases being complementary?*”. By ‘complete’ we mean ‘such that we can completely characterise a quantum state using these bases’[‡]. We call such a set of bases a complete set of Mutually Unbiased Bases (MUBs) and say that two bases are mutually unbiased if they satisfy the inner product from last paragraph. In any given dimension, a complete set of MUBs consists of $N + 1$ MUBs. Schwinger and many after him have tried to answer this simple question, but to this day it remains an open question. Partial results have been proven though, Schwinger proved that there exist pairs of complementary bases in each dimension and it has since been shown that there exist complete sets of MUBs in all prime power dimensions [34].

Another concept central to this thesis which is a way related to MUBs is the Positive Operator Valued Measure (POVM). This is a generalisation of the von Neumann measurements. Whereas

*By certain eccentrics, ‘Hermitean’ (with a silent ‘H’, phonetic: $\varepsilon\beta'mi:f\grave{a}n$), from French.

[†]Specifically Bohr studied the wave particle duality as a result of position and impulse being complementary.

[‡]The technical term for characterising a quantum state being ‘quantum tomography’.

von Neumann measurements require orthonormal (ON) eigenbases of Hermitian operators there are no such requirement for a POVM. Certainly an ON-basis is a special case of an POVM, but the POVM also allows for over complete bases. In fact, the POVM captures the most general idea of a measurement in quantum mechanics.

We might of course enquire as to whether there exists any other special POVMs, except for the ON-basis. One extraordinary POVM, and indeed the main focus of this thesis, is the Symmetric Informationally Complete POVM (SIC-POVM; commonly just 'SIC'). This is a set of unit vectors with constant inner products and whose outer products sum to identity. Furthermore, there are N^2 vectors in a SIC, this enables us to do quantum tomography using SICs and corresponds to the 'informationally complete' part of the SIC. While the definition of a SIC is simpler than that of a MUB, they have proven even harder to construct, although it seems as though they exists in every dimension [30].

As far as applications to physics goes both MUBs and SICs are both active research subjects. Between January and September this year 30 papers on MUBs were published (source: *arXiv*). MUBs are especially popular in quantum information theory where they are used in a variety of contexts, for instance in quantum cryptography and signal processing [17]. The subject of MUBs engages both respected experimentalists such as A. Zeilinger, who arranged a conference on the matter [1], as well as leading mathematicians. Despite the popularity of MUBs they have only been successfully constructed in prime power dimensions.

The research on SICs is more limited, with 7 articles between January and September this year (source: *arXiv*). Still, SICs are an emerging concept with many promising applications in quantum information theory, including being a candidate for succeeding the von Neumann measurements [23], as well as potentially being useful in quantum computing [32].

However, our motivation for investigating the SICs runs much deeper than these applications, it really has its roots in one of Hilbert's famous problems[§]. Hilbert's 12th problem states: "*Extend the Kronecker-Weber theorem on abelian extensions of the rational numbers to any base number field.*". While we will avoid any entanglement with this sophisticated mathematical problem itself, it is curious to note that all numbers occurring in a SIC sit in such a number field. Specifically they all sit in a kind of number field which, it is agreed, forms the first extension of this theorem: an abelian extension field of a real quadratic field [9].

An intuitive, and not too bad, picture of such number fields is that they are made up of roots of unity and Euclidean numbers, which is what we call the numbers that can be realised within Euclidean geometry using only unscaled rulers and pairs of compasses (e.g. nested roots, all rational numbers, etc.).

Apart from this observation there is a group that adds significant structure to the SICs. This is a group well known to quantum mechanics called the Weyl-Heisenberg group and it has strong ties to both MUBs and SICs. We shall see that this group introduces a natural framework for working with SICs and we shall use it extensively to generate SICs among other things.

In the spirit of Weil and encouraged by leading researchers in the field [24] we shall take it upon ourselves to give this puzzling entity called a 'SIC' the closest attention, in hope that we might one day understand it, and that from this understanding something big shall emerge.

[§]1902 D. Hilbert compiled a list of, at the time, open mathematical questions, much like the modern 'Millennium Problems' posed by Clay Institute.

Chapter 0

Introduction

The purpose of this chapter is to introduce the subject of this thesis on an as non-technical level as possible. We will arrive at two dimensional versions of most central concepts, it is our ambition that this two dimensional case-study shall provide some intuition as to what roles these concepts actually play. In the main part of this thesis we shall formulate all our theory in the most general manner possible. Hopefully, this chapter will ease the grasping of this imminent abstract formulation.

This chapter should be regarded as something of a pre-appendix, that is to say, an appendix before the main text—as opposed to after. The reader familiar with theoretical aspects of quantum information theory or foundations of quantum mechanics can skip ahead to Chapter 1. For the same very reason, there may be some minor repetitions in the main text of what is stated here.

0.1 A sphere of states

Regard a two level quantum system and a two dimensional Hilbert space. The prime example of such a system would be the spin space of an electron, though any two dimensional quantum system will suffice. We will consider the polarisation space of a single photon as this more closely relates to quantum information as it is implemented in the lab.

The point of this first section is to convince the reader that the set of states of any two level quantum system is readily realised as a sphere and that the orientation of states on this sphere is relevant. We shall start to argue this from pure physical grounds using photon polarisation as our example. At this point we shall involve a minimal amount of mathematical constructions. Afterwards, we shall develop a mathematical description of this argument which applies to any two level system, convincing ourselves that this is the model we should use when talking about the set of quantum states.

0.1.1 The physical approach

Generic light is said to be 'unpolarised', which is kind of an inapt terminology, rather it has a maximally mixed polarization, that is to say, it has components in all polarisation directions. Polarised light on the other hand, in its most simple implementation, is *linearly polarised*. We obtain linearly polarised light by letting unpolarised light pass through a linear polarisation filter, as is shown in Figure 1.

Notice that a linear polariser imposes a polarisation direction on the light. In Figure 1 we filter every component but the vertical part, and we say that the obtained light is polarised along

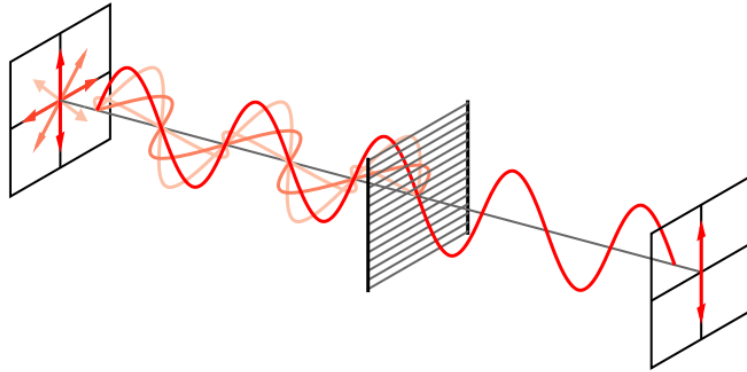


Figure 1: A vertical polarisation filter. Image credit: Bob Mellish at Wikimedia commons, image used under the Creative Commons Attribution-Share Alike 3.0 Unported-licence.

the y -axis, or, simply, that it is vertically polarised. We see from the figure that every linear polarisation can be expressed in terms of two polarisation modes, horizontal (x -) and vertical (y -) polarisation, as such we might take them for bases vectors for the linear polarisation space.

In this *polarisation plane* we may represent any given linear polarisation by a normalised polarisation vector, pointing at a unit circle of polarisation states. E.g. the vector $(1/\sqrt{2}, 1/\sqrt{2})$ points at the state having equal amounts of horizontal and vertical polarisation, which makes an angle of $\pi/4$ with the x -axis, this polarisation vector corresponds to a diagonal polarisation. There are two diagonal polarisation directions, we call them left and right diagonal polarisations, with the $\pi/4$ one being right diagonal polarisation. Note that there is some potential ambiguity going on here, the polarisation vector is not effected by the sign, such that the polarisation vectors (x, y) and $(-x, -y)$ both correspond to the same polarisation. This mishap will be compensated for in a moment.

This is a good point to introduce the concept of orthogonality at a physical level. If we apply a vertical polarisation filter it is known that only vertically polarised light passes through it. If one then applies a horizontal polarisation filter to the obtained light, all light will be filtered out, as is hinted in Figure 1. We say that these states are opposite, or, that they are *orthogonal* with respect to the horizontal-vertical polarisation basis*. In general, having polarised light in any given direction, the amount of light passing through a second filter is given by sine square of the angle between the polarisation axes.

This pattern can be understood within the context of measurements. Regard a polariser as a device preparing copies of some quantum state. Let us say, for the sake of the argument, that this is a horizontal polariser. A second polariser might then be viewed as a measurement. If we measure these prepared states by asking: “*Is this a horizontally polarised photon?*” to each and every photon, the answer will always be ‘yes’. Similarly, if we ask every photon if it is vertically polarised, the answer will always be ‘no’, and no light will be allowed to pass through. Finally, we know from last paragraph that half of the light should be filtered by a right diagonal polariser. This corresponds to half of the photons resulting in ‘yes’ and the other half resulting in ‘no’.

From this observation and by the superposition principle we can not only verify that the states of vertical and horizontal polarisation are orthogonal—we can also conclude that the right diagonal polarisation state sit equidistant to these states. Regarding the polariser as a

*Note that this is not the x - y -base introduced for the polarisation plane. This has to do with the sign dependency.

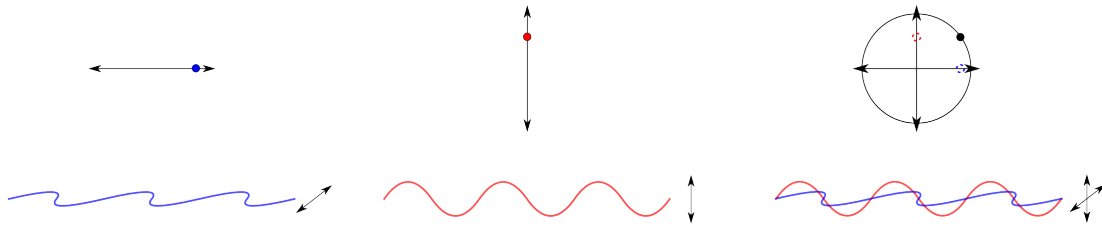


Figure 2: Decomposition of circular polarisation.

measurement (which is all in order), the photons stacking up in half 'yes', half 'no', corresponds to each measurement having probability $1/2$ for yielding 'yes' or 'no'. This is equivalent of saying that there is no bias with respect to horizontal or vertical polarisation when making this measurement. Hence, this measurement corresponds to a measurement in a different basis, specifically an unbiased basis, more on this later.

In order to obtain a more general description of photon polarisation we need to regard polarisation states where the polarisation vector rotates. This is conceived by letting the x and y components oscillate with time. The result is illustrated in Figure 2.

We see that the result is a circular polarisation. Note that we obtain two different kinds of circular polarisation states since the polarisation vector can either rotate in the positive or negative direction. This is determined by the relative oscillatory motion of the x and y components. Figure 2 might be of help to visualise this. We label the respective polarisation states as right and left circular polarisation.

Note that any linear polarisation state can be realised as a combination of these circular polarisation states. But what about elliptical polarisation states? An ellipse in the polarisation plane would correspond to the oscillatory range being different in the x and y directions in Figure 2. This renders the set of polarisations into a sphere, with the circular polarisation modes at the poles; the circle of linear polarisations situated at the equator; and where the rest corresponds to various elliptic polarisations. This is shown in Figure 3. A more rigid argument can be found e.g. here [28].

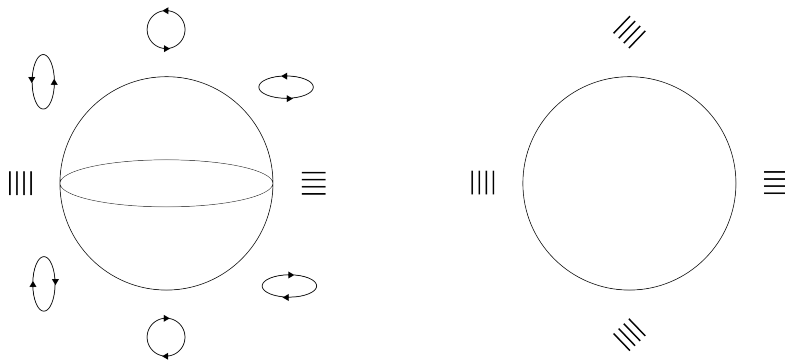


Figure 3: The sphere of photon polarisations.

Also, note that through the introduction of this polarisation picture, the before mentioned ambiguity of the circle of linear polarisations have been resolved. Now points of opposite sign correspond to orthogonal states – as it should be.

u	v	$ \psi\rangle$	State vector	Polarisation
0	1	$ 1\rangle$	$\begin{pmatrix} 0 \\ 1 \end{pmatrix}$	
1	0	$ 0\rangle$	$\begin{pmatrix} 1 \\ 0 \end{pmatrix}$	
1	1	$\frac{1}{\sqrt{2}} 0\rangle + \frac{1}{\sqrt{2}} 1\rangle$	$\frac{1}{\sqrt{2}}\begin{pmatrix} 1 \\ 1 \end{pmatrix}$	
1	-1	$\frac{1}{\sqrt{2}} 0\rangle - \frac{1}{\sqrt{2}} 1\rangle$	$\frac{1}{\sqrt{2}}\begin{pmatrix} 1 \\ -1 \end{pmatrix}$	
1	i	$\frac{1}{\sqrt{2}} 0\rangle + i\frac{1}{\sqrt{2}} 1\rangle$	$\frac{1}{\sqrt{2}}\begin{pmatrix} 1 \\ i \end{pmatrix}$	
1	$-i$	$\frac{1}{\sqrt{2}} 0\rangle - i\frac{1}{\sqrt{2}} 1\rangle$	$\frac{1}{\sqrt{2}}\begin{pmatrix} 1 \\ -i \end{pmatrix}$	

Table 1: Certain superpositions of interest. In this table we have imposed normalisation. In the case of photon polarisation the resulting polarisation is also given in this table.

0.1.2 The mathematical approach

Photon polarisation is a good example of why we use mathematics as the language to express physics – the reasoning above is exquisitely described in mathematics. We start out by introducing two distinct state vectors

$$|0\rangle = \begin{pmatrix} 1 \\ 0 \end{pmatrix} \quad |1\rangle = \begin{pmatrix} 0 \\ 1 \end{pmatrix} \quad (1)$$

and we identify these with the left- and right circular polarization modes of the photon.

In accordance with the laws of quantum mechanics we may very well (and should!) consider superposition of these *basis vectors*. A superposition would then be some state

$$|\psi\rangle = u|0\rangle + v|1\rangle \quad (2)$$

where $u, v \in \mathbb{C}$.

We immediately single out some interesting states in table 1.

Now, we know from quantum mechanics that a state vector scaled by some arbitrary complex number still corresponds to the same physical state. As such, any physical, two dimensional, state (equation 2) is uniquely determined by the quotient of the complex coefficients u and v . Hence, we introduce

$$z = \frac{u}{v} \quad (3)$$

Let us investigate this claim. We can easily calculate z for the states given in the table above[†].

[†]The attentive reader might at this point argue that this quotient does not handle $v = 0$ very well – which is bad, since this is one of our basic states given in table 1. However, this will be compensated for in a moment!

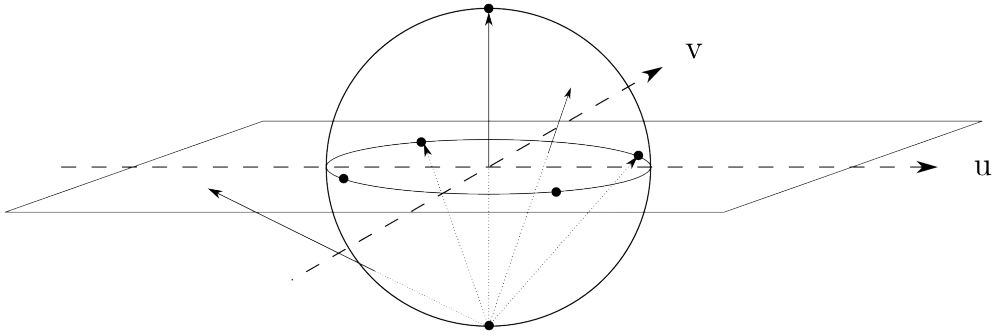


Figure 4: The stereographic projection of the Bloch sphere.

However, these nice states are exceptions, a general state does not sit in any of these 'privileged' positions. Moreover, z assumes values from the whole of $\mathbb{C}_\infty^\ddagger$, so it is obviously not the length of some state on the sphere. Rather u and v spans a \mathbb{C}^2 -plane.

In fact, the quotient z corresponds to a stereographic projection from the south pole of the sphere[§] [28]. By imposing this stereographic projection every state is uniquely labelled by a complex number, though we need to add infinity to deal with the point of projection. This stereographic projection is illustrated in Figure 4.

This sphere is referred to as 'the Bloch sphere'[¶]. In a complex 3-space this sphere would be oriented around the origin with the special points in table 1 situated oppositely at a distance of $1/2$ along respective axis, forming an octahedron. The radius $1/2$ is chosen by convention and is motivated by the fact that we want the maximum distance between two states to be $\pi/2$. The Bloch sphere is given in Figure 5.

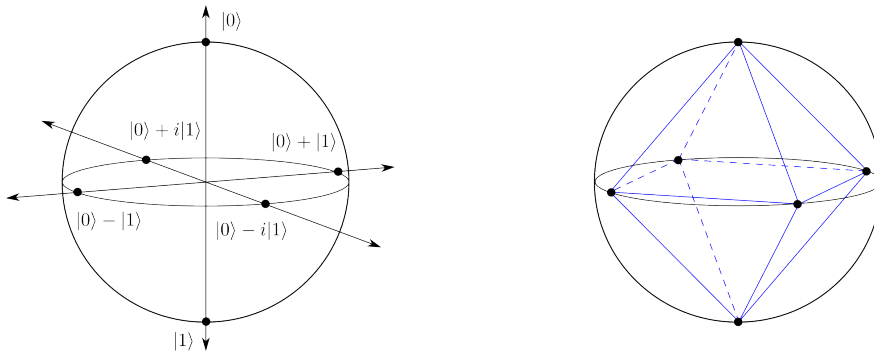


Figure 5: The Bloch sphere of quantum states, where the MUB-vectors form an octahedron.

The introduction of a Bloch sphere is a very deep result that is one of the founding blocks of quantum information. Realising the orthogonal states $|0\rangle$ and $|1\rangle$ as left and right circular polarisation the equatorial states are required to represent linear polarisation, as is stated in table 1. This observation renders the remaining states on the Bloch sphere elliptic polarisation states, the result is given in 3.

[‡]This is the field of complex numbers including infinity.

[§]Such a projective space is called a Riemann sphere.

[¶]Named after the Swiss physicist Felix Bloch.

We shall use the Bloch sphere picture to calculate the probability of finding $|\psi\rangle$ in some specific state is. Assume that $|\psi\rangle$ is in the state $|0\rangle + |1\rangle$. Assume also, for simplicity, that we restrict ourselves to states that sit on the equator of the Bloch sphere. The result will be qualitatively the same regardless of initial state and whether we choose states on the equator or not, since we can always orient our coordinate system such that this is the case. Writing $|\psi\rangle$ as $|\psi\rangle = \frac{1}{\sqrt{2}}(|0\rangle + e^{i\phi}|1\rangle)$, the probability for finding some state is

$$p = \left| \langle \psi | \left(\frac{1}{\sqrt{2}}|0\rangle + \frac{1}{\sqrt{2}}|1\rangle \right) \right|^2 = \frac{1}{4}|1 + e^{i\phi}|^2 = \frac{1}{2}(1 + \cos \phi) \quad (4)$$

where ϕ is the angle between the vectors.

Hence, the probability of finding $|\psi\rangle$ in the same very state is unity while it is 0 for finding the state in the orthogonal state, as it should be. More interestingly however, if we calculate the probability of finding $|0\rangle + i|1\rangle$ or $|0\rangle - i|1\rangle$ we find that it is precisely $\frac{1}{2}$. Noting how these states are situated on the Bloch sphere we realise that they sit in two completely different bases. In fact, this corresponds to the two corresponding observables being complementary. Recall that we introduced complementarity as: *“If we know everything about a state in some base, then we know nothing at all about it in the complementary base”*, thus the complete set of complementary bases in the Bloch sphere forms a complete set of Mutually Unbiased Bases (MUBs) such that they satisfy the MUB criterion

$$|\langle e_i | f_j \rangle| = \frac{1}{2} \quad \forall i, j \quad (5)$$

where $|e_i\rangle$ and $|f_j\rangle$ are basis vectors in two different bases.

This mathematical description is well in tune with the photon polarisation discussed before. The orthogonality of states and the statement that horizontal and diagonal polarisation sit in mutually unbiased bases is in agreement with this formalism.

Before we move on, we shall emphasise two statements of great importance.

“The set of states of a two level system constitutes a sphere.”

We have derived this result from both a physical and a mathematical line. This carries over to higher dimensions in a similar but more complicated fashion.

“The position on this sphere is important.”

Not only do the states sit on a sphere (or make up a sphere, depending on your perspective), the relative positioning of the states is also of relevance. We have seen that certain positions of states corresponds to orthogonality among other things.

Both these observations play a key role as structural elements throughout this thesis.

0.2 The notion of a group

We now introduce the operators

$$Z = \begin{pmatrix} 1 & 0 \\ 0 & -1 \end{pmatrix} \quad X = \begin{pmatrix} 0 & 1 \\ 1 & 0 \end{pmatrix} \quad ZX = \begin{pmatrix} 0 & -1 \\ 1 & 0 \end{pmatrix} \quad (6)$$

Acting with Z on our special states in table 1 while disregarding normalising factors we find

$$Z \begin{pmatrix} 1 \\ 0 \end{pmatrix} = \begin{pmatrix} 1 \\ 0 \end{pmatrix} \quad (7)$$

$$Z \begin{pmatrix} 1 \\ 1 \end{pmatrix} = \begin{pmatrix} 1 \\ -1 \end{pmatrix} \quad (8)$$

$$Z \begin{pmatrix} 1 \\ i \end{pmatrix} = \begin{pmatrix} 1 \\ -i \end{pmatrix} \quad (9)$$

Looking at Figure 5 we realise that this operation actually corresponds to a rotation by π about the 'z-axis', or rather, about the orthonormal (ON) base spanned by $\begin{pmatrix} 0 \\ 1 \end{pmatrix}$ and $\begin{pmatrix} 1 \\ 0 \end{pmatrix}$, which is mutually unbiased to the other two ON-bases spanning the Bloch sphere. Similarly, the X and ZX operations correspond to rotations about the 'x' and 'y' axes respectively.

Now, this structure right here, is due to an underlying group, and moreover a – for this thesis – very important group; the Weyl-Heisenberg group. The two dimensional Weyl-Heisenberg group is given by the operators above and the identity operator. We will use this group extensively throughout the rest of this thesis.

Regarding, once again, that the MUBs form a octahedron we identify another potentially interesting configuration of points on the Bloch sphere, namely the eight points that maximise the distance from the MUB-vectors. These special points should correspond to something remarkable – and indeed, they form two Symmetric Informationally Complete Positive Operator Valued Measures (SIC-POVMs; or just SICs) – the key player of this thesis. A SIC is a set of states on the Bloch sphere given by equiangular vectors that, in two dimensions, span a tetrahedron. Moreover, in any dimension these states are situated as to maximise the distance from the MUB-vectors. A SIC is given in Figure 6.

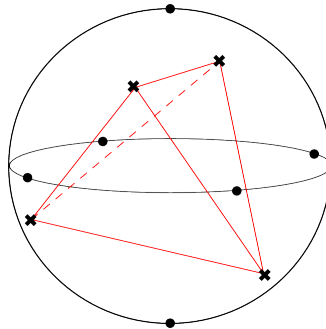


Figure 6: A SIC on the Bloch sphere with MUB-vectors given as balls for reference. The SIC forms an inscribed tetrahedron.

That the SIC-vectors span a tetrahedron is derived from the fact that the vectors are equiangular. This structure is preserved as we advance to higher dimensions. The SICs will always span regular polyhedra—albeit in a slightly more complicated implementation. Since the vectors are equiangular, the inner product of any two vectors in the SIC is constant, in two dimensions it is

$$|\langle \psi_i | \psi_j \rangle|^2 = \frac{1}{3} \quad (10)$$

A SIC is generated by acting on any one state in the set with all elements in the Weyl-Heisenberg group. We call such a vector a SIC-fiducial vector and say that the SIC is an orbit

under the Weyl-Heisenberg group. Recall that we have just learnt that acting with the Weyl-Heisenberg group elements corresponds to doing certain rotations on the Bloch sphere. A fiducial vector in two dimensions is [35]

$$\psi_0 = \begin{pmatrix} \sqrt{\frac{1}{2} \left(1 + \frac{1}{\sqrt{3}}\right)} \\ e^{i\pi/4} \sqrt{\frac{1}{2} \left(1 - \frac{1}{\sqrt{3}}\right)} \end{pmatrix} \quad (11)$$

Acting with the Weyl-Heisenberg elements on this state we find some more vectors like this one. Even from a quick glance we decide that these states are a great deal more complicated than the ones found before. This observation foreshadows the hardship of finding SICs in higher dimensions. We will use the Weyl-Heisenberg group in similar ways later on.

The introduction of SICs introduces yet another important operator – the Zauner operator U_Z .[‡] This is an order 3 operator that acts in a similar way on SIC-vectors as the Weyl-Heisenberg group did on MUB-vectors. Fixating one state in the SIC, the Zauner operator will embody the order 3 rotational symmetry of the tetrahedron around the symmetry axis passing through this state on the Bloch sphere.

Since both the Zauner operator and the Weyl-Heisenberg group are realised as rotations of the Bloch sphere – and by the fact that they both relate to SICs – we might suspect that there is a connection between the two. By imposing that the tetrahedron spanned by the SIC is oriented in a special way (such that they maximise the distance to the MUB-vectors), the Zauner operator and the Weyl-Heisenberg group become simultaneously meaningful as illustrated in Figure 7. This further strengthens the statement that the relative positioning of states are important on the Bloch sphere.

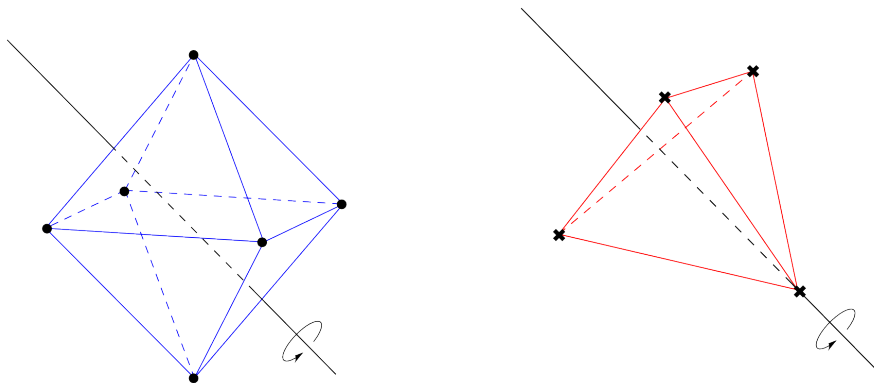


Figure 7: Acting with the Zauner operator corresponds to a rotation of $\frac{2\pi}{3}$. This permutes the vectors in the SIC- and MUB-vectors.

Without having to do any calculation we can see from this picture that the Zauner operator will permute the set of MUBs. Hence, starting from one single MUB-vector we can generate the set of MUBs by consecutively acting with the Zauner operator. As such the Zauner operator is a 'MUB-cycler' in two dimensions.

[‡]It is labelled U since it is a unitary operator.

0.3 Looking ahead

Summarising we have studied some of the most central concepts of this thesis in two dimensions: the MUBs, the SIC, and the Weyl-Heisenberg group. We even got to mention the MUB-cycler in the end, to which we will return in the last chapter of this thesis.

Be aware that not all the structure present in this two dimensional case study will carry over to higher dimensions. We will clarify why this is the case in the Chapter 1. However, the outline will be the same. We will, at length, study the interaction between these key players, and while some of the structure is specific to two dimensions much is inherited to higher dimensions.

As the thesis progresses it will become increasingly hard to provide decent pictures of the spaces which we study. In fact, being able to visualise the whole Hilbert space is a luxury enjoyed solely in two dimensions. Even in \mathbb{C}^3 , being the next dimension, the Bloch space is eight dimensional. As such we will largely rely on algebra to express our results. However, we will try to illustrate our results to the extent it is possible, there are some nice geometrical tricks yet to be unveiled!

Part I

BACKGROUND

Chapter 1

On the Geometry of Quantum States

In this chapter we shall introduce the quantum theory required for this thesis. We will scope the idea of a measurement of a quantum system and adopt a geometry for quantum states. The reader is assumed to have previous knowledge of quantum mechanics and the Dirac formalism equivalent to that of an undergraduate, e.g. Sakurai's "Modern Quantum Mechanics" [29].

1.1 Classification of states

At the heart of quantum mechanics dwells the idea of a state. A state is *that* which contains all conditional information of any given system. To specify this entity in more detail using general terms is *hard* – if at all possible – and at any rate not the purpose of this text. Rather, we shall arrive at a precise mathematical definition in the language of convexity and density matrices.

1930-1932 P.A.M. Dirac and J. von Neumann developed the axiomatic formalism of quantum mechanics. Herein they postulated the intrinsic probabilistic nature of all quantum theory [20] [33]; this is where we start our journey.

Regard the following two situations

1. A set-up preparing half of the states as $|0\rangle$ and the other half of the states as $|1\rangle$ written

$$\rho = \frac{1}{2}|0\rangle\langle 0| + \frac{1}{2}|1\rangle\langle 1| \quad (1.1)$$

2. A set-up producing states in the superposition $\frac{1}{\sqrt{2}}|0\rangle + \frac{1}{\sqrt{2}}|1\rangle$ written

$$\rho = \frac{1}{2}(|0\rangle + |1\rangle)(\langle 0| + \langle 1|) = \frac{1}{2}|0\rangle\langle 0| + \frac{1}{2}|1\rangle\langle 1| + \frac{1}{2}|0\rangle\langle 1| + \frac{1}{2}|1\rangle\langle 0| \quad (1.2)$$

Measuring either of these systems the probability for finding the system in the state $|0\rangle$ is the same, namely $\frac{1}{2}$. It is a philosophical question whether the nature of these probabilities are *the same*. Regardless of your take on that issue there is, as of today, no way of distinguishing between the two when making a measurement. That is to say; they are numerically identical.

As such we must have a mathematical description of quantum states that incorporate both of these probabilities.

Any measurement in quantum mechanics can be represented by a Positive Operator Valued Measure (hereinafter POVM), we define a POVM as

Definition 1. *Positive Operator Valued Measures (POVMs)*

Let E_i be an operator. We say that it is a POVM if it satisfies

I *Completeness*

$$\sum_{i=1}^N E_i = \mathbb{1} \quad (1.3)$$

II *Hermiticity*

$$E_i = E_i^\dagger \quad (1.4)$$

III *Non negativity*¹

$$E_i \geq 0 \quad (1.5)$$

Additionally, if E_i is an ON-base the POVM corresponds to a projective measurement, which is typically the kind of measurement we do in the lab.

In this formalism, the probability for the outcome numbered i given a state $|\psi\rangle$ is

$$p_i = |\langle\psi|E_i|\psi\rangle| \quad (1.6)$$

It follows from the definition of POVMs that

$$p_i \geq 0 \quad (1.7)$$

$$\sum_{i=1}^N p_i = 1 \quad (1.8)$$

Suppose that we have a source that by some means generates a set of states $\{|\psi_j\rangle\}$ with some corresponding probabilities p'_j . Measuring this *ensemble* of states we find

$$p_i = \sum_{j=1}^K p'_j \langle\psi_j|E_i|\psi_j\rangle = \text{Tr} \left(E_i \sum_{j=1}^N p'_j |\psi_j\rangle\langle\psi_j| \right) \quad (1.9)$$

We now define the density matrix

Definition 2. *Density Matrix*

Let $\{|\psi_j\rangle\}$ be a set of states with associated probabilities p'_j , then the density matrix for any given state is

$$\rho = \sum_{j=1}^N p'_j |\psi_j\rangle\langle\psi_j| \quad (1.10)$$

satisfying

¹It has non negative real eigenvalues, λ_i .

I Hermiticity

$$\rho_i = \rho_i^\dagger \quad (1.11)$$

II Non negative eigenvalues

$$\rho \geq 0 \quad (1.12)$$

III Normalisation

$$\text{Tr } \rho = 1 \quad (1.13)$$

We can take the density matrix to be a more mathematical definition of a state. In the formalism of density matrices we write 1.9 as

$$p_i = \text{Tr}(E_i \rho) \quad (1.14)$$

This is a rather enjoyable expression. Since the trace is the same regardless of basis we may choose to evaluate this in any convenient basis.

The density matrix contains all the viable information of a quantum system. Combining density matrices and POVMs in this way we find a very concise formalism for calculating the probabilities of a given system.

If ρ represents a pure state we have

$$\rho^2 = |\psi\rangle\langle\psi|\psi\rangle\langle\psi| = |\psi\rangle\langle\psi| = \rho \quad (1.15)$$

Which means that for a pure state

$$\text{Tr } \rho^2 = 1 \quad (1.16)$$

This means that we can always chose a basis such that ρ is of the form

$$\rho = \begin{pmatrix} 1 & 0 & \cdots & 0 \\ 0 & 0 & \cdots & 0 \\ \vdots & \vdots & \ddots & \vdots \\ 0 & 0 & \cdots & 0 \end{pmatrix} \quad (1.17)$$

Or equivalently

$$\lambda_j = 1 \quad \lambda_i = 0 \quad \forall i \neq j \quad (1.18)$$

We say that ρ has the spectrum $(1, 0, \dots, 0)$.² Conversely $\text{Tr } \rho^2 < 1$ implies that the state is mixed.

The notion of density matrices may be expanded by introducing the convex mixing of density matrices.

$$\rho = p\rho_1 + (1-p)\rho_2 \quad (1.19)$$

where p is some probability.

This convex mixing of states accounts for the mixed states and it is the most general notion of a state that we will use. However, we shall mainly concern ourselves with pure states why from here on all states are assumed to be pure if nothing else is explicitly stated.

²Of course any one diagonal element can be 1, we just chose the first one for convenience.

1.2 The geometry of density matrices

For pure states we recognise that $|\psi\rangle$ and $e^{i\theta}|\psi\rangle$ both represents the same physical state. We express this relation as

$$e^{i\theta}|\psi\rangle_{\mathcal{H}} \longleftrightarrow |\psi\rangle_{\mathbb{C}\mathbb{P}^{N-1}} \quad (1.20)$$

Such that there exists a bijection between physical states and rays in Hilbert space. This is illustrated in Figure 1.1. The set of rays spans the complex projective $N - 1$ -plane $\mathbb{C}\mathbb{P}^{N-1}$ where every point corresponds to a state. Accounting for the phase in equation 1.20 and for normalisation ($\langle\psi|\psi\rangle = 1$) this space has $2(N - 1)$ real dimensions, cf. \mathcal{H}^N which has $2N$ real dimensions. This property of quantum states (1.20) is very important since it greatly reduces the number of states which are physically relevant.

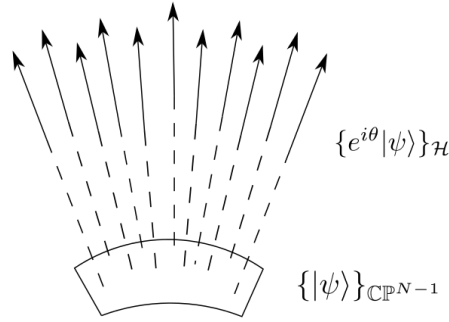


Figure 1.1: The bijection between points in the complex projective space ($\mathbb{C}\mathbb{P}^{N-1}$) and rays in Hilbert space (\mathcal{H}) illustrated. The complete set of rays in \mathcal{H}^N spans $\mathbb{C}\mathbb{P}^{N-1}$, the space of all quantum states.

We introduce the $N^2 - 1$ real dimensional vector space, V , of all traceless, Hermitian $N \times N$ matrices. $N^2 - 1$ -dimensional because a general Hermetian matrix has N^2 parameters but the requirement of tracelessness removes one degree of freedom, leaving us with $N^2 - 1$ parameters.

In V

$$\psi \mapsto |\psi\rangle\langle\psi| - \frac{1}{N}\mathbf{1} \quad (1.21)$$

is a $2(N - 1)$ dimensional vector.

We introduce the following geometry on V

I *Scalar product*

$$\mathbf{A} \circ \mathbf{B} = \frac{1}{2} \text{Tr } AB \quad (1.22)$$

II *Norm*

$$\|\mathbf{A}\|^2 = \frac{1}{2} \text{Tr } A^2 \quad (1.23)$$

Let's work out some of the features of this vector space given the geometry above.

For any two, orthogonal, basis vectors in \mathbb{R}^N

$$\langle e_i | e_j \rangle = 0 \quad (1.24)$$

We transfer these into V by the transformations

$$\mathbf{e}_i = |e_i\rangle\langle e_i| - \frac{1}{N}\mathbb{1} \quad (1.25)$$

$$\mathbf{e}_j = |e_j\rangle\langle e_j| - \frac{1}{N}\mathbb{1} \quad (1.26)$$

and check the consequences of orthogonality

$$\begin{aligned} \mathbf{e}_i \circ \mathbf{e}_j &= \frac{1}{2} \text{Tr} \left[\left(|e_i\rangle\langle e_i| - \frac{1}{N}\mathbb{1} \right) \left(|e_j\rangle\langle e_j| - \frac{1}{N}\mathbb{1} \right) \right] \\ &= \frac{1}{2} \text{Tr} \left[-\frac{1}{N}|e_i\rangle\langle e_i| - \frac{1}{N}|e_j\rangle\langle e_j| + \frac{1}{N^2}\mathbb{1} \right] \\ &= \frac{1}{2} \left(-\frac{1}{N} - \frac{1}{N} + \frac{1}{N} \right) = -\frac{1}{2N} \end{aligned} \quad (1.27)$$

This calculation shows us that we have lost the familiar orthogonality of the basis vectors. However, it also tells us that the basis vectors now span a regular simplex, since all the inner products take the same value.

We can verify this by calculating the distance between two basis vectors.

$$\begin{aligned} \|\mathbf{e}_i - \mathbf{e}_j\|^2 &= \frac{1}{2} \text{Tr} \left(|e_i\rangle\langle e_i| - |e_j\rangle\langle e_j| - 2\frac{1}{N}\mathbb{1} \right)^2 \\ &= \frac{1}{2} \text{Tr}(|e_i\rangle\langle e_i| + |e_j\rangle\langle e_j|) \\ &= \frac{1}{2}(1 + 1) = 1 \end{aligned} \quad (1.28)$$

In order to get a feeling for this coordinate system we shall investigate the case $N = 3$. By equations 1.27 and 1.28 the distance between any two basis vectors is 1 and their scalar product is $-\frac{1}{6}$ accounting for an angle $\frac{2\pi}{3}$ between them. This forces the length of the basis vectors to be $\frac{1}{\sqrt{3}}$. Hence the three basis vectors \mathbf{e}_1 , \mathbf{e}_2 and \mathbf{e}_3 spans a 2-simplex as shown in Figure 1.2.

The intuitive coordinate system on a simplex is the barycentric coordinate system. An arbitrary vector in this coordinate system can be written

$$\mathbf{v} = \alpha_1\mathbf{e}_1 + \alpha_2\mathbf{e}_2 + \cdots + \alpha_N\mathbf{e}_N \quad \alpha_i \geq 0 \quad \forall i \quad (1.29)$$

We note that $\mathbf{e}_1 + \mathbf{e}_2 + \cdots + \mathbf{e}_N = 0$ by symmetry; this is easily realised by regarding the $N = 3$ case. We may choose the following normalisation as a constraint for the coefficients α_i

$$\alpha_1 + \alpha_2 + \cdots + \alpha_N = 1 \quad (1.30)$$

Using this normalisation we can realise the coefficients as probabilities and we relabel them appropriately as p_1, p_2, \dots, p_N . This provides a nice, intuitive, picture of what a vector, \mathbf{v} , in the

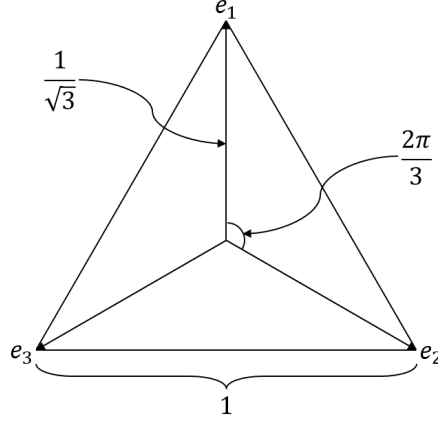


Figure 1.2: In three dimensions the basis vectors of the vector space V forms a 2-simplex.

simplex actually represents. Regard Figure 1.2 once again, equations 1.27 and 1.28 tell us that at the furthest top of \mathbf{e}_1 we have $p_1 = 1$, $p_2 = p_3 = 0$, hence this is where we find the pure state with eigenvalues $(1, 0, 0)$. Likewise the other pure states are found at respective vertex. Whereas in the middle of the edges we find states like $p_1 = 0$, $p_2 = p_3 = 1/2$ (bottom line) which corresponds to the mixed state with eigenvalues $(0, 1/2, 1/2)$. The maximally mixed state sits in the middle with $p_1 = p_2 = p_3 = 1/3$. We call this density matrix ρ_* .

We calculate the length of an arbitrary vector \mathbf{v} in the simplex as

$$\begin{aligned}
 \mathbf{v} \circ \mathbf{v} &= \left(\sum_{i=1}^N p_i \mathbf{e}_i \right)^2 = \sum_{i=1}^N p_i^2 \mathbf{e}_i \circ \mathbf{e}_i + \left(\sum_{\substack{i=1 \\ i \neq j}}^N \sum_{\substack{j=1 \\ j \neq i}}^N p_i p_j \mathbf{e}_i \circ \mathbf{e}_j \right) \\
 &= \left\langle \mathbf{e}_i \circ \mathbf{e}_i = \frac{N-1}{2N} \quad \mathbf{e}_i \circ \mathbf{e}_j = -\frac{1}{2N} \right\rangle \\
 &= \frac{N-1}{2N} \sum_{i=1}^N p_i^2 - \frac{1}{2N} \sum_{\substack{i=1 \\ i \neq j}}^N \sum_{\substack{j=1 \\ j \neq i}}^N p_i p_j = \frac{N-1}{2N} \sum_{i=1}^N p_i^2 - \frac{1}{N} \left(\frac{1}{2} \left(\sum_{i=1}^N p_i \right)^2 - \frac{1}{2} \sum_{i=1}^N p_i^2 \right) \\
 &= \frac{N-1}{2N} \sum_{i=1}^N p_i^2 + \frac{1}{2N} \sum_{i=1}^N p_i^2 - \frac{1}{2N} = \frac{1}{2} \sum_{i=1}^N p_i^2 - \frac{1}{2N}
 \end{aligned} \tag{1.31}$$

Summarising, the barycentric coordinates p_i are subject to the following constraints

$$\sum_{i=1}^N p_i = 1 \tag{1.32}$$

$$\sum_{i=1}^N p_i^2 = 2\|\mathbf{v}\|^2 + \frac{1}{N} \tag{1.33}$$

1.3 Mutually unbiased bases

The attentive reader might recall that the state $|\psi\rangle$ sits in an $N^2 - 1$ -dimensional real space, \mathbb{R}^{N^2-1} , and argue that insofar, in $N = 3$, we have only talked about some vector in a 2-simplex, which is a vector in, \mathbb{R}^2 , rather than a vector in \mathbb{R}^8 . This is however all in order, note that a vector in a 2-simplex is actually a vector in some 2-dimensional plane. The simplex from last section is but one simplex sitting in one out of four totally orthogonal planes in \mathbb{R}^8 . There are three additional simplices orthogonal to this one, making a total of $2 \times 4 = 8$ dimensions. However, in order to construct them we need to introduce the concept of Mutually Unbiased Bases [26][34]

Definition 3. *Mutually Unbiased Bases (MUBs)*

Let $\{e_i\}$ and $\{f_j\}$ be two complete sets of basis vectors spanning the bases E and F . These are said to be mutually unbiased if and only if

$$|\langle e_i | f_j \rangle|^2 = \frac{1}{N} \quad \forall i, j \quad (1.34)$$

Taking the inner product of two basis vectors from two different MUBs in V we find,

$$\begin{aligned} \mathbf{e}_i \circ \mathbf{f}_j &= \frac{1}{2} \text{Tr} \left[\left(|e_i\rangle\langle e_i| - \frac{1}{N} \mathbb{1} \right) \left(|f_j\rangle\langle f_j| - \frac{1}{N} \mathbb{1} \right) \right] \\ &= \frac{1}{2} \text{Tr} \left[-\frac{1}{N} |e_i\rangle\langle e_i| - \frac{1}{N} |f_j\rangle\langle f_j| + \underbrace{|e_i\rangle\langle e_i | f_j\rangle\langle f_j|}_{= |\langle e_i | f_j \rangle|^2 = \frac{1}{N}} + \frac{1}{N^2} \mathbb{1} \right] \\ &= \frac{1}{N} \left(-\frac{1}{N} - \frac{1}{N} + \frac{1}{N} + \frac{1}{N} \right) = 0 \end{aligned} \quad (1.35)$$

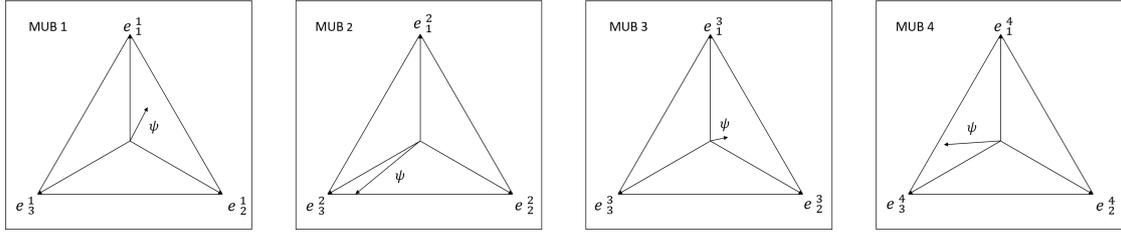
thus the simplices are MUBs and sit in totally orthogonal planes in V .

This completes the example of the 3-dimensional Hilbert space by concluding that any state $|\psi\rangle$ is given by its projection onto four totally orthogonal simplices as shown in Figure 1.3. The length of each component corresponds to the convex mixing of density matrices in that basis. Note that this is all valid for both mixed and pure states, hence this formalism incorporates classical mixing of states as well as *quantum* probabilities. This will be further exemplified in the end of this section.

It follows from equation 1.31 that the total length of some vector $|\psi\rangle$ in V is

$$\|\psi\| = \sum_{j=1}^{N+1} \left(\sum_{i=1}^N \frac{p_i^{(j)^2}}{2} - \frac{1}{2N} \right) \quad (1.36)$$

We can generalise this case study by arguing that in N dimensions the MUBs form $N - 1$ -simplices with $N - 1$ real parameters. We also know that any state can be decomposed with projective measurements onto the MUBs. Hence, in N dimensions there must be at least $\frac{N^2-1}{N-1} = N + 1$ MUBs. Furthermore, if $N \in \mathbb{P}$ then the number of MUBs is always $N + 1$, where \mathbb{P} is the set of prime numbers [26][34].

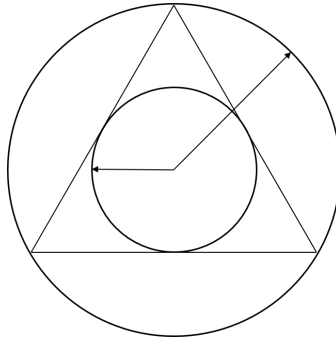
Figure 1.3: ψ decomposed into four MUBs.

Having introduced MUBs we turn to a related piece in the puzzle of quantum state geometry; the notion of minimum uncertainty states [8].

Definition 4. *Minimum Uncertainty State (MUS)*

Let $|\psi\rangle$ be a state in Hilbert space and let $p_i^{(j)}$ be the component of $|\psi\rangle$ along the i :th basis vector in the j :th MUB such that $p_i^{(j)} = |\langle\psi|e_i^{(j)}\rangle|^2$. Then $|\psi\rangle$ is a minimum uncertainty state if and only if

$$\sum_{i=1}^N (p_i^{(j)})^2 = \frac{2}{N+1} \quad \forall j \in [1, N+1] \quad (1.37)$$

Figure 1.4: The inner sphere of MUS and the outer sphere of MUB-states in $N = 3$.

In V , MUSs are in a way antipodal to the MUB vectors (the basis vectors of the MUBs). Once again turning to the 3-dimensional case for intuition, we realise from equation 1.37 and Figure 1.2 that while MUB vectors have coordinates such as $(1, 0, 0)$ the MUSs have coordinates such as $(0, \frac{1}{2}, \frac{1}{2})$. Thus the MUB vectors are situated as far away from their corresponding MUS as possible [21], see Figure 1.4. Note that a state $|\psi\rangle$ which is a MUB vector in one MUB is projected to ρ_* in all other MUBs, hence the antipodal analogy only holds in one MUB. On the contrary MUSs have components of equal length in all four MUBs. This property of MUSs is the direct geometrical realisation of equation 1.37, thus we may take it to be the defining quality of a MUS.

This nicely generalises to an arbitrary prime dimension N as [21]

1. ψ sits in a $N^2 - 1$ dimensional space.
2. ψ is decomposed into $N + 1$ MUBs being $N - 1$ -simplices.

3. The pure states sit at a distance

$$d_{pure}^2 = \frac{1}{2} \sum_{i=1}^N p_i^2 - \frac{1}{2N} = \frac{1}{2} - \frac{1}{2N} = \frac{N-1}{2N} \quad (1.38)$$

where we used

$$p_j = 1 \implies p_i = 0 \quad \forall i \neq j \quad (1.39)$$

4. The MUS sit at a distance

$$d_{MUS}^2 = \frac{1}{2} \sum_{i=1}^N p_i^2 - \frac{1}{2N} = \frac{1}{N-1} - \frac{1}{2N} = \frac{N-1}{2N(N+1)} \quad (1.40)$$

where we used the MUS condition from Definition 4.

All quantum states ψ – mixed and pure – are enclosed by a sphere. This sphere has dimension $N^2 - 2$ since the sphere of highest dimension that can be embedded in R^{N^2-1} (the space of all quantum states) is \mathcal{S}^{N^2-2} . The set of pure states, $\mathbb{C}\mathbb{P}^{N-1}$, forms a submanifold on the surface of this sphere and has dimension $2(N-1)$ [21].

Note that $N = 2$ is quite special. Here the dimension of V is \mathbb{R}^3 which makes two dimensions exceptional for working out some intuition as to how this geometry is realised. According to subsequent sections the MUBs in two dimensions are pairs of opposite lines (1-simplices) emerging from ρ_* with lengths $\frac{1}{4}$. Hence all the pure states are sitting on a sphere of radius $\frac{1}{4}$ enclosing the mixed states. But this is just the Bloch ball(!), which is the set of all quantum states for a two level system (widely recognised as a *qubit*).

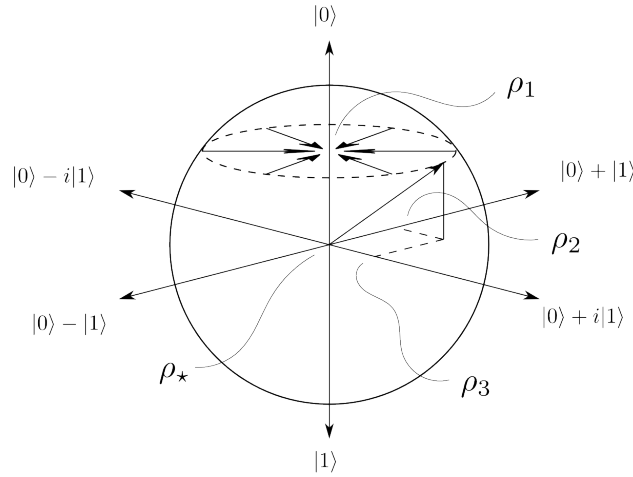


Figure 1.5: $|\psi\rangle$ decomposed into three 1-simplices (lines). Each simplex is spanned by two basis vectors corresponding to the spin directions of a 2-dimensional quantum system. A state is projected onto these MUBs where it is assigned a value corresponding the probability in that base.

For the sake of intuition we include a figure showing how the states are geometrically related to the simplices, see Figure 1.5. We see that there is a disc of states orthogonal to every point on

a given MUB vector which are projected onto this point, this is also the case in higher dimensions albeit it is hard to visualise, eg. in $N = 3$ at every point in the simplex there is a sphere of points orthogonal to that point being projected to that point. Any state ket $|\psi\rangle$ is decomposed into the MUBs with lengths corresponding to the probabilities for that outcome.

We conclude this chapter by proving the following theorem which shall be useful later on.

Theorem 1. *Probability when summing over all MUBs*

Given an arbitrary state vector in \mathbb{C}^N

$$|\psi\rangle = \begin{pmatrix} \sqrt{p_1} \\ \sqrt{p_2} e^{\mu_{1i}} \\ \vdots \\ \sqrt{p_n} e^{\mu_{ni}} \end{pmatrix} \quad (1.41)$$

and an inner product

$$p_i = |\langle\psi|e_i^{(j)}\rangle|^2 \quad (1.42)$$

where $e_i^{(j)}$ is the i :th basis vector of the j :th MUB in dimension N , $N \in \mathbb{P}$

Then

$$\sum_{j=0}^{N+1} \sum_{i=1}^N p_i^{(j)} = 2 \quad (1.43)$$

Proof.

By equations 1.36 and 1.38

$$\begin{aligned} \frac{N-1}{2N} &= \sum_{j=1}^{N+1} \left(\sum_{i=1}^N \frac{p_i^{(j)^2}}{2} - \frac{1}{2N} \right) \iff \\ \sum_{j=1}^{N+1} \sum_{i=1}^N p_i^{(j)^2} &= 2 \left(\frac{N-1}{2N} + \frac{N+1}{2N} \right) = 2 \end{aligned} \quad (1.44)$$

and the proof is done.

□

Chapter 2

Exploring the Weyl-Heisenberg Group

The subject of group theory is an elegant part of abstract algebra. Although being a subject that is sometimes overlooked in the undergraduate physics programmes, it has a lot of applications in physics. With this in mind we shall assume no prior knowledge of groups from the reader. While we cannot spend a lot of time on giving a thorough introduction to group theory, we shall at least have the common courtesy of formally define (most of) the group theoretical concepts to be used.

The reader who is inclined towards learning more about the fascinating subject of groups is referred to the literature; e.g. Flaleigh's "A First Course in Abstract Algebra" [22] or for a more comprehensive (and more advanced) reference Lang's "Algebra" [27]. We hope that the reader already familiar with group theory bears with us.

Throughout this chapter Einstein summation convention for tensors is implied¹.

2.1 Mathematical definitions

Like any proper text in mathematics we inaugurate this chapter with a definition. We will define the abstract algebraic entity called a group. This is a very general notion defined as follows

Definition 5. *Group*

We define a group (G, \star) as a set, G , under a binary operation, \star , satisfying the so called group axioms

I Closure

$$a \star b = c \in G \quad \forall a, b \in G \quad (2.1)$$

II Associativity

$$(a \star b) \star c = a \star (b \star c) \quad \forall a, b, c \in G \quad (2.2)$$

¹Contracted indices implies summation, eg. $A_{ij}x^\alpha y^\beta g_{\alpha\beta} = A_{ij} \sum_{\alpha=1}^l \sum_{\beta=1}^l x^\alpha y^\beta g_{\alpha\beta}$. Note that all terms in an expression are *elements* of some tensors in this formalism, as such they commute: $g_{\alpha\beta}x^\alpha b^\beta = g_{\alpha\beta}b^\beta x^\alpha$.

III Existence of identity element

$$\exists e \in G \mid e \star a = a \star e = a \quad \forall a \in G \quad (2.3)$$

IV Existence of inverse element

$$\exists a' \in G \mid a' \star a = a \star a' = e \quad \forall a \in G \quad (2.4)$$

When working with groups it is inevitable to come across the concept of homomorphisms, so we define it right away

Definition 6. *Homomorphism*

Let (G, \star) and $(H, *)$ be two groups, we define the homomorphism to be a function such that

$$\exists \phi : G \mapsto H \mid \phi(u \star v) = \phi(u) * \phi(v) \quad \forall u, v \in G \quad (2.5)$$

The homomorphism can be thought of as a generic function between two groups. We can formulate other functions, but generally the functions have to obey this criterion to make any sense. In accordance with common group theory practice we shall emphasise two special types of homomorphisms worthy of their own definitions.

Definition 7. *Isomorphism*

Let the homomorphism $\phi : G \mapsto H$ be bijective. Then we call ϕ an isomorphism and we say that G and H are isomorphic.

Isomorphisms can be thought of as the group theoretical analogue to congruence. If two groups are isomorphic they are in every practicable sense the same.

Definition 8. *Automorphism*

Let the homomorphism $\phi : G \mapsto G$ be bijective. Then we call ϕ an automorphism.

A general automorphism does not have a clear counterpart in ordinary functions, it is a function whose domain and codomain are the same. An example of an automorphism is the permutation of a set; it sends all the elements in the set to the set itself, but it changes the order of the elements. We shall introduce two automorphisms right away to be used later on: Let $\phi(g) = h^{-1}gh$ be some automorphism. If h is an element in G , ϕ is called an *inner automorphism*. If h is an element in a larger group containing G , ϕ is called an *outer automorphism*.

We are now fit to define our first group through the following presentation²

Definition 9. *The Weyl-Heisenberg group*

Let G_{WH} be a group with the following defining representation³

²The proper definition of a presentation is rather lengthy and not very enlightening, as such will omit its formal definition. Rather we shall take the *presentation* of a group to be *the set of generators along with some relation that generate all elements of the group as products of powers of the generators subject to the relation* and be happy about it.

³This is a concept from the branch of mathematics called representation theory. We will not define it. In this specific case we can think of it as a way of mimicking the group with non-unitary matrices.

$$\omega = \begin{pmatrix} 1 & 0 & i \\ 0 & 1 & 0 \\ 0 & 0 & 1 \end{pmatrix}$$

$$X = \begin{pmatrix} 1 & 0 & 0 \\ 0 & 1 & j \\ 0 & 0 & 1 \end{pmatrix}$$

$$Z = \begin{pmatrix} 1 & k & 0 \\ 0 & 1 & 0 \\ 0 & 0 & 1 \end{pmatrix}$$

for $i, j, k \in \mathbb{Z}_N$ – the set of integers modulo N .

Also let G_{WH} have the following presentation

$$G_{WH} = \left\{ \begin{array}{l} ZX = \omega XZ \\ X^N = Z^N = \omega^N = \mathbf{1} \end{array} \right. \quad (2.6)$$

Then G_{WH} forms the Weyl-Heisenberg group under matrix multiplication within \mathbb{Z}_N . G_{WH} has N^3 group elements $\omega^k X^i Z^j$ called words.

The Weyl-Heisenberg group is instrumental to this thesis, the observant reader shall identify it as a key background player throughout the rest of the text. We use the following essentially unique unitary representation of the Weyl-Heisenberg group

$$Z|r\rangle = \omega^r |r\rangle \quad (2.7)$$

$$X|r\rangle = |r+1\rangle \quad (2.8)$$

$$\omega = e^{\frac{2\pi i}{N}} \quad (2.9)$$

with $r \in \mathbb{Z}_N$.

Using this representation we can reconstruct all elements of the Weyl-Heisenberg group in any given basis. Specifically, in an orthogonal N dimensional base

$$\langle r|s\rangle = \delta_{r,s} \quad (2.10)$$

Using the unitary representations 2.7 and 2.8 we find

$$\langle r|Z|s\rangle = \omega^s \delta_{r,s} \quad (2.11)$$

$$\langle r|X|s\rangle = \delta_{r,s+1} \quad (2.12)$$

and a general element is written

$$\begin{aligned}
\langle r|\omega^k X^i Z^j|s\rangle &= \\
&= \langle r|\omega^k X^i (\omega^s)^j|s\rangle \\
&= \langle r|\omega^{k+sj} X^i|s\rangle \\
&= \langle r|\omega^{k+sj}|s+i\rangle \\
&= \omega^{k+sj} \langle r|s+i\rangle \\
&= \omega^{k+sj} \delta_{r,s+i}
\end{aligned} \tag{2.13}$$

We now define the displacement operators as [6]

Definition 10. *Displacement Operators*

Let $\tau = -e^{\frac{i\pi}{N}}$ and let $X^i Z^j$ be a general element in the Weyl Heisenberg group.⁴ Then the displacement operator is

$$D_{ij} = \tau^{ij} X^i Z^j = \tau^{ij+2sj} \delta_{r,s+i} \tag{2.14}$$

where $i, j, r, s \in \mathbb{Z}_N$

We note that

$$D_{ij}^\dagger = D_{-i-j} \tag{2.15}$$

This gives us a nice way of writing a general element in the Weyl-Heisenberg group, where the indices of D in a way labels the elements by their order in X and Z , e.g.

$$D_{01} = Z \tag{2.16}$$

$$D_{10} = X \tag{2.17}$$

Taking the product of two general elements in the Weyl Heisenberg group we find

$$D_{kl} D_{kj} = \omega^{kj-il} D_{kj} D_{kl} \tag{2.18}$$

We assert that $kj - il$ comes from an anti symmetric quadratic form, Ω , on a discrete phase space, W . This is realised by introducing the matrix

$$\Omega = \begin{pmatrix} 0 & -1 \\ 1 & 0 \end{pmatrix} \tag{2.19}$$

and the vectors

$$\mathbf{p} = \begin{pmatrix} i \\ j \end{pmatrix} \quad \mathbf{q} = \begin{pmatrix} k \\ l \end{pmatrix} \tag{2.20}$$

Then

$$\Omega(\mathbf{p}, \mathbf{q}) = p^i q^j \Omega_{ij} = kj - il \tag{2.21}$$

⁴The attentive reader will realise that $\tau = -e^{\frac{i\pi}{N}} = -\sqrt{\omega}$. We introduce τ because the displacement operators do not make sense in even dimensions without this notion. Even though we shall mostly concern ourselves with prime dimensions in this thesis we introduce this formalism for completion.

hence, Ω_{ab} is a quadratic form. Furthermore, it is a quadratic form on a discrete space since the vectors \mathbf{p}_1 and \mathbf{p}_2 are defined for integer i, j, k, l . Also we note that it is anti-symmetric

$$\Omega(\mathbf{p}, \mathbf{q}) = -\Omega(\mathbf{q}, \mathbf{p}) \quad (2.22)$$

Having identified the indices of equation 2.18 with the vectors 2.20 we reformulate the displacement operators in accordance with current conventions [6]

$$D_{\mathbf{p}}D_{\mathbf{q}} = \omega^{\Omega(\mathbf{q}, \mathbf{p})} D_{\mathbf{q}}D_{\mathbf{p}} \quad (2.23)$$

One should be restrained towards introducing new notation without good reason. But it shall soon be clear why this is a superior notation.

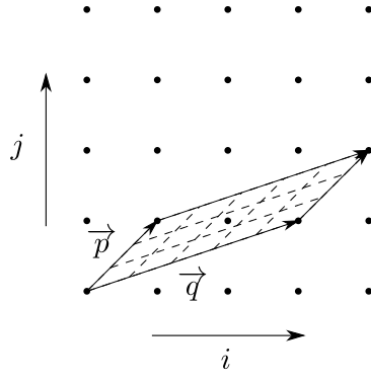


Figure 2.1: The quadratic form on the discrete phase space spanned by i and j .

There is a real analogue of equation 2.21 such that

$$\mathbf{x} = \begin{pmatrix} x_1 \\ x_2 \end{pmatrix} \quad \mathbf{y} = \begin{pmatrix} y_1 \\ y_2 \end{pmatrix} \quad x_i, y_i \in \mathbb{R} \quad (2.24)$$

$$\Omega(\mathbf{x}, \mathbf{y}) = x^i \Omega_{ij} y^j = x_2 y_1 - x_1 y_2 \quad (2.25)$$

This is the (oriented) area in a \mathbb{R}^2 -plane spanned by the vectors \mathbf{x} and \mathbf{y} . In just the same way, equation 2.21 is really the *area* spanned by the vectors \mathbf{p} and \mathbf{q} as shown in Figure 2.1.

Before we can proceed from this point we need to define two additional abstract algebraic constructions.

Define a subgroup as

Definition 11. *Subgroup*

Let (G, \star) be a group. Then H is said to be a subgroup of G if and only if

I H is closed under \star .

II The identity element, e , of G is also in H .

III Every element in H has an inverse in H .

Now define the normaliser of a group to be

Definition 12. *Normaliser*

Let G be a group and let S be a subset of group elements. The normaliser of S with respect to G is again a set of group elements such that

$$N_G(S) = \{g \in G \mid gSg^{-1} = S\} \quad (2.26)$$

If S is chosen such that it is a subgroup of G then the normaliser is also a subgroup of G containing S , in symbols $S \subseteq N_G(S) \subseteq G$.

Now define the Clifford group as the normaliser of the Weyl-Heisenberg group within the group of unitary matrices

Definition 13. *The Clifford Group*

Let U be the group of unitary matrices under matrix multiplication and call the group elements U and let G_{WH} be the Weyl-Heisenberg group. Then the Clifford group is the normaliser of G_{WH} with respect to U

$$G_C = \{U \in U \mid U^\dagger G_{WH} U = G_{WH}\} \quad (2.27)$$

From here on we shall apply the convention that whenever we write U we mean an element in the Clifford group rather than any unitary matrix.

Since we have chosen a unitary representation of the Weyl-Heisenberg group it is a subgroup of U . It follows from the definition of the normaliser and the subgroup that the Weyl-Heisenberg group is also a subgroup of the Clifford group.

Regard the following outer automorphism of an arbitrary element in the Weyl-Heisenberg group

$$U^\dagger D_{\mathbf{p}} U = D_{\mathbf{p}'} \quad (2.28)$$

The product of two general elements in the Weyl-Heisenberg group can be written

$$D_{\mathbf{p}} D_{\mathbf{q}} = \omega^{\Omega(\mathbf{q}, \mathbf{p})} D_{\mathbf{q}} D_{\mathbf{p}} \quad (2.29)$$

By means of 2.28 we can write the left hand side as

$$U D_{\mathbf{p}} D_{\mathbf{q}} U^\dagger = U^\dagger D_{\mathbf{p}} U U^\dagger D_{\mathbf{q}} U = D_{\mathbf{p}'} D_{\mathbf{q}'} \quad (2.30)$$

whereas the right hand side can be written

$$U \omega^{\Omega(\mathbf{q}, \mathbf{p})} D_{\mathbf{q}} D_{\mathbf{p}} U^\dagger = \omega^{\Omega(\mathbf{q}, \mathbf{p})} U D_{\mathbf{q}} D_{\mathbf{p}} U^\dagger = \omega^{\Omega(\mathbf{q}, \mathbf{p})} D_{\mathbf{q}'} D_{\mathbf{p}'} \quad (2.31)$$

thus,

$$D_{\mathbf{p}'} D_{\mathbf{q}'} = \omega^{\Omega(\mathbf{q}, \mathbf{p})} D_{\mathbf{q}'} D_{\mathbf{p}'} \quad (2.32)$$

It is also trivially true from equation 2.29 that

$$D_{\mathbf{p}'} D_{\mathbf{q}'} = \omega^{\Omega(\mathbf{q}', \mathbf{p}')} D_{\mathbf{q}'} D_{\mathbf{p}'} \quad (2.33)$$

why it had better be true that

$$\Omega(\mathbf{q}, \mathbf{p}) = \Omega(\mathbf{q}', \mathbf{p}') \quad (2.34)$$

let's assume that the transformation $\mathbf{p} \mapsto \mathbf{p}'$ is linear and that it is mediated by

$$\begin{pmatrix} p'_1 \\ p'_2 \end{pmatrix} = \underbrace{\begin{pmatrix} \alpha & \beta \\ \gamma & \delta \end{pmatrix}}_{=G_k^j} \begin{pmatrix} p_1 \\ p_2 \end{pmatrix} \quad (2.35)$$

where G is an arbitrary element in the group of general linear 2×2 matrices modulo N , $GL(2, \mathbb{Z}_N)$. This is plausible and can be proved [6]. We require that $\Omega(\mathbf{q}, \mathbf{p})$ is invariant under $GL(2, \mathbb{Z}_N)$, hence

$$G_i^k G_j^l \Omega_{kl} = \Omega_{ij} \quad (2.36)$$

If we solve this equation we find that G is subject to

$$\alpha\delta - \beta\gamma = 1 \quad (2.37)$$

or equivalently that G has unit determinant. This constraint further restricts G to the special linear group of 2×2 matrices $SL(2, \mathbb{Z}_N)$ which incidentally is isomorphic to the symplectic group $SP(2, \mathbb{Z}_N)$ for 2×2 matrices.

We introduce the following unitary representation of the special linear group [6],

Definition 14. *Unitary representation of $SL(2, \mathbb{Z}_N)$*

$$\left(\mathcal{U}_{\begin{pmatrix} \alpha & \beta \\ \gamma & \delta \end{pmatrix}} \right)_{rs} = \frac{e^{i\theta}}{\sqrt{N}} \tau^{\frac{1}{\beta}(\delta r^2 - 2rs + \alpha s^2)} \quad (2.38)$$

where $\alpha, \beta, \gamma, \delta, r, s \in \mathbb{Z}_N$, θ is a phase, $\alpha\delta - \beta\gamma = 1$ modulo N and β^{-1} is the inverse of β within \mathbb{Z}_N .

If β is non-invertible we need to tweak this equation somewhat. Using 2.38 it is straight forward to show that

$$\mathcal{U}_{\begin{pmatrix} \alpha & 0 \\ \gamma & \delta \end{pmatrix}} \equiv \mathcal{U}_{\begin{pmatrix} 0 & -1 \\ 1 & 0 \end{pmatrix}} \mathcal{U}_{\begin{pmatrix} \gamma & \delta \\ -\alpha & -\beta \end{pmatrix}} \quad (2.39)$$

Using this definition a unitary representation of any 2×2 matrix in equation 2.35 can be found.

Putting subsequent definitions together we find the following: A general transformation of p into p' is given by 2.35. This transformation is mediated by the group $SL(2, \mathbb{Z}_N)$. Furthermore there is a set of unitary matrices that take the displacement operator of p into the displacement operator of p' , equation 2.28. But the $SL(2, \mathbb{Z}_N)$ in 2.35 has a unitary representation by equation 2.38. It follows that the unitary operators in 2.28 are the unitary representation of the $SL(2, \mathbb{Z}_N)$ element in 2.35, hence these two equations are very much related and can even be seen as the same equation written in two different representations. If we recall the definition of a normaliser it follows from this argument that $SL(2, \mathbb{Z}_N)$ is a subgroup of the Clifford group.

An alternative definition of the Clifford group arises from this argument. We could equally well have defined the Clifford group (modulo phases) as the semi-direct product⁵ $SL(2, \mathbb{Z}_N) \rtimes G_{WH}$ [6].

2.2 Orbits under the Weyl-Heisenberg group

We shall start out this section by wrapping up some missing group theoretical definitions. However, in order to make powerful definitions we shall first indulge the concepts of equivalence relations and equivalence classes. These are two very general algebraic structures; a lot of fundamental concepts in mathematics can be understood within the context of equivalence relations and classes. Furthermore, we shall see that physical structure can also be realised within this framework.

Definition 15. *Equivalence Relations and Equivalence Classes*

Let \sim be a binary relation on a set X , we call \sim an equivalence relation if it satisfies

I Reflexivity

$$a \sim a \quad \forall a \in X \quad (2.40)$$

II Symmetry

$$a \sim b \iff b \sim a \quad \forall a, b \in X \quad (2.41)$$

III Transitivity

$$a \sim b \wedge b \sim c \implies a \sim c \quad \forall a, b, c \in X \quad (2.42)$$

We define an equivalence class of an element, a , as the set of elements such that

$$[a] = \{x \in X \mid a \sim x\} \quad (2.43)$$

A powerful consequence of the definition of an equivalence class is that

$$x \sim y \iff [x] = [y] \quad (2.44)$$

thus any two equivalence classes are either disjoint or equal, consequently the set of equivalence classes form a partition⁶ of X .

We will now introduce the quotient group and as a prerequisite to that the cosets of a group. These might seem remote abstract concept at first glance, but we shall shortly relate them to what we did in last section.

Definition 16. *Coset*

⁵We will not bother to give a formal definition of the semi-direct product as it relies on several group theoretical definitions which we have not introduced. Also one ought to be careful not to digress for too long amongst the beautiful subject of group theory lest one intends to stay. Think of the semi-direct product as the composition rule $(a_1, b_1) \rtimes (a_2, b_2) = (a_1 a_2, b_1 + a_1 b_2)$.

⁶A division of a set into non overlapping subsets such that every element in the set is found in one and only one subset.

Let H be a subgroup of G and let \sim be the equivalence relation such that $g_i \sim g_j$ if and only if $g_i h = g_j$ for some $h \in H$, then the left coset of H is the equivalence classes under \sim , in symbols⁷

$$g_i H = \{g_j \in G \mid g_i \sim g_j\} \quad (2.45)$$

We could of course, analogously, have defined the right coset. Finally we define the quotient group as follows

Definition 17. *Quotient Group*

Let N be a normal subgroup⁸ of G . The quotient group, G/N is the set of left (or right) cosets of N , written

$$G/N = \{S \in G \mid S = gN, g \in G\} \quad (2.46)$$

with the binary operation

$$(g_i N)(g_j N) = (g_i g_j)N \quad (2.47)$$

We now return to the statement that \mathbf{p} and \mathbf{q} are vectors in a discrete phase space, Figure 2.1. Recall that the coordinates of a point in this plane can be written as the components of a vector pointing at that point. Furthermore, recall that these components are the indices of the displacement operators which in turn corresponds to different elements in the Weyl-Heisenberg group. Doing this identification each point in the discrete phase space corresponds to an element in the Weyl-Heisenberg group. However only elements on the form $X^i Z^j$ are being indexed in this way. To describe this properly we introduce the centraliser of a group

Definition 18. *Centraliser*

Let H be a subgroup of G then the centraliser of H is the set of elements in G that commute with every element in H ,

$$C(H) = \{x \in G \mid xh = hx \forall h \in H\} \quad (2.48)$$

Note that we can likewise define the centraliser of an element by trading H for h .

The elements of the form $X^i Z^j$ indeed forms a group, it forms the quotient group of the Weyl-Heisenberg group and the centraliser of the Weyl-Heisenberg group within the group of unitary matrices, $G_{WH}/C(G_{WH})$. This is the Weyl-Heisenberg group modulo phases; which serves us just fine since we are ultimately interested in applying this framework to physical systems where we regard a state and a state with an attached phase to be equivalent, cf. equation 1.20. Note however, that this is not a subgroup of the Weyl-Heisenberg group since $X^i Z^j X^k Z^l = \omega X^{i+k} Z^{j+l}$, which is not in this quotient group. Actually, for the remainder of the thesis, whenever we refer to the Weyl-Heisenberg group it will be this group we refer to rather than the Weyl-Heisenberg group with phases. This group is sometimes called the collineation group⁹.

In terms of equivalence classes we define the orbit to be

⁷Usually the left coset is defined as $xH = \{xh \mid h \in H\}$ but it is nice to think of the cosets as equivalence classes, so we make this slightly more unorthodox definition. For one part, with this definition it is obvious that the set of cosets is a partition of G . Both definitions are in every practical sense equivalent.

⁸A normal subgroup is a subgroup with the additional criteria that $xHx^{-1} = H \forall x \in G$. For a normal subgroup the right and left cosets coincide.

⁹The collineation group is the set of all transformations which conserves the collineation of points.

Definition 19. *Orbit*

Let g and h be elements in some group G , and let X be some set. Let \sim be the equivalence relation such that $g \sim h$ if and only if there exists an x in X such that $x \star g = h$, in symbols

$$g \sim h \iff \exists x \in X \mid x \star g = h \tag{2.49}$$

We define the orbits as the equivalence classes under this equivalence relation. In symbols,

$$[g] = \{h \in G \mid g \sim h\} \tag{2.50}$$

The set of orbits forms a partition of G .

Notice that this definition allows for orbits within a group under different sets. We shall mostly look at orbits under $SL(2, \mathbb{Z}_N)$ within the Weyl-Heisenberg group. In this case the orbits are given by consecutively applying the following operation until the original element is returned

$$\mathcal{U}_{\begin{pmatrix} \alpha & \beta \\ \gamma & \delta \end{pmatrix}} D_{\begin{pmatrix} i \\ j \end{pmatrix}} \mathcal{U}_{\begin{pmatrix} \alpha & \beta \\ \gamma & \delta \end{pmatrix}}^\dagger = D_{\begin{pmatrix} i\alpha + j\beta \\ i\gamma + j\delta \end{pmatrix}} \iff \begin{pmatrix} \alpha & \beta \\ \gamma & \delta \end{pmatrix} \begin{pmatrix} i \\ j \end{pmatrix} = \begin{pmatrix} i\alpha + j\beta \\ i\gamma + j\delta \end{pmatrix} \tag{2.51}$$

This explains how equation 2.28 from previous section works.

The set of elements in the Weyl-Heisenberg group that can be generated by consecutively acting on some element with an element in $SL(2, \mathbb{Z}_n)$ forms an orbit under that element. The size of the orbit will be the same as the order of the matrix chosen. Also it follows from the definition of an orbit that all elements in the Weyl-Heisenberg group will be in some (but only one!) orbit. E.g. if we choose the order five matrix $\begin{pmatrix} 2 & 1 \\ -1 & 0 \end{pmatrix}$ we calculate an orbit as presented in equation 2.52 and illustrated in Figure 2.2

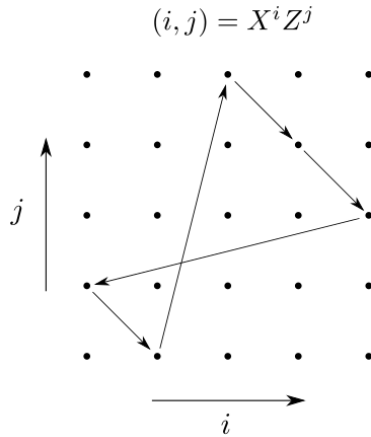


Figure 2.2: An orbit in the Weyl-Heisenberg group under an element in $SL(2, \mathbb{Z}_N)$

$$\begin{aligned}
\begin{pmatrix} 2 & 1 \\ -1 & 0 \end{pmatrix} \begin{pmatrix} 1 \\ 0 \end{pmatrix} &= \begin{pmatrix} 2 \\ -1 \end{pmatrix} = \begin{pmatrix} 2 \\ 4 \end{pmatrix} \\
\begin{pmatrix} 2 & 1 \\ -1 & 0 \end{pmatrix} \begin{pmatrix} 2 \\ 4 \end{pmatrix} &= \begin{pmatrix} 8 \\ -2 \end{pmatrix} = \begin{pmatrix} 3 \\ 3 \end{pmatrix} \\
&\dots \\
\begin{pmatrix} 2 & 1 \\ -1 & 0 \end{pmatrix} \begin{pmatrix} 0 \\ 1 \end{pmatrix} &= \begin{pmatrix} 1 \\ 0 \end{pmatrix}
\end{aligned} \tag{2.52}$$

Another useful partition of the Weyl-Heisenberg group is the decomposition of the group into cyclic subgroups¹⁰ generated by powers of the elements in the group. Since the Weyl-Heisenberg group is taken modulo N , we are sure to obtain cyclic subgroups as

$$\begin{aligned}
\begin{pmatrix} i \\ j \end{pmatrix} \begin{pmatrix} i \\ j \end{pmatrix} &= \begin{pmatrix} 2i \\ 2j \end{pmatrix} \\
\begin{pmatrix} i \\ j \end{pmatrix} \begin{pmatrix} 2i \\ 2j \end{pmatrix} &= \begin{pmatrix} 3i \\ 3j \end{pmatrix} \\
&\dots
\end{aligned} \tag{2.53}$$

where $\begin{pmatrix} i \\ j \end{pmatrix}$ corresponds to the element $X^i Z^j$ in the Weyl-Heisenberg group.

This concludes the group theoretical background needed for this thesis.

2.3 A note on calculating MUBs

Having introduced all group theory necessary for this thesis, we shall at once put it to good use in discussing how to explicitly calculate the MUBs introduced in Chapter 1. MUBs are in themselves an intriguing subject of great importance for e.g. quantum computing [18] (though in quantum computing they are commonly recognised as stabiliser states) and there are several ways available for calculating them. We will here present two ways; the standard way, which one ought to know as a reference, and an elegant way [13].

The standard way of calculating the MUBs is to find the eigenbases of the elements of the Weyl-Heisenberg group. There are N^2 elements in the Weyl-Heisenberg group but only $N + 1$ MUBs. Excluding the identity matrix given by $X^0 Z^0$ we are left with $N^2 - 1$ elements – calculating the eigenbases of these we find that the group elements arrange themselves into $N + 1$ cyclic groups with $N - 1$ elements, where all elements in the same cyclic groups generate the same eigenbasis (MUB). These cyclic groups are exactly the once introduced in the end of last section, generated by equation 2.53. Hence we only need to calculate the eigenbase of one element from each cyclic subgroup in order to obtain all the MUBs. The grouping is illustrated in Figure 2.3 for $N = 5$.

Be aware that there is some ambiguity going on here. When calculating the eigenbases—or rather when calculating the eigenvectors to form the eigenbases, the ordering of the eigenvectors depend on the ordering with which we index our eigenvalues. This will not be a problem though;

¹⁰A cyclic group is a group where all elements can be generated by successively taking powers of any one element. All cyclic groups are abelian, which is what a group where all elements commute is called in honour of the Norwegian mathematician Niels Abel.

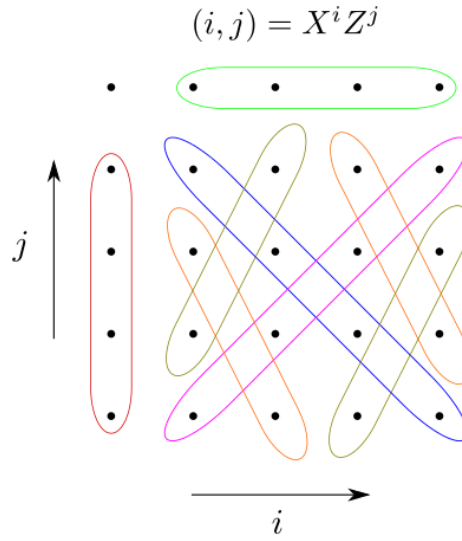


Figure 2.3: Illustrating which elements $X^i Z^j$ that corresponds to the same *MUB* when calculating the eigenbases.

since all MUBs are, per definition, bases, the specific order of the basis vectors is irrelevant. Each time we use the MUBs in a calculation we will sum over all the basis vectors.

The elegant way of calculating the MUBs is to find an $SL(2, \mathbb{Z}_N)$ element of order N under which the MUBs form an orbit and adding the computational basis (the standard base) to these. Apart from the computational basis, the so called Fourier basis is the MUB that is most easily calculated. It is written, by equation 2.38, as

$$\mathcal{U}_F = \mathcal{U} \begin{pmatrix} 0 & 1 \\ -1 & 0 \end{pmatrix} = \frac{1}{\sqrt{N}} \omega^{ij} \delta_{ij} \quad (2.54)$$

The element that we use to cycle through the MUBs is the following [13]

$$\mathcal{U}_S = \mathcal{U} \begin{pmatrix} 1 & 0 \\ 0 & 1 \end{pmatrix} = \frac{1}{\sqrt{N}} \omega^{\frac{i^2}{2}} \delta_{ij} \quad (2.55)$$

Acting with \mathcal{U}_S $N - 1$ times on \mathcal{U}_F we obtain all the MUBs.

Chapter 3

Getting to Know the SIC-POVM

In this last background chapter we will define the SIC and survey the task ahead of trying to find SICs. We will start out by defining the SIC and tie it to concepts introduced in previous chapters. Next we will introduce a brute force, but exhaustive, way of searching for SICs. Finally we will state the main conjectures on SICs as of today, which will guide us on our quest to find SICs. We shall also prove a theorem of paramount importance for the later parts of this thesis concerning SICs and MUSs.

Parts of this chapter might seem abstract at first glance to a physicist, but there are good physics to be found within the framework of SICs and while it requires us to think in terms of groups, the rewards of linking abstract algebra to physics are great.

3.1 Mathematical definition

Preceding chapters have been dedicated to formulating the physical and mathematical framework necessary to study the SIC-problem to some extent. Now we may finally formulate the definition of the SIC [19]; the protagonist of this thesis

Definition 20. *Symmetric Informationally Complete Positive Operator Valued Measure (SIC-POVM)*

Let $\{\psi\}$ be a set of N -dimensional unit vectors, we say that $\{\psi\}$ constitutes a Symmetric Informationally Complete Positive Operator Valued Measure (SIC-POVM; commonly just SIC) if, for any two vectors ψ_μ and ψ_ν in $\{\psi\}$

$$\sum_{\mu=0}^{N^2-1} \frac{1}{N} |\psi_\mu\rangle\langle\psi_\mu| = \mathbb{1} \quad (3.1)$$

and

$$|\langle\psi_\nu|\psi_\mu\rangle|^2 = \begin{cases} 1 & \text{if } \nu = \mu \\ \frac{1}{N+1} & \text{if } \nu \neq \mu \end{cases} \quad (3.2)$$

Take heed that while the formulation of a SIC is deviously simple, the SIC-problem has eluded physicists and mathematicians since the early 90's. This is indeed both the charm and

the nuisance of the SIC-problem!

Equation 3.1 in the SIC-POVM definition corresponds to the POVM part. We verify this for self-consistency

I *Completeness*

This follows directly from equation 3.1 by setting $E_k = |\psi_\mu\rangle\langle\psi_\mu|$.

II *Hermiticity*

$\rho = |\psi_\mu\rangle\langle\psi_\mu|$ is a density matrix, as such it is Hermitian by definition.

III *Non negative real eigenvalues*

Being a density matrix this requirement is also met by construction.

We have scaled the left hand side of equation 3.1 with a factor $\frac{1}{N}$ in order to ensure that it sums to identity. This is realised by taking the trace of both sides and noting that since $|\psi_\mu\rangle\langle\psi_\mu|$ is a density matrix, it has unit trace.

Likewise equation 3.2 in the definition corresponds to the SIC part. Symmetric means that the inner products are all the same, whereas informationally complete means that making measurements in all the basis vectors completely determines the density matrix. The symmetry part follows directly from the equation 3.2. As for the informational completeness there are $N^2 - 1$ elements in a density matrix and there are a total of N^2 inner products. Acknowledging that the probabilities of these inner products sum to unity, we are left with $N^2 - 1$ parameters, which are just as many we need to determine the density matrix.

As of today, every SIC found except one¹ is formed as the complete set of orbits under the Weyl-Heisenberg group of any one vector in that SIC [6][30]. That is to say, given any vector in a SIC, $|\psi_0\rangle$, the full SIC is found by consecutively acting with all elements of the Weyl-Heisenberg group on this vector, $D_{ij}|\psi_0\rangle$. We call such a vector a SIC-fiducial vector. There are no proof ensuring that we can always find a SIC in any finite dimension, but numerical searches strongly suggests so [30].

We therefore formulate the following conjecture

Conjecture 1. *Fiducial Vector Existence*

In every dimension there exists at least one vector $|\psi_0\rangle$ such that $\{D_{ij}|\psi_0\rangle\}$ forms a SIC.

Take notice that there may be – and are usually – more than one SIC in any given dimension. Thus we need to straighten out our terminology. While it is true that any vector in a SIC generate the other vectors as orbits under the Weyl-Heisenberg group we shall see that when we search for SICs we will always (except in two dimensions) find one and only one vector from each SIC. Hence we reserve the term 'SIC-fiducial vector' (from here on only 'fiducial vector') for the vectors associated with different SICs.

¹In $N = 8$ there is a SIC formed as the group $G_{WH}(2) \times G_{WH}(2) \times G_{WH}(2)$ which is slightly different from the ordinary $G_{WH}(8)$ [25]

3.2 The SICness function

The remainder of this text will be about finding SICs in one way or an other. Conjecture 1 strongly suggests that a good way of finding SICs is to search for fiducial vectors, why we introduce the following function [10][11]

Definition 21. *The SICness function*

Let $|\psi\rangle$ be any normalised vector and let $|\psi_{ij}\rangle = D_{ij}|\psi\rangle$, then we define the SICness function as

$$f_{SIC}(|\psi\rangle) = \frac{1}{2} \sum_{i=0}^{N-1} \sum_{j=0}^{N-1} \left(|\langle\psi|\psi_{ij}\rangle|^2 - \frac{1}{1+N} \right)^2 \quad (3.3)$$

where we require that $(i, j) \neq (0, 0)$.

Spelled out this is a function which is zero if and only if $|\psi\rangle$ is a vector that forms a SIC under orbits in the Weyl-Heisenberg group; i.e. a fiducial vector $|\psi_0\rangle$. Conjecture 1 states that there exists such a vector in every dimension. Hence we may use equation 3.3 to search for fiducial vectors and we name it appropriately as the SICness function since it quantifies how much of a SIC fiducial vector any given state is.

It is possible to rewrite 3.3 in a more computation friendly way by introducing the frame potential [10][11]

$$F_t = \sum_{I=1}^K \sum_{J=1}^K |\langle\psi_I|\psi_J\rangle|^{2t} \quad (3.4)$$

Relabelling the indices of equation 3.3

$$\begin{aligned} f_{SIC} &= \frac{1}{2} \sum_{\substack{I=0 \\ J=0 \\ I \neq J}}^{N^2-1} \left(|\langle\psi_I|\psi_J\rangle|^2 - \frac{1}{N+1} \right)^2 \\ &= \frac{1}{2} \sum_{\substack{I=0 \\ J=0}}^{N^2-1} \left(|\langle\psi_I|\psi_J\rangle|^2 - \frac{1}{N+1} \right)^2 - \frac{1}{2} \sum_{I=J}^{N^2-1} \left(\underbrace{|\langle\psi_I|\psi_J\rangle|^2}_{=1} - \frac{1}{N+1} \right)^2 \\ &= \frac{1}{2} \sum_{\substack{I=0 \\ J=0}}^{N^2-1} |\langle\psi_I|\psi_J\rangle|^4 - \frac{1}{N+1} \sum_{\substack{I=0 \\ J=0}}^{N^2-1} |\langle\psi_I|\psi_J\rangle|^2 + \frac{N^4}{2(N+1)^2} - \frac{N^4}{2(N+1)^2} \\ &= \frac{1}{2} \sum_{\substack{I=0 \\ J=0}}^{N^2-1} |\langle\psi_I|\psi_J\rangle|^4 - \frac{1}{N+1} \sum_{\substack{I=0 \\ J=0}}^{N^2-1} |\langle\psi_I|\psi_J\rangle|^2 \\ &= \frac{1}{2} F_2 - \frac{1}{N+1} F_1 \end{aligned} \quad (3.5)$$

Here we have played the trick of trading $\sum_{ij} |\langle\psi|\psi_{ij}\rangle|^2$ for $\sum_{ij} |\langle\psi_i|\psi_j\rangle|^2$. Be aware that we are well within our rights to do so since we can always find some D_{ij} such that

$$\sum_{ij} |\langle \psi_i | \psi_j \rangle|^2 = \sum_{ij} |\langle D_{kl} D_i D_{kl}^\dagger \psi_i | D_{kl} D_j D_{kl}^\dagger \psi_j \rangle|^2 = \sum_{ij} |\langle \psi | \psi_{ij} \rangle|^2 \quad (3.6)$$

It is required by the definition of a SIC that $|\psi_I\rangle$ is a unit vector. We let

$$\sum_{I=1}^K |\psi_I\rangle \langle \psi_I| = \frac{K}{N} \mathbf{1} \quad (3.7)$$

be an equally weighted POVM. Taking the trace of the left hand side we find

$$\text{Tr} \sum_{I=1}^K |\psi_I\rangle \langle \psi_I| = \sum_{I=1}^K \text{Tr} |\psi_I\rangle \langle \psi_I| = \sum_{I=1}^K |\langle \psi_I | \psi_I \rangle| = \sum_{I=1}^K 1 = K \quad (3.8)$$

the second equality is true because we have restricted ourselves to unit vectors.

While for the right hand side

$$\text{Tr} \frac{K}{N} \mathbf{1} = K \quad (3.9)$$

Having concluded 3.8 and 3.9 we play the following trick; taking the trace of two such sums, we find that

$$\text{Tr} \sum_{I=1}^K |\psi_I\rangle \langle \psi_I| \sum_{J=1}^K |\psi_J\rangle \langle \psi_J| = \text{Tr} \frac{K}{N} \mathbf{1} \frac{K}{N} \mathbf{1} = \frac{K^2}{N} \quad (3.10)$$

But it is also true that

$$\text{Tr} \sum_{I=1}^K |\psi_I\rangle \langle \psi_I| \sum_{J=1}^K |\psi_J\rangle \langle \psi_J| = \sum_{I=1}^K \sum_{J=1}^K \text{Tr} |\psi_I\rangle \langle \psi_I | \psi_J \rangle \langle \psi_J| = \sum_{I=1}^K \sum_{J=1}^K |\langle \psi_I | \psi_J \rangle|^2 = F_1 \quad (3.11)$$

Finally, our POVM has N^2 elements thus

$$F_1 = N^3 \quad (3.12)$$

and we find

$$f_{SIC} = \frac{1}{2} F_2 - \frac{N^3}{N+1} \quad (3.13)$$

Written out

$$f(\psi) = \frac{1}{2} \sum_{i=0}^{N-1} \sum_{j=0}^{N-1} |\langle \psi | \psi_{ij} \rangle|^4 - \frac{N^3}{N+1} \quad (3.14)$$

Even though this expression is computationally more desirable than its original form 3.3 we will stick to the original form in the text since it is more intuitive to look upon.

Note that while the SICness function is minimised when all the inner products are $\frac{1}{\sqrt{N+1}}$ it is maximised when all inner products are equal to one. This happens exactly for the MUB-basis vectors [21]. This is realised by noting that the unitary representation of the Weyl-Heisenberg

d	1	$e^{i\frac{2\pi}{3}}$	$e^{i\frac{4\pi}{3}}$
$3m$	$m+1$	m	$m-1$
$3m+1$	$m+1$	m	m
$3m+2$	$m+1$	$m+1$	m

Table 3.1: The dimensions of the Zauner subspaces of any given dimension can be found using this table. E.g. $d = 5$ is on the form $3m + 2$ for $m = 1$ why 5-dimensional Hilbert space is split into two 2-dimensional and one 1-dimensional subspace.

group elements (equation 2.13) are monomials with roots of unity in some pattern. Taking the modulus inner product of a vector on the form $(1, 0, \dots, 0)$ and such matrices always result in one.

3.3 Zauner subspaces

All fiducial vectors found sit in very special (and small!) subspaces of Hilbert space [6][30]. This is not at all to be expected and it further adds to the mystery shrouding the SIC-problem. Specifically, all fiducial vectors sit in a subspace which is spanned by the eigenvectors of a unitary representation of an element in $SL(2, \mathbb{Z}_N)$ of order 3 and with negative unit trace. We call such a subspace a Zauner subspace and we call the unitary operator a Zauner operator [6][35], named after Gerhard Zauner who pioneered the study of SICs.

The Zauner operator always have the following eigenvalues $1, \omega^1, \omega^2$ where ω is the third root of unity [35]. Technically the Zauner operator splits Hilbert space into three subspaces, each with the same dimension as the degeneracy of the associated eigenvalue. These eigenspaces then form the Zauner subspaces. The dimensionality of the Zauner subspaces are given given in table 3.1

We conjecture that

Conjecture 2. Fiducial Vector Confinement

Every fiducial vector is an eigenvector of an order 3 element, U , in the Clifford group with $\text{Tr}U = -1$ and that is the unitary representation of an element in $SL(2, \mathbb{Z}_N)$. Additionally, in prime dimensions, all fiducial vectors sit in the largest of the subspaces generated by this operator.

Together Conjecture 1 and 2 make up Zauner's original conjecture from 1991 [35].

In a 2-dimensional space we can search exhaustively for fiducial vectors by choosing $|\psi\rangle$ according to

$$|\psi\rangle = \begin{pmatrix} \cos \frac{\theta}{2} |e_i\rangle \\ \sin \frac{\theta}{2} e^{i\phi} |e_j\rangle \end{pmatrix} \quad (3.15)$$

and calculate the SICness function for all θ and ϕ to some sufficient numerical precision. But this is precisely the parametrisation of the Bloch sphere. Hence, plotting the contours of the

SICness-function for this choice of $|\psi\rangle$ we can map the SIC-function onto the Bloch sphere. However, 3-dimensional objects – such as a sphere – are not very apt for printing on paper, therefore we do the mapping presented in Figure 3.1.

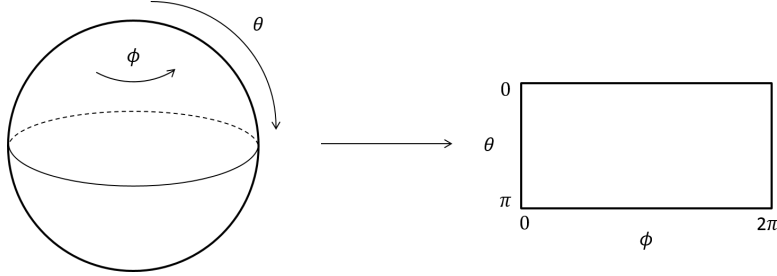


Figure 3.1: Schematic description of how the surface of \mathcal{S}^2 is transformed into a plane with the vertical sides topologically identified. Note that this transformation will distort the image, especially close to the poles.

At times we shall want to search for fiducial vectors in spaces of dimension larger than two, we shall then construct 2-dimensional subspaces from the basis vectors according to

$$|\psi\rangle = \frac{\cos\theta}{2}|e_i\rangle + \frac{\sin\theta}{2}e^{i\phi}|e_j\rangle \quad (3.16)$$

3.4 The MUS connection

In this section we shall prove a very important result for this thesis; we shall prove that all fiducial vectors are MUS. Note that the converse is not true—all MUS are not fiducial vectors! This is a known result, but it is of such decisive importance to this thesis that we shall formulate it as a theorem and provide a proof. The original proof can be found here [8].

Theorem 2. *SIC-MUS relation*

A state which is a SIC is also a MUS.

Proof.

Let $|\psi\rangle$ be a general state,

$$|\psi\rangle = \begin{pmatrix} z_0 \\ z_2 \\ \vdots \\ z_{N-1} \end{pmatrix} \quad (3.17)$$

with $z_a = \sqrt{p_a}e^{i\mu_a}$

We use the following matrix representation of an element in the Weyl-Heisenberg group

$$X^i Z^j = \omega^{bj} \delta_{a,b+i} \quad (3.18)$$

For a general $|\psi\rangle$ the following is true

$$\langle\psi|X^iZ^j|\psi\rangle = \sum_{a,b=0}^{N-1} z_a^* \omega^{bj} \delta_{a,b+i} z_b = \sum_{a=0}^{N-1} \omega^{(a-i)j} z_a^* z_{a-i} \quad (3.19)$$

and as usual with $(a, b) \neq (0, 0)$.

Thus,

$$|\langle\psi|X^iZ^j|\psi\rangle|^2 = \sum_{a,b=0}^{N-1} \omega^{(a-b)j} z_a^* z_{a-i} z_{b-i}^* z_b \quad (3.20)$$

Keep i fixed and take the discrete Fourier transform

$$\begin{aligned} \sum_{j=0}^{N-1} \omega^{kj} |\langle\psi|X^iZ^j|\psi\rangle|^2 &= \sum_{j,a,b=0}^{N-1} \omega^{(k+a-b)j} z_a^* z_{a-i} z_{b-i}^* z_b = \\ &= N \sum_{a,b=0}^{N-1} \delta_{b,k+a} z_a^* z_{a-i} z_{b-i}^* z_b = \\ &= N \sum_{a=0}^{N-1} z_a^* z_{a-i} z_{a+k-i}^* z_{a+k} \end{aligned} \quad (3.21)$$

Assume that $|\psi\rangle = |\psi_0\rangle$ which is a fiducial vector and set $i = 0$. This is all in order since all cyclic subgroups of the Weyl-Heisenberg group are all equivalent in this calculation.

$$\sum_{j=0}^{N-1} \omega^{kj} |\langle\psi_0|Z^j|\psi_0\rangle|^2 = N \sum_{a=0}^{N-1} p_a p_{a+k} \quad (3.22)$$

We are left with two cases, if $k=0$ the left hand side of equation 3.22 becomes

$$\sum_{j=0}^{N-1} |\langle\psi_0|Z^j|\psi_0\rangle|^2 = 1 + \frac{N-1}{N+1} = \frac{2N}{N+1} \quad (3.23)$$

and the right hand side becomes

$$N \sum_{a=0}^{N-1} p_a p_a \quad (3.24)$$

such that

$$\sum_{a=0}^{N-1} p_a^2 = \frac{2}{N+1} \quad (3.25)$$

If $k \neq 0$, the left hand side of equation 3.22 becomes,

$$|\langle\psi|\psi\rangle|^2 + \sum_{j=0}^{N-2} \omega^{kj} |\langle\psi_0|Z^j|\psi_0\rangle|^2 = 1 + \frac{1}{N+1} \sum_{j=1}^{N-2} \omega^{kj} = 1 - \frac{1}{N+1} = \frac{N}{N+1} \quad (3.26)$$

such that

$$\sum_{a=0}^{N-1} p_a p_{a+k} = \frac{1}{N+1} \quad (3.27)$$

Notice that equations 3.25 and 3.27 together define a simplex with size corresponding to a MUS and with correct scalar products. Hence all SICs spans simplices and furthermore the fiducial vectors are MUSs.

This completes the proof. □

We shall conclude the background part of this thesis by taking a quick detour to do a curious remark about finding SICs. The problem of finding SICs can equivalently be reformulated as a geometrical optimisation problem rather than a numerical minimisation problem.

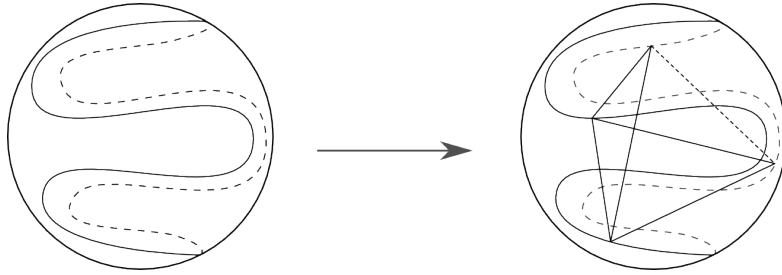


Figure 3.2: The submanifold of pure states.

We have already declared that all fiducial vectors are pure states, as such they sit in $\mathbb{C}\mathbb{P}^{N-1}$, we have also just shown that complete sets of fiducial vectors spans regular simplices. Recalling that $\mathbb{C}\mathbb{P}^{N-1}$ forms a submanifold on \mathcal{S}^{N^2-2} (equation 1.40) we can conclude that the simplices (SICs) must be inscribed in this sphere. This is known since the requirement that fiducial vectors are pure states places them *on the surface* of the sphere, and in order to have the correct inner products (equation 3.27) they must *span simplices in R^{N^2-1}* . Hence the SIC-existence problem may equally well be formulated as fitting regular simplices into a certain (known!) submanifold of a higher dimensional sphere. This is illustrated in Figure 3.2.

Part II

RESULTS

Chapter 4

SICs in Low Dimensions

For the remainder of the text we will either be presenting, or commenting on, our own results. It is our ambition that the reader shall be able to follow our line of reasoning after having understood the first part of this thesis.

The main goal of this chapter is to work out some intuition about the SICness function; equation 3.3. We shall go about this by dissecting the SICness function in the low dimensions 2, 3, 4 and 5. Like before we shall put some extra effort into dimension 2 as it is an excellent dimension to be thorough in due to its simplicity.

That said we encourage the reader to pay close attention to the attached plots as they most likely are more illuminating than trying to decipher the SICness function or the fiducial vectors by themselves. It will be evident that finding fiducial vectors is, even numerically, a formidable task already in low dimensions.

4.1 Two dimensions

As stated before, the 2-dimensional case is an extraordinary case in that we can actually view the *full* space since everything interesting collapses to a 2-sphere embedded in \mathbb{R}^3 (cf. section 1.3 “Mutually Unbiased Bases”). Hence we will investigate the 2-dimensional case a bit further in order to build some intuition.

In two dimensions we may write out $f_{SIC}(\psi)$ explicitly—this is not possible, or rather, not at all convenient, in dimensions higher than two since the number of terms in the SICness function increase very rapidly with increasing dimension. The SICness function is given by equation 3.3

$$f_{SIC}(\psi) = \frac{1}{96}(31 + 12 \cos 2\theta + 21 \cos 4\theta + 24 \cos 4\phi \sin^4 \theta) \quad (4.1)$$

The contour plot of $f_{SIC}(\psi)$ is given in Figure 4.1.

There is a lot to be learnt from this map and we shall dwell on it for a while to make some remarks. Firstly we note that there are eight minima (black dots). Probing the minima with *Mathematica* we find that they are actually zeroes of $f_{SIC}(\psi)$ and thus fiducial vectors. We know that these eight vectors constitute two SICs since the definition of a SIC requires that each SIC

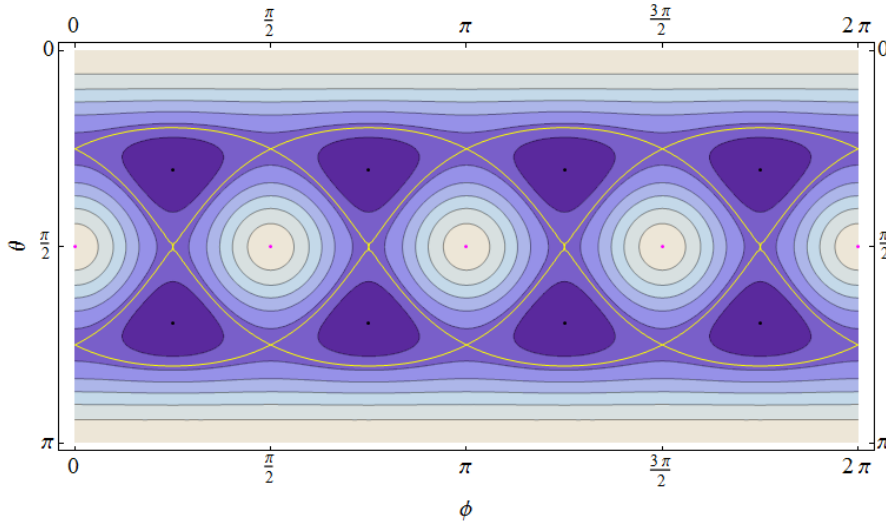


Figure 4.1: The map of $f_{SIC}(\psi)$ in two dimensions. Dark areas represent low function values whilst light ones represent high values. Minima are given as black dots and maxima as magenta dots. The yellow contour is the contour consisting of all saddle points for the function. On the ϕ -axis we have the azimuthal angle and on the θ -axis we have the polar angle

be made of $N^2 = 4$ vectors. Accounting for a total of eight zeroes.

As per our deliberations on the geometry of SICs from last chapter, we expect the vectors of the SICs to arrange themselves into regular polytopes. We note that the minima come with a period of $\frac{\pi}{2}$ in ψ for two separate θ , which is exactly what we would expect for two tetrahedra, and indeed, extracting the coordinates of the minima we recover the two tetrahedra, see Figure 4.2.

Another, slightly more technical, argument arriving at the same number of SICs stems from the fact that acting on a fiducial vector with an element in the Clifford group will again result in a fiducial vector – this is shown in the end of this chapter in lemma 1. In dimensions two through six all fiducial vectors line up nicely as an orbit under an order 3 element of the Clifford group [30]. Noting that the Clifford group has cardinality

$$|G_C| = \underbrace{|SL(2, \mathbb{Z}_2)|}_{24} \times \underbrace{|G_{WH}|}_{6} \times \underbrace{|G_{WH}|}_{4} \quad (4.2)$$

using the requirement of an order 3 element we find that the size of the orbit is $\frac{24}{3} = 8$. Since the SICs spans tetrahedra, we have $\frac{8}{4} = 2$ SICs in two dimensions. We emphasise, however, that this is not true in general.

We have also found six maxima¹ (magenta dots), these correspond to the six basis vectors of the three MUBs in two dimensions, cf. MUBs on the Bloch sphere, Figure 1.5, and note that the coordinates of the MUBs are identical. Given the existences of minima and maxima we anticipate some kind of distribution of saddle points. These lie exactly on the yellow contour in

¹Two maxima sit at the poles, in this crude projection these points are maximally distorted to lines.

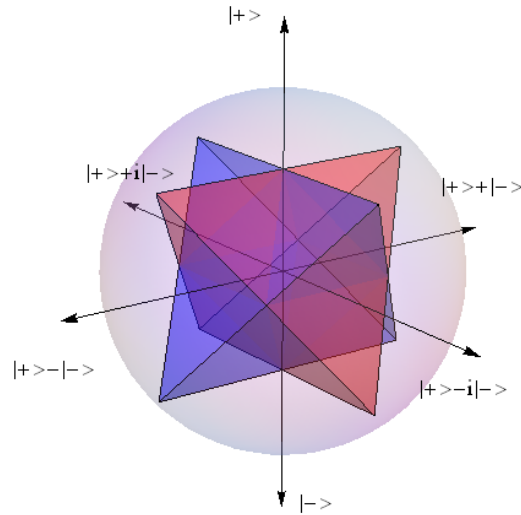


Figure 4.2: The SICs in the Bloch sphere.

the map conspicuously given by $f_{SIC}(\psi) = \frac{1}{6}$. It so happens that the Alltop MUB vectors² lie in the self intersections of this curve [4][13]. As a curious remark we note that this contour makes four great circles on the sphere.

The preceding results are summed up in table 4.1. For the sake of intuition we also include a snapshot of the function as seen on an actual sphere, Figure 4.3.

Lastly, one might inquire as to the total number of distinct inner products $|\langle \psi | \psi_{ij} \rangle|^2$ that occur in $f_{SIC}(\psi)$. In Figure 4.4 we give the contours $|\langle \psi | \psi_{ij} \rangle|^2 = \frac{1}{1+d}$ for the three distinct inner products on the background of $f_{SIC}(\psi)$. We know that they must all intersect at the minima. This is realised by noting that at these coordinates all three distinct inner products are zero, since these are the zeroes of the SICness function. Note that this is by no means a trivial statement. Picking three random one dimensional curves represented by three equations in two variables we would not expect a simultaneous solution to the given system of equation, and hence we would not expect them to intersect in the same point. This observation shall be important in the next chapter.

²Alltop MUBs are a different sets of MUBs that can be constructed. They are however not however within the scope of this thesis, and we shall not do more with them then note that they are present.

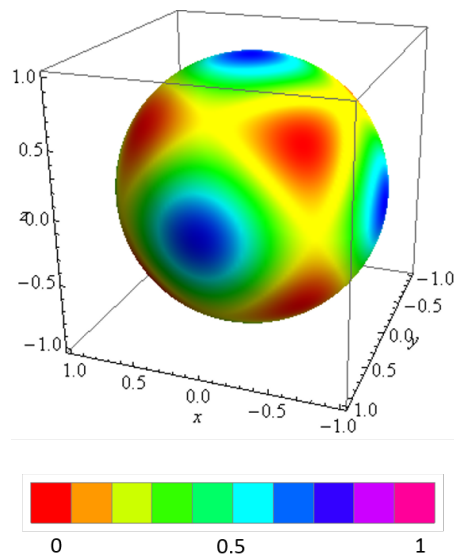


Figure 4.3: The map of $f_{SIC}(\psi)$ in two dimensions. The yellow lines are great circles made up of saddle points.

Minima		Maxima	
(ϕ, θ)	$f(\phi, \theta)$	(ϕ, θ)	$f(\phi, \theta)$
$(\frac{\pi}{4}, \frac{\pi}{4})$	0	$(0, \frac{\pi}{2})$	$\frac{2}{3}$
$(\frac{3\pi}{4}, \frac{\pi}{4})$	0	$(\frac{\pi}{2}, \frac{\pi}{2})$	$\frac{2}{3}$
$(\frac{5\pi}{4}, \frac{\pi}{4})$	0	$(\pi, \frac{\pi}{2})$	$\frac{2}{3}$
$(\frac{7\pi}{4}, \frac{\pi}{4})$	0	$(\frac{3\pi}{2}, \frac{\pi}{2})$	$\frac{2}{3}$
$(\frac{\pi}{4}, \frac{3\pi}{4})$	0	$(-, 0)$	$\frac{2}{3}$
$(\frac{3\pi}{4}, \frac{3\pi}{4})$	0	$(-, \pi)$	$\frac{2}{3}$
$(\frac{5\pi}{4}, \frac{3\pi}{4})$	0		
$(\frac{7\pi}{4}, \frac{3\pi}{4})$	0		

Table 4.1: Extrema for $f(\phi, \theta)$ in two dimensions

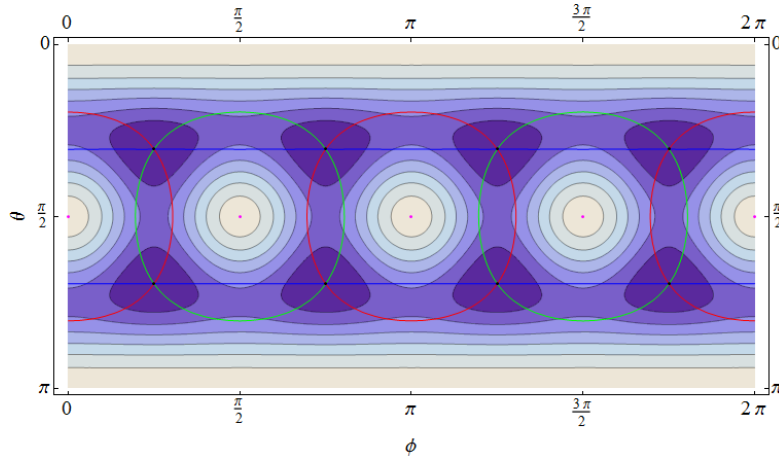


Figure 4.4: In two dimensions $f_{SIC}(\psi)$ has three distinct inner products. For each of these we give the contour $|\langle \psi | \psi_{ij} \rangle|^2 = \frac{1}{1+d}$ on the background of the SICness function.

4.2 Three dimensions

As per our discussion about the space of pure states, $\mathbb{C}\mathbb{P}^{N-1}$, in Chapter 1, it is now no longer possible to plot the whole space due to the dimensionality. Rather, we shall have to be content with looking at subspaces spanning Bloch spheres. This is achieved according to the decomposition presented in Chapter 3, equation 3.16. In the Zauner case we have conjectured that all SIC fiducial vectors sit in the largest Zauner subspace. If this subspace is 2-dimensional we may use the basis vectors to form a Bloch sphere using the same trick as before. This only works for dimensions three through five though, after dimension five the largest Zauner subspace is of dimension three or greater.

In three dimensions the level curves of the SICness function in all the subspaces of \mathbb{C}^3 and the Zauner subspace are almost the same, hence we will only study the Zauner subspace and merely make a note on the difference to the picture in \mathbb{C}^3 . In three dimensions we find the following basis vectors to the Zauner subspace [35]

$$\psi_1 = \frac{1}{\sqrt{6}} \begin{pmatrix} 2 \\ -\alpha^2 \\ -\alpha^2 \end{pmatrix} \quad \psi_2 = \frac{1}{\sqrt{2}} \begin{pmatrix} 0 \\ 1 \\ -1 \end{pmatrix} \quad (4.3)$$

Taking ψ to be a general vector in this subspace we find the contour plot of the SICness function to be as in Figure 4.5.

There are no isolated zeroes in this plot, rather there is a straight line of zeroes for $\theta = \frac{\pi}{2}$. The only difference in \mathbb{C}^3 is that this line is not zero, otherwise the plots are very much similar. Hence, we have a one parameter family of SICs in one dimension. This one parameter solution can be written [35]

$$\psi_x = \cos x \psi_1 + \alpha^2 \sin x \psi_2 \quad (4.4)$$

for $x \in \mathbb{R}$ [35]. Such that any vector, ψ_x , written on that form is a fiducial vector.

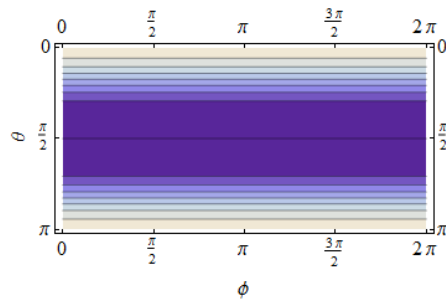


Figure 4.5: The map of $f_{SIC}(\psi)$ in three dimensions. The dark line in the middle is a line of zeroes.

Since there is a one parameter solution of SICs in this dimension we expect that there should only be one distinct inner product of the form $|\langle \psi | \psi_{ij} \rangle|^2 = \frac{1}{1+d}$. It is the sole inner product that makes up the line in the plot. Compare this situation to the one in two dimensions. In two dimensions we had several distinct inner products and we concluded that the fiducial vectors must lay in the intersection of these curves, this generated a set of distinct fiducial vectors. In three dimensions we only have one equation which generate a one dimensional family of SICs. Thus, we are left with a single distinct inner product which is given in Figure 4.6.

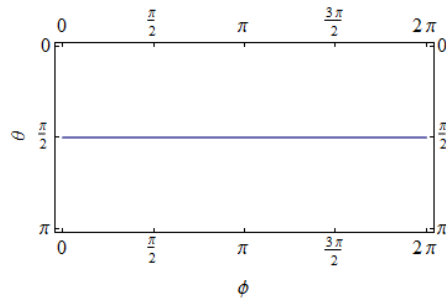


Figure 4.6: The single distinct inner product in three dimensions.

4.3 Four dimensions

4.3.1 The standard base

In four dimensions, we can construct six different subspaces spanned by the basis vectors of the standard base. In these we find two kinds of contour plots. The subspaces $\mathbf{e}_1 - \mathbf{e}_2$, $\mathbf{e}_1 - \mathbf{e}_4$, $\mathbf{e}_2 - \mathbf{e}_3$ and $\mathbf{e}_3 - \mathbf{e}_4$ generate a plot which is just like the one in \mathbb{C}^3 , so we omit this plot.

On the other hand, in the subspaces $\mathbf{e}_1 - \mathbf{e}_3$ and $\mathbf{e}_2 - \mathbf{e}_4$ the SICness function exhibits some more intriguing structure and is given in Figure 4.7.

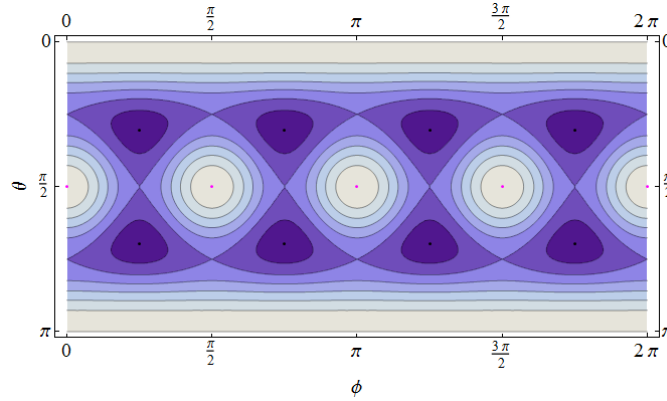


Figure 4.7: The map of $f_{SIC}(\psi)$ in the subspaces $\mathbf{e}_2 - \mathbf{e}_3$ and $\mathbf{e}_3 - \mathbf{e}_4$ in four dimensions. On the ϕ -axis we have the azimuthal angle and on the θ -axis we have the polar angle.

We observe that this plot is suspiciously like its 2-dimensional counterpart. The same distribution of extrema is evident and we can easily spot the same curve of saddle points. In fact, this map is just a scaled version of the map in two dimensions given by

$$f_{4D}(\psi) = 16/15 + 2f_{2D}(\psi) \quad (4.5)$$

There are three distinct inner products in the subspaces $\mathbf{e}_1 - \mathbf{e}_2$, $\mathbf{e}_1 - \mathbf{e}_4$, $\mathbf{e}_2 - \mathbf{e}_3$ and $\mathbf{e}_3 - \mathbf{e}_4$ while there are five distinct inner products in subspace $\mathbf{e}_1 - \mathbf{e}_3$ and $\mathbf{e}_2 - \mathbf{e}_4$. Accounting for a total of eight inner products. None of them are very interesting though since we have found no fiducial vectors in these subspaces. Most of the distinct inner products generate no plot at all, and the ones who do generate two straight lines equally separated from the equator.

4.3.2 The Zauner subspace

Guided by Conjecture 2 and table 3.1, we construct the basis vectors for the Zauner subspace by finding the eigenvectors corresponding to the degenerate eigenvalue 1 of a Zauner unitary. The following will suffice

$$\mathcal{U}_{\begin{pmatrix} -1 & -1 \\ 1 & 0 \end{pmatrix}} = \begin{pmatrix} \frac{1}{2}e^{i\frac{\pi}{4}} & -\frac{i}{2} & -\frac{1}{2}e^{i\frac{\pi}{4}} & -\frac{i}{2} \\ \frac{1}{2}e^{i\frac{\pi}{4}} & \frac{1}{2} & \frac{1}{2}e^{i\frac{\pi}{4}} & -\frac{1}{2} \\ \frac{1}{2}e^{i\frac{\pi}{4}} & \frac{i}{2} & -\frac{1}{2}e^{i\frac{\pi}{4}} & \frac{i}{2} \\ \frac{1}{2}e^{i\frac{\pi}{4}} & -\frac{1}{2} & \frac{1}{2}e^{i\frac{\pi}{4}} & \frac{1}{2} \end{pmatrix} \quad (4.6)$$

we find the basis vectors [35]

$$\psi_a = \frac{1}{\sqrt{6}} \begin{pmatrix} \rho + 1 \\ i \\ \rho - 1 \\ i \end{pmatrix} \quad \psi_b = \frac{1}{\sqrt{2}} \begin{pmatrix} 0 \\ 1 \\ 0 \\ -1 \end{pmatrix} \quad (4.7)$$

where $\rho = e^{\frac{i\pi}{4}}$.

The contour plot of $f_{SIC}(\psi)$ in the Zauner subspace is shown in 4.8.

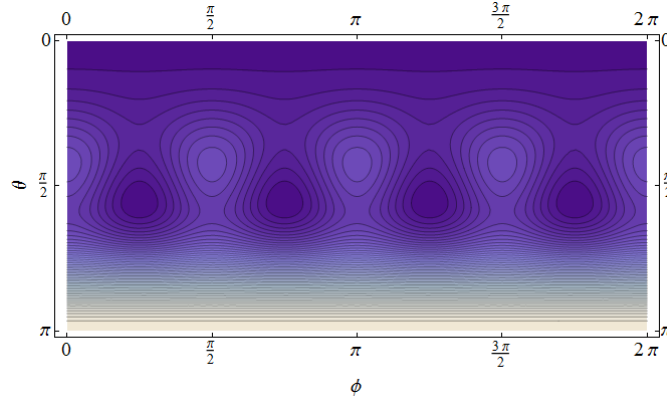


Figure 4.8: The map of $f_{SIC}(\psi)$ in the Zauner subspace of \mathbb{C}^4 .

As mentioned in the beginning of this chapter the complexity of the SICness function increases rapidly. In four dimensions we are starting to see the effects of this. The contour plot is looking less ordered than the one in two dimensions. We can make out four minima just below the equator and four maxima just above, however their θ -coordinate is no longer obvious. There also seems to be something going on with large respectively small values at the poles. The curve of saddle points is still present, though it does not have any self intersections. Probing the points of interest we find that the minima near the equator are zeroes to the SICness function and that the south pole is a global maximum. Hence we have found four fiducial vectors and consequently four SICs. The fiducial vectors are [35]:

$$\psi_k = X\psi_a + \rho^k Y\psi_b \quad (4.8)$$

for

$$X = \frac{1}{2} \sqrt{3 - \frac{3}{\sqrt{5}}} \quad Y = \frac{1}{2} \sqrt{1 + \frac{3}{\sqrt{5}}} \quad (4.9)$$

with $k = 1, 3, 5, 7$ and ρ as above.

Note that we cannot vouch for the fact that the south pole corresponds to a MUB vector, since this is just a global maxima in the *Zauner subspace*. Recall that in two dimensions we were actually looking at the full space, that is why we could determine that the global maxima were MUB vectors. We also observe that the SICness function has an overall periodicity of $\frac{\pi}{2}$.

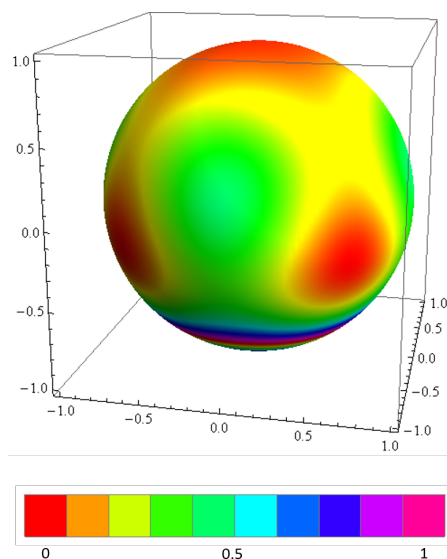


Figure 4.9: The map of $f_{SIC}(\psi)$ in the Zauner subspace of \mathbb{C}^4 plotted on the surface of a sphere.

We also include $f_{SIC}(\psi)$ as plotted on a sphere to remind ourselves that this is actually the case (Figure 4.9).

In the Zauner subspace we find three distinct inner products. These are shown on the background of the SICness function in 4.10. Note that all the contours of the distinct inner products converge at the minima, in agreement with our observations in dimension two.

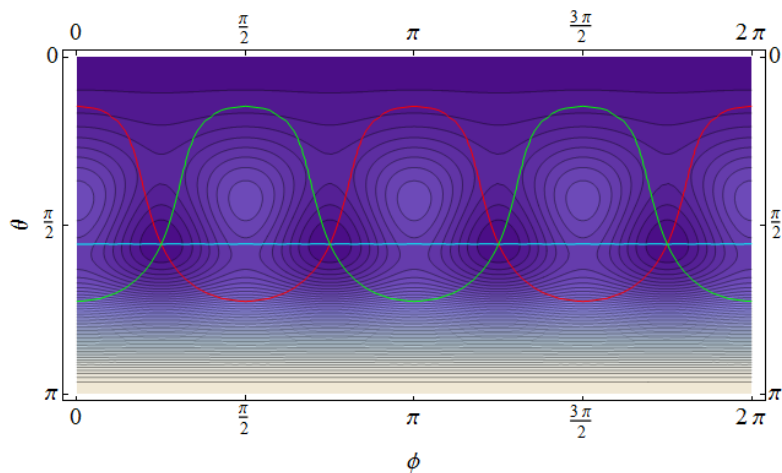


Figure 4.10: The distinct inner products of $f_{SIC}(\psi)$ in the Zauner subspace in four dimensions.

Minima		Maxima	
(ϕ, θ)	$f(\phi, \theta)$	(ϕ, θ)	$f(\phi, \theta)$
$(\frac{\pi}{4}, \sim 1.74)$	0	$(0, \sim 1.33)$	~ 0.40
$(\frac{3\pi}{4}, \sim 1.74)$	0	$(\frac{\pi}{2}, \sim 1.33)$	~ 0.40
$(\frac{5\pi}{4}, \sim 1.74)$	0	$(\pi, \sim 1.33)$	~ 0.40
$(\frac{7\pi}{4}, \sim 1.74)$	0	$(\frac{3\pi}{2}, \sim 1.33)$	~ 0.40
$(-, 0)$	$\frac{4}{135}$	$(-, \pi)$	$\frac{12}{5}$

Table 4.2: Local maxima and global minima for $f(\phi, \theta)$ in the Zauner subspace of four dimensions. The global maximum sits at the south pole. One could probably, with the right amount of determination and patience, find closed forms of the approximate values above.

4.4 Five dimensions

4.4.1 The standard base

In five dimensions all 2-dimensional subspaces that can be constructed by taking pairs of the standard basis vectors result in the same contour plot. This plot is independent of ψ and only consists of constant lines for different θ ; just like the 3-dimensional plot but without the zeroes, hence we omit the plot. For this choice of subspaces we find five distinct inner products, only two of which yield contours in the SICness function, though they are just as the those described in the 4-dimensional case (two separate constant lines equally spaced from the equator), so we omit these plots too in favour for more interesting results and without further ado we fast forward to the Zauner subspace.

4.4.2 The Zauner subspace

We introduce the basis vectors of the Zauner subspace as the two eigenvectors corresponding to the eigenvalue one of the unitary matrix

$$\mathcal{U} \begin{pmatrix} -1 & -1 \\ 1 & 0 \end{pmatrix} = \begin{pmatrix} \frac{e^{i\theta}}{\sqrt{5}} & -\frac{e^{\frac{i\pi}{5}+i\theta}}{\sqrt{5}} & \frac{e^{\frac{4i\pi}{5}+i\theta}}{\sqrt{5}} & -\frac{e^{-\frac{i\pi}{5}+i\theta}}{\sqrt{5}} & \frac{e^{-\frac{4i\pi}{5}+i\theta}}{\sqrt{5}} \\ \frac{e^{i\theta}}{\sqrt{5}} & -\frac{e^{\frac{3i\pi}{5}+i\theta}}{\sqrt{5}} & \frac{e^{-\frac{2i\pi}{5}+i\theta}}{\sqrt{5}} & \frac{e^{i\theta}}{\sqrt{5}} & \frac{e^{\frac{4i\pi}{5}+i\theta}}{\sqrt{5}} \\ \frac{e^{i\theta}}{\sqrt{5}} & \frac{e^{i\theta}}{\sqrt{5}} & \frac{e^{\frac{2i\pi}{5}+i\theta}}{\sqrt{5}} & -\frac{e^{\frac{i\pi}{5}+i\theta}}{\sqrt{5}} & \frac{e^{\frac{2i\pi}{5}+i\theta}}{\sqrt{5}} \\ \frac{e^{i\theta}}{\sqrt{5}} & -\frac{e^{-\frac{3i\pi}{5}+i\theta}}{\sqrt{5}} & \frac{e^{-\frac{4i\pi}{5}+i\theta}}{\sqrt{5}} & -\frac{e^{-\frac{3i\pi}{5}+i\theta}}{\sqrt{5}} & \frac{e^{i\theta}}{\sqrt{5}} \\ \frac{e^{i\theta}}{\sqrt{5}} & -\frac{e^{-\frac{i\pi}{5}+i\theta}}{\sqrt{5}} & \frac{e^{i\theta}}{\sqrt{5}} & -\frac{e^{\frac{3i\pi}{5}+i\theta}}{\sqrt{5}} & \frac{e^{-\frac{2i\pi}{5}+i\theta}}{\sqrt{5}} \end{pmatrix} \quad (4.10)$$

with the eigenvectors [35]

$$\psi_a = \frac{e^{\frac{i\pi}{10}}}{2\sqrt{30}} \begin{pmatrix} 2\sqrt{2(5+\sqrt{5})} \\ (\sqrt{15} + \sqrt{5-2\sqrt{5}})\epsilon \\ (-\sqrt{15} + \sqrt{5-2\sqrt{5}})\epsilon^4 \\ (-\sqrt{15} + \sqrt{5-2\sqrt{5}})\epsilon^4 \\ (\sqrt{15} + \sqrt{5-2\sqrt{5}})\epsilon \end{pmatrix} \quad \psi_b = \frac{1}{2\sqrt{15}} \begin{pmatrix} 0 \\ \sqrt{15 + \sqrt{15(5+2\sqrt{5})}} \\ -\sqrt{15 - \sqrt{15(5+2\sqrt{5})}}\epsilon^3 \\ \sqrt{15 - \sqrt{15(5+2\sqrt{5})}}\epsilon^3 \\ -\sqrt{15 + \sqrt{15(5+2\sqrt{5})}} \end{pmatrix} \quad (4.11)$$

where $\epsilon = e^{\frac{2\pi}{5}}$

The curious reader might inquire as to why the chosen unitary matrices in dimensions four and five both are representations of the same element in respective $SL(2, \mathbb{Z}_N)$ group. Note that there is nothing special about this particular element. In accordance with Conjecture 2, any order 3 element in $SL(2, \mathbb{Z}_N)$ with negative unit determinant will suffice. In this chapter we are, for historical reasons, using the Zauner convention ($\mathcal{U}_{\begin{pmatrix} -1 & \\ & 1 \end{pmatrix}}$), though for the rest of the thesis we will use the Appleby convention ($\mathcal{U}_{\begin{pmatrix} 0 & -1 \\ 1 & -1 \end{pmatrix}}$).

The contour plot of the SICness function is given in Figure 4.11. This plot is losing even more structure as compared to its four and 2-dimensional counterparts. By inspection we can now no longer identify neither the ϕ nor the θ coordinate of the extrema. There is some structure to the minima though; they come as two mirrored pairs separated in θ by π .

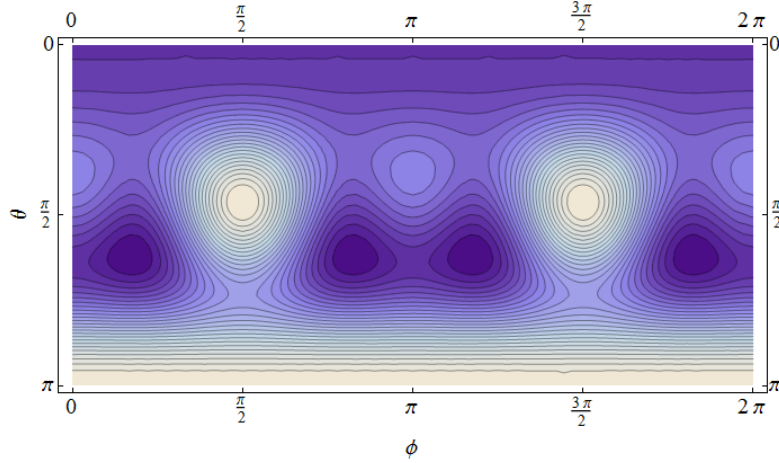


Figure 4.11: The map of $f_{SIC}(\psi)$ in the Zauner subspace of \mathbb{C}^5 . On the ϕ -axis we have azimuthal angle and on the θ -axis we have the polar angle.

The fiducial vectors are given by [35]

$$\psi_{k,l} = X\psi_a + k\beta^l Y\psi_b \quad k, l = \pm 1 \quad (4.12)$$

with

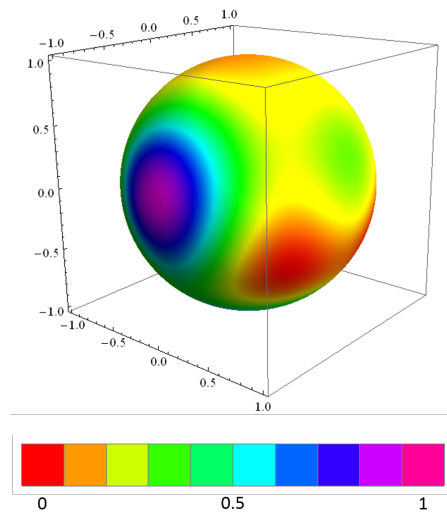


Figure 4.12: The map of $f_{SIC}(\psi)$ in the Zauner subspace in five dimensions on the surface of a sphere.

$$X = \frac{1}{2}\sqrt{3 - \sqrt{3}} \quad Y = \frac{1}{2}\sqrt{3 + \sqrt{3}} \quad \beta = \sqrt{\frac{1}{10}(5 + \sqrt{5})} + i\sqrt{\frac{1}{10}(5 - \sqrt{5})} \quad (4.13)$$

Once again we include a table of the maxima and minima as well as a spherical plot of the SICness function, these are given in table 4.3 and Figure 4.12.

There are four distinct inner products in five dimensions. These are given in Figure 4.13.

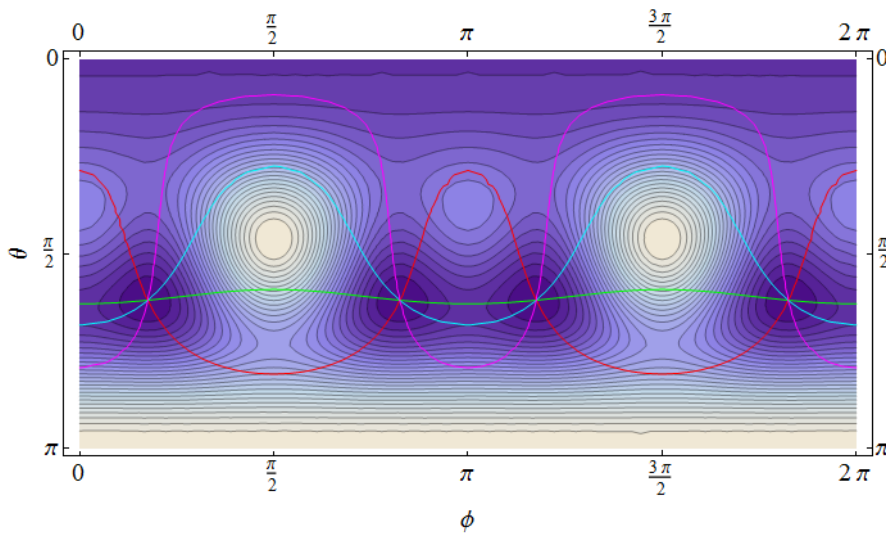


Figure 4.13: The distinct inner products of $f_{SIC}(\psi)$ in the Zauner subspace in five dimensions.

Minima		Maxima	
(ϕ, θ)	$f(\phi, \theta)$	(ϕ, θ)	$f(\phi, \theta)$
$(\sim 0.55, \sim 1.95)$	0	$(\frac{\pi}{2}, \sim 1.45)$	~ 0.84
$(\sim 3.70, \sim 1.95)$	0	$(\frac{3\pi}{2}, \sim 1.45)$	~ 0.84
$(\sim 2.59, \sim 1.95)$	0	$(-, \pi)$	$\frac{5}{6}$
$(\sim 5.73, \sim 1.95)$	0		
$(-, 0)$	$\frac{5}{54}$		

Table 4.3: Local maxima and global minima for $f(\phi, \theta)$ in the Zauner subspace in five dimensions. One could probably, with the right amount of determination and patience, find closed forms of the approximate values above.

4.5 A note on the number of distinct inner products

In this section we shall wrap up the loose ends on the number of distinct inner products. Chapter 2 supplies all the information needed to understand how many distinct inner products there are in a Zauner subspace. We formulate the following two lemmas to answer that question.

Lemma 1. *Closure of the set of SICs under the Clifford group*

Let $|\psi\rangle$ be a vector in a SIC and let \mathcal{U} be an element in the Clifford group. Then

$$\mathcal{U}^{-1}|\psi\rangle\mathcal{U} = |\psi'_0\rangle \quad (4.14)$$

where $|\psi'_0\rangle$ is some vector in the SIC.

Proof.

Suppose that we have a fiducial vector $|\psi\rangle$, such that

$$|\langle\psi|\psi_{ij}\rangle|^2 = c \quad \forall i, j \quad (4.15)$$

with $i \neq j$ where c is some constant.

Let $\mathcal{U} \in G_C$ such that,

$$|\psi'_0\rangle = \mathcal{U}|\psi\rangle \quad (4.16)$$

Then,

$$|\langle\psi'_0|\psi'_{ij}\rangle|^2 = |\langle\mathcal{U}\psi|D_{ij}\mathcal{U}|\psi\rangle|^2 = |\langle\psi|\mathcal{U}^{-1}D_{ij}\mathcal{U}|\psi\rangle|^2 \quad (4.17)$$

But by equation 2.51 and 4.15

$$|\langle \psi | \mathcal{U}^{-1} D_{ij} \mathcal{U} | \psi \rangle|^2 = |\langle \psi | D_{nm} | \psi \rangle|^2 = c \quad (4.18)$$

Thus, the set of vectors in a SIC is taken to the same set under Clifford group³. And the proof is done. \square

This lemma proves the statement in the beginning of this chapter when we argued the number of SICs in two dimensions. We can now formulate the lemma relating certain inner products in the Zauner subspace.

Lemma 2. *Orbits within the Zauner subspace under the Clifford group*

Let $|\psi\rangle$ be a vector in a SIC and choose the Zauner operator $\mathcal{U}_Z = \mathcal{U}_{\begin{pmatrix} 0 & -1 \\ 1 & -1 \end{pmatrix}}$ then the following equivalence holds true

$$|\langle \psi | D_{\begin{pmatrix} k \\ l \end{pmatrix}} | \psi \rangle|^2 = |\langle \psi | D_{\begin{pmatrix} -l \\ k-l \end{pmatrix}} | \psi \rangle|^2 \quad (4.19)$$

Proof.

By equation 2.51 it follows that

$$\mathcal{U}_Z^\dagger D_{\begin{pmatrix} k \\ l \end{pmatrix}} \mathcal{U}_Z = D_{\begin{pmatrix} 0 & -1 \\ 1 & -1 \end{pmatrix}} \begin{pmatrix} k \\ l \end{pmatrix} = D_{\begin{pmatrix} -l \\ k-l \end{pmatrix}} \quad (4.20)$$

thus

$$|\langle \psi | D_{\begin{pmatrix} k \\ l \end{pmatrix}} | \psi \rangle|^2 = |\langle \psi | \mathcal{U}_Z^\dagger \mathcal{U}_Z D_{\begin{pmatrix} k \\ l \end{pmatrix}} \mathcal{U}_Z^\dagger \mathcal{U}_Z | \psi \rangle|^2 = |\langle \psi | D_{\begin{pmatrix} -l \\ k-l \end{pmatrix}} | \psi \rangle|^2 \quad (4.21)$$

and conversely

$$|\langle \psi | D_{\begin{pmatrix} -l \\ k-l \end{pmatrix}} | \psi \rangle|^2 = |\langle \psi | \mathcal{U}_Z^\dagger D_{\begin{pmatrix} -l \\ k-l \end{pmatrix}} \mathcal{U}_Z | \psi \rangle|^2 = |\langle \psi | D_{\begin{pmatrix} k \\ l \end{pmatrix}} | \psi \rangle|^2 \quad (4.22)$$

\square

Note that a direct consequence of this lemma is that the inner products in the Zauner subspace will divide into orbits under the Zauner operator⁴, cf. Figure 2.2.

We will actually use a slightly modified version of this lemma to argue the specific amount of inner products, since our inner products are subject to both a Zauner operator and complex conjugation. Complex conjugation can be realised within the framework of displacement operators as

$$\mathbf{C} = \begin{pmatrix} -1 & 0 \\ 0 & -1 \end{pmatrix} \quad (4.23)$$

³The set of vectors in a SIC is partitioned into permutation groups by the Clifford group. It is not probable that all vectors in the SIC end up in the same permutation group. Hence, the set of vectors in a SIC is generically not given as an orbit under the Clifford group.

⁴This lemma holds for any Zauner operator, although which elements that are in the same orbit varies with the choice of Zauner operator.

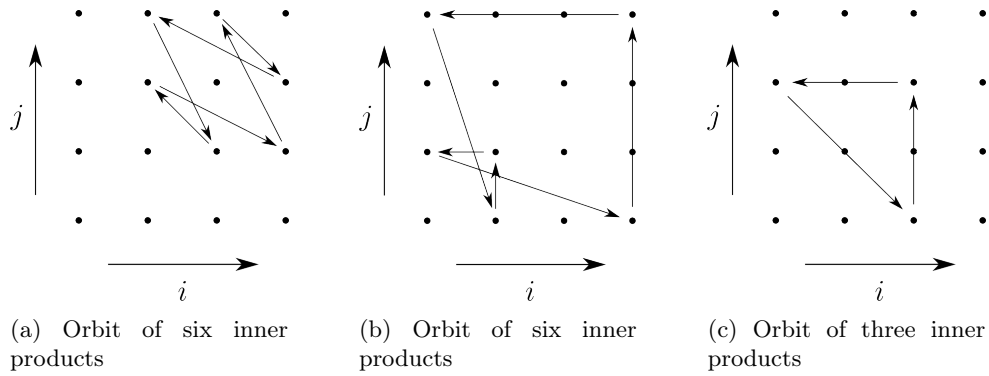


Figure 4.14: The inner products in four dimensions arranged into a lattice. The orbits corresponding to inner products being equal as per lemma 2. Each of these orbits corresponds to an inner product in Figure 4.10. The orbits is calculated as done in equation 2.52.

Hence we are actually looking at the combined order $2 \times 3 = 6$ Zauner and complex conjugation operator

$$\mathcal{U}_{\begin{pmatrix} 0 & 1 \\ -1 & 1 \end{pmatrix}} = \mathcal{U}_{\begin{pmatrix} -1 & 0 \\ 0 & -1 \end{pmatrix}} \mathcal{U}_{\begin{pmatrix} 0 & -1 \\ 1 & -1 \end{pmatrix}} \tag{4.24}$$

We call this type of operators anti-unitary and introduce an apt terminology

$$\mathcal{A}_{\begin{pmatrix} 0 & -1 \\ 1 & -1 \end{pmatrix}} = \mathcal{C} \times \mathcal{U}_{\begin{pmatrix} 0 & -1 \\ 1 & -1 \end{pmatrix}} \tag{4.25}$$

Inner products within the same orbits will be equated through lemma 2. Hence the number of unique inner products will decrease. We also know that the size of the orbits is 6.⁵ From this information it's possible to calculate the unique number of inner products in low dimensions, since there exists a unique way of combining $N^2 - 1$ (the number of inner products) elements into orbits of this given size. E.g. in dimension four we find $4^2 = 15 = 6 + 6 + 3$ (the '3' is explained in the footnote below), why we expect three inner products. Comparing with Figure 4.10 we find that this is the case. To be thorough we include a figure of the orbits in four dimensions, see Figure 4.14.

⁵The attentive reader might object that this argument only holds for dimensions that are zero modulo 6. While this is true there is a loophole hidden in the technicalities; in these cases we will find that there is a set of three inner products that are equal and real. Hence they are unaffected by the complex conjugation and remain order 3, and we can add an order 3 orbit.

Chapter 5

MUSs and SICs in Seven Dimensions

We previously stated that for dimensions larger than five we cannot use the trick from last chapter to look for fiducial vectors since the Zauner subspace is no longer represented by a Bloch sphere. However, we shall see that there is another special 2-dimensional subset in seven dimensions where there actually sit fiducial vectors. We shall implement a new method of finding all fiducial vectors in this subspace by relating to their apparent relationship to MUSs as is stated in Theorem 2.

5.1 Setting the scene

So far our approach to finding fiducial vectors has been to plot the SICness function and by guided numerical searches trying to locate the minima. This proved successful in dimensions 2, 3, 4 and 5. However, in dimensions higher than five the Zauner subspaces are no longer 2-dimensional, hence we can no longer plot the subspaces to look for fiducial vectors in a practical way [35]. In more general terms, the SICness function is getting too complicated for brute force numerical searches to be a viable option. We could of course apply some intelligent numerical search algorithm, but most likely it would converge at some local minimum instead of a global one. We shall, however, duly note that successful numerical searches have been conducted for $N \leq 67$, though these are of very sophisticated nature [30].

In this chapter we shall look at the case $N = 7$. The methods used in both this chapter and the next relies heavily on the fact that all fiducial vectors are minimum uncertainty states [8] as proved in Chapter 4, see Theorem 2.

In 2005 it was shown showed that the following vector is a fiducial vector [6]

$$|\psi_0\rangle = a_0|e_0\rangle + \sum_{k=1}^6 a_1 e^{ik\theta} |e_k\rangle \quad (5.1)$$

with

$$a_0 = \sqrt{\frac{2 + 3 + \sqrt{2}}{14}} \quad a_1 = \sqrt{\frac{4 - \sqrt{2}}{28}} \quad \theta = \cos^{-1} \left(-\frac{\sqrt{\sqrt{2} - 1}}{2} \right) \quad (5.2)$$

and where l_k is the Legendre symbol¹ which is,

$$l_k = \begin{cases} 1 & \text{if } k = 1, 2, 4 \\ -1 & \text{if } k = 3, 5, 6 \end{cases} \quad (5.3)$$

Writing out this fiducial vector we note that it is of a very special form

$$|\psi\rangle \sim \begin{pmatrix} x_0 \\ z \\ z \\ z^* \\ z \\ z^* \\ z^* \end{pmatrix} \quad (5.4)$$

where x_0 is real and z is complex.

We note that any vector of this form is characterised by three real parameters. Hence these vectors are restricted to a very small region of \mathcal{H}^7 , namely a real 3-dimensional subspace. However, we shall soon discover that this space can even be made into a 2-dimensional manifold. We now inquire as to whether any other fiducial vectors reside in this extraordinary corner of Hilbert space. Our strategy shall be to find all MUSs in this space and check whether they are fiducial vectors or not.

We remind ourselves that the MUS criterion is (equation 1.37)

$$\sum_{k=1}^N |\langle \psi | e_k^{(l)} \rangle|^4 = \frac{2}{N+1} \quad \forall l \quad (5.5)$$

also recall that there are $N + 1$ MUBs.

5.2 The special case

Let us start out by surveying the task of finding the MUSs. We regard a vector $|\psi\rangle$ on the form presented in equation 5.4, plugging this vector into the MUS criterion we obtain eight equations $\sum_{k=1}^7 |\langle \psi | e_k^{(l)} \rangle|^4 = \frac{1}{4}$. Solving these equations simultaneously we find all MUS. Without providing any additional information this indeed seems like a fool's errand. We would certainly not expect a system of eight equations in three variables to have any unique solution since it is (very) overdetermined.

The key is that we indeed are investigating a very special subspace. But in order to understand *how special* we must make some additional remarks about the elements of the Clifford group. Acting with these matrices on the set of MUBs will merely permute them. That is to say, acting with \mathcal{U} on the set of basis vectors of one MUB takes that set of basis vectors to the set of basis vectors of some other MUB. Note that we use *other* in a very mathematical sense here and that this operation can take some MUBs to themselves. E.g. acting with $\mathcal{U}_{\begin{pmatrix} 4 & 0 \\ 0 & 2 \end{pmatrix}}$ on the set of basis vectors of the first MUB in 7D will just permute the basis vectors within the MUB, hence it

¹The Legendre symbol is 1 if k is a quadratic residue, else it is 0. If we regard the equation $q = x^2 \pmod p$ over the integers with $x < 0 < p$, then q are the quadratic residues of p

takes the first MUB to itself. However, acting with the same matrix on the third MUB takes the set of basis vectors to the set of basis vectors of fourth MUB; thus it takes the third MUB to the fourth MUB. Continuing this we get the grouping of MUBs shown in Figure 5.1.

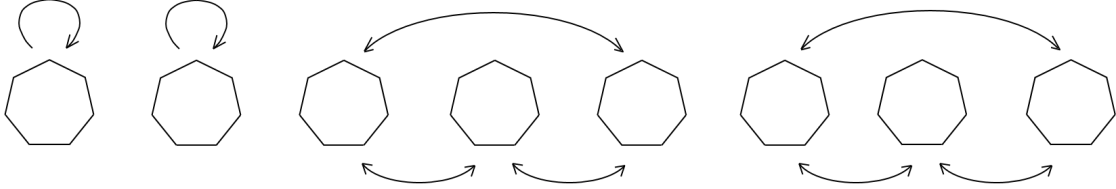


Figure 5.1: An example of how \mathcal{U} can permute the the sets of MUBs in seven dimensions using $\mathcal{U}_{\begin{pmatrix} 4 & 0 \\ 0 & 2 \end{pmatrix}}$.

It is no coincidence that we chose the specific \mathcal{U} unitary above. Let us investigate the problem of finding fiducial vectors in seven dimensions from a more general point of view.

Conjecture 2 tells us that given *any* order 3 unitary representation of an $SL(2, \mathbb{Z}_7)$ -element with negative unit trace, that unitary matrix is a Zauner operator and the eigenvectors of that operator span subspaces where fiducial vectors are found. We are of course keen to choose as simple a unitary as possible since it is getting increasingly difficult to find the eigenvectors with the increasing dimension cf. the eigenvectors we used in five dimensions. Looking at the formula for actually calculating the unitary matrix from Chapter 2 (equation 2.38)

$$\left(\mathcal{U}_{\begin{pmatrix} \alpha & \beta \\ \gamma & \delta \end{pmatrix}} \right)_{rs} = \frac{e^{i\theta}}{\sqrt{d}} \tau^{\frac{1}{\beta}(\delta r^2 - 2rs + \alpha s^2)} \quad (5.6)$$

with the additional special case if no inverse to β exists

$$\mathcal{U}_{\begin{pmatrix} \alpha & 0 \\ \gamma & \delta \end{pmatrix}} \equiv \mathcal{U}_{\begin{pmatrix} 0 & -1 \\ 1 & 0 \end{pmatrix}} \mathcal{U}_{\begin{pmatrix} \gamma & \delta \\ -\alpha & -\beta \end{pmatrix}} \quad (5.7)$$

we note that setting $\beta = \gamma = 0$ we obtain a monomial unitary matrix which is exceedingly simple to handle. Thus we look for an order 3 element in $SL(2, \mathbb{Z}_7)$ on the form

$$\begin{pmatrix} \alpha & 0 \\ 0 & \delta \end{pmatrix} \quad (5.8)$$

Guided by the fact that the sought matrix must have negative unit trace and unit determinant we try the following

$$M = \begin{pmatrix} \alpha & 0 \\ 0 & -(1 + \alpha) \end{pmatrix} \quad (5.9)$$

Since we are in the SL group

$$\det M = 1 \iff \alpha(1 + \alpha) = -1 \quad (5.10)$$

Solving this equation for in \mathbb{Z}_7 we find the solutions $\alpha = 2$ and $\alpha = 4$. Checking that it cubes to the identity matrix we find

$$\begin{pmatrix} 4 & 0 \\ 0 & 2 \end{pmatrix}^3 = \begin{pmatrix} 36 & 0 \\ 0 & 8 \end{pmatrix} \equiv \begin{pmatrix} 1 & 0 \\ 0 & 1 \end{pmatrix} \quad (5.11)$$

thus we have shown that $\mathcal{U}_{\begin{pmatrix} 4 & 0 \\ 0 & 2 \end{pmatrix}}$ is a monomial matrix that complies with Conjecture 2. Using equation 5.6 we can give the unitary matrix explicitly

$$\mathcal{U}_{\begin{pmatrix} 4 & 0 \\ 0 & 2 \end{pmatrix}} = \begin{pmatrix} 1 & 0 & 0 & 0 & 0 & 0 & 0 \\ 0 & 0 & 1 & 0 & 0 & 0 & 0 \\ 0 & 0 & 0 & 0 & 1 & 0 & 0 \\ 0 & 0 & 0 & 0 & 0 & 0 & 1 \\ 0 & 1 & 0 & 0 & 0 & 0 & 0 \\ 0 & 0 & 0 & 1 & 0 & 0 & 0 \\ 0 & 0 & 0 & 0 & 0 & 1 & 0 \end{pmatrix} \quad (5.12)$$

Acting with this matrix on a general state $|\psi\rangle$ we find

$$\begin{pmatrix} 1 & 0 & 0 & 0 & 0 & 0 & 0 \\ 0 & 0 & 1 & 0 & 0 & 0 & 0 \\ 0 & 0 & 0 & 0 & 1 & 0 & 0 \\ 0 & 0 & 0 & 0 & 0 & 0 & 1 \\ 0 & 1 & 0 & 0 & 0 & 0 & 0 \\ 0 & 0 & 0 & 1 & 0 & 0 & 0 \\ 0 & 0 & 0 & 0 & 0 & 1 & 0 \end{pmatrix} \begin{pmatrix} x_0 \\ z_1 \\ z_2 \\ z_3 \\ z_4 \\ z_5 \\ z_6 \end{pmatrix} = \begin{pmatrix} x_0 \\ z_2 \\ z_4 \\ z_6 \\ z_1 \\ z_3 \\ z_5 \end{pmatrix} \quad (5.13)$$

this equality enables us to find an eigenvector of $\mathcal{U}_{\begin{pmatrix} 4 & 0 \\ 0 & 2 \end{pmatrix}}$ by subjecting $|\psi\rangle$ to

$$\begin{cases} x_0 = x_0 \\ z_1 = z_2 = z_4 \\ z_3 = z_5 = z_6 \end{cases} \quad (5.14)$$

such that

$$|\psi\rangle = \begin{pmatrix} x_0 \\ z_1 \\ z_1 \\ z_2 \\ z_1 \\ z_2 \\ z_2 \end{pmatrix} \quad (5.15)$$

We note that this is almost of the same form as the form of the fiducial vector 5.4. Introducing the anti unitary operator $\mathcal{A}_{\begin{pmatrix} -2 & 0 \\ 0 & -3 \end{pmatrix}}$ and acting on the vector above we find

$$\begin{pmatrix} 1 & 0 & 0 & 0 & 0 & 0 & 0 \\ 0 & 0 & 0 & 1 & 0 & 0 & 0 \\ 0 & 0 & 0 & 0 & 0 & 0 & 1 \\ 0 & 0 & 1 & 0 & 0 & 0 & 0 \\ 0 & 0 & 0 & 0 & 0 & 1 & 0 \\ 0 & 1 & 0 & 0 & 0 & 0 & 0 \\ 0 & 0 & 0 & 0 & 1 & 0 & 0 \end{pmatrix} \times \mathcal{C} \begin{pmatrix} x_0 \\ z_1 \\ z_1 \\ z_2 \\ z_1 \\ z_2 \\ z_2 \end{pmatrix} = \begin{pmatrix} x_0 \\ z_2^* \\ z_2^* \\ z_1^* \\ z_2^* \\ z_1^* \\ z_1^* \end{pmatrix} \quad (5.16)$$

where \mathcal{C} denotes complex conjugation.

Which gives us a system of equations for finding an eigenvector of \mathcal{A} with the solution

$$\begin{cases} x_0 = x_0 \\ z_1 = z_2^* \\ z_2 = z_1^* \end{cases} \quad (5.17)$$

such that

$$|\psi\rangle = \begin{pmatrix} x_0 \\ z \\ z \\ z^* \\ z \\ z^* \\ z^* \end{pmatrix} \quad (5.18)$$

which is a vector of the form given in equation 5.4. Thus we find that the fiducial vector 5.1 sits in the same subspace as this eigenvector to the anti unitary operator $\mathcal{A}_{\begin{pmatrix} -2 & 0 \\ 0 & -3 \end{pmatrix}}$. Writing the complex components in Cartesian form we obtain the vector

$$|\psi\rangle = \begin{pmatrix} x_0 \\ x_1 + ix_2 \\ x_1 + ix_2 \\ x_1 - ix_2 \\ x_1 + ix_2 \\ x_1 - ix_2 \\ x_1 - ix_2 \end{pmatrix} = x_0 \begin{pmatrix} 1 \\ 0 \\ 0 \\ 0 \\ 0 \\ 0 \\ 0 \end{pmatrix} + x_1 \begin{pmatrix} 0 \\ 1 \\ 1 \\ 1 \\ 1 \\ 1 \\ 1 \end{pmatrix} + x_2 \begin{pmatrix} 0 \\ i \\ i \\ -i \\ i \\ -i \\ -i \end{pmatrix} \quad (5.19)$$

with the normalisation

$$x_0^2 + 6x_1^2 + 6x_2^2 = 1 \quad (5.20)$$

This renders the subspace a *real* 3-dimensional subspace of \mathbb{C}^7 – and a real 3-dimensional subspace where we know that there sits at least one fiducial vector nonetheless!

Summarising we have three different spaces hanging around here. There are the space of all quantum states in seven dimensions (\mathbb{C}^7) which has seven complex dimensions; the Zauner subspace (equation 5.15) which has three complex dimensions; and the real subspace of the Zauner subspace (equation 5.18) which has three real dimensions.

Now, acting with $\mathcal{A}_{\begin{pmatrix} -2 & 0 \\ 0 & -3 \end{pmatrix}}$ on the MUBs permutes the MUBs in almost the same way as $\mathcal{U}_{\begin{pmatrix} 4 & 0 \\ 0 & 2 \end{pmatrix}}$ as shown in Figure 5.2.

Having declared that 5.4 is an eigenvector of $\mathcal{A}_{\begin{pmatrix} -2 & 0 \\ 0 & -3 \end{pmatrix}}$ and that as far as $\mathcal{A}_{\begin{pmatrix} -2 & 0 \\ 0 & -3 \end{pmatrix}}$ is concerned there are but three MUBs, we have shown that there will only be three independent equations in 5.5. Thus we are left with three polynomials in three variables. The situation would seem to be convoluted by the fact that Theorem 1 from Chapter 1 adds one unique equation, making the system overdetermined. But it turns out enforcing this theorem is equivalent with imposing normalisation. This is realised by recalling that normalisation is a prerequisite of Theorem 1.

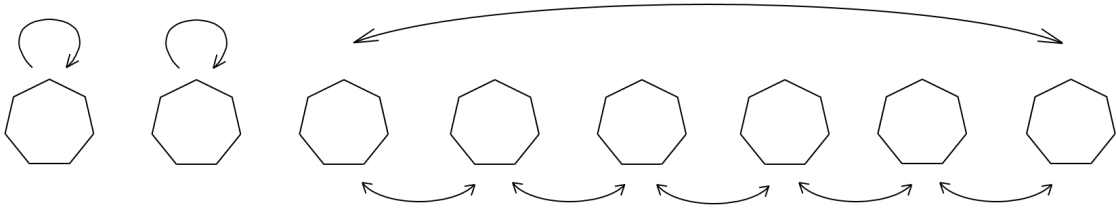


Figure 5.2: Schematic overview of how $\mathcal{A}_{\begin{pmatrix} -2 & 0 \\ 0 & -3 \end{pmatrix}}$ permutes the MUBs in seven dimensions.

Glancing at equation 5.5 we realise that solving these equations is no easy task. Each sum contributes seven quartic inner products of 7-dimensional vectors, the problem is possibly huge. Simplifying the three unique equations given by the MUS-criterion we find

$$\begin{cases} p_1 = x_0^4 + 6(x_1^2 + x_2^2)^2 \\ p_2 = \frac{1}{7}(x_0^4 + 36x_0^2x_1^2 + 120x_0x_1^3 + 186x_1^4 + 36(x_0 - x_1)^2x_2^2 + 42x_2^4) \\ p_3 = \frac{1}{7}(x_0^4 + 46x_1^4 + 148x_1^2x_2^2 + 70x_2^4 + 22x_0^2(x_1^2 + x_2^2) + 4x_0x_1(-5x_1^2 + 3x_2^2)) \end{cases} \quad (5.21)$$

We solve the resulting equations (eq. 5.22) by using *Mathematica's* command `Reduce`. This is a generalisation of the more widely known command `Solve`. It operates by reworking the polynomial in a specified way rather than trying to solve it right away. This allows for a more sophisticated approach to work with polynomials than the often quite blunt `Solve` algorithm. By inspection we gather that the polynomial system 5.21 is probably best solved in terms of x_2 . This variable comes into many of the terms and moreover it always comes in even powers. Asking *Mathematica* to eliminate all x_0 's and x_1 's in the system

$$\begin{cases} p_1 = \frac{1}{4} \\ p_2 = \frac{1}{4} \\ p_3 = \frac{1}{4} \end{cases} \quad (5.22)$$

under the normalisation given in equation 5.20 we find 12 exact solutions being minimum uncertainty states. The solutions are, however, not very enlightening to look upon so we will not give them here explicitly. As a reference we present them in Appendix C.

Before we comment on the MUSs found, we shall visualise the MUSs using the tricks from last chapter. In order to make a contour plot we are required find a parametrisation of the submanifold. Firstly we recognise that we are solely interested in pure states, hence we are really only regarding the submanifold of pure states of the real subspace 5.18 (or 5.19). However, is just the real counterpart of $\mathbb{C}\mathbb{P}^2$, called the real projective space², $\mathbb{R}\mathbb{P}^2$, which is what we get if we subject the real subspace 5.19 to the normalisation 5.20. The parametrisation for $\mathbb{R}\mathbb{P}^2$ is

²The real projective plane is a 2-dimensional manifold that consists of all lines in \mathbb{R}^3 passing through the origin. This space is topologically equivalent to the standard sphere, S^2 , with antipodal points identified.

$$\begin{cases} x_0 = \cos \theta \\ x_1 = \cos \phi \sin \theta \\ x_2 = \sin \phi \sin \theta \end{cases} \quad (5.23)$$

such that a general, correctly normalised, vector is written

$$\begin{pmatrix} \cos \theta \\ \frac{1}{\sqrt{6}}(\cos \phi \sin \theta + i \sin \phi \sin \theta) \\ \frac{1}{\sqrt{6}}(\cos \phi \sin \theta + i \sin \phi \sin \theta) \\ \frac{1}{\sqrt{6}}(\cos \phi \sin \theta - i \sin \phi \sin \theta) \\ \frac{1}{\sqrt{6}}(\cos \phi \sin \theta + i \sin \phi \sin \theta) \\ \frac{1}{\sqrt{6}}(\cos \phi \sin \theta - i \sin \phi \sin \theta) \\ \frac{1}{\sqrt{6}}(\cos \phi \sin \theta - i \sin \phi \sin \theta) \end{pmatrix} \quad (5.24)$$

Figure 5.3 shows where in $\mathbb{R}\mathbb{P}^2$ the MUSs sit.

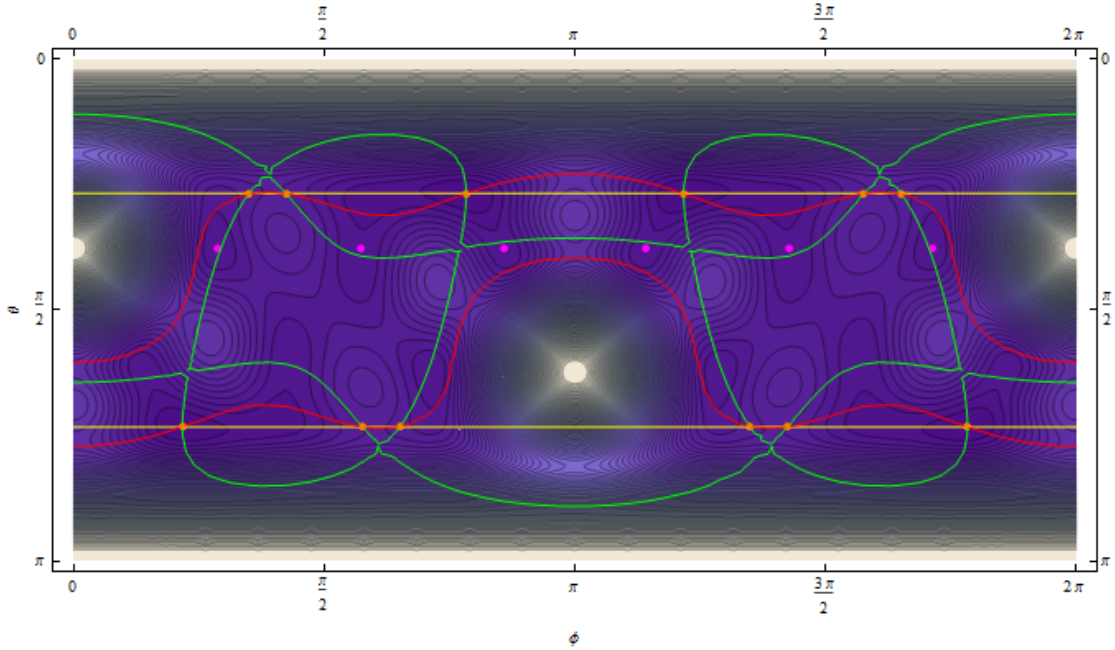


Figure 5.3: The SICness function in the submanifold where the fiducial vector 5.1 sits. The coloured lines are the unique MUS equations. The orange dots sitting in the intersections of these lines are the MUSs and the magenta dots are the Alltop-MUBs.

This figure provides nice means of giving some intuition to the MUSs we just derived. We see that there is an apparent mirroring of the MUSs in both the θ -plane and the ϕ -plane. We write “apparent” because this is a plot in $\mathbb{R}\mathbb{P}^2$, thus antipodal points are identified. Hence antipodal points not mirror images, but the *same* physical state. Apart from this identification there is a mirroring in the ϕ axis. This is inherited from the complex conjugation of the anti unitary

operator.

In the end, we have essentially found three interesting MUSs and a complex conjugated relative to each of these, making up a total of $3 \times 2 = 6$ MUSs. Checking whether these are fiducial vectors or not we find that one of the primordial MUSs is indeed a fiducial vector, this is precisely the fiducial vector found by D. M. Appleby presented in the beginning of this chapter. The complex conjugate of this state is also a fiducial vector, although not being as interesting.

Our next step is to investigate whether we can make a slight generalisation to this situation or not.

5.3 The general case

Having found all MUS in the real subspace (eq. 5.4) we ask whether it is possible to find all MUS in the full complex Zauner subspace (eq. 5.15).

$$|\psi\rangle \equiv \begin{pmatrix} z_0 \\ z_1 \\ z_1 \\ z_2 \\ z_1 \\ z_2 \\ z_2 \end{pmatrix} \quad (5.25)$$

This situation is considerably more complex. While the system of equations we need to solve now consists of four equations (cf. Figure 5.1) we have also added two real variables to a total of five real variables. Thus we are naively looking for a one parameter family of solutions.

Even simplifying the polynomials in this case is a great ordeal. Simplifying the polynomials with *Mathematica's* `FullSimplify` we generate our adversities

$$\left\{ \begin{array}{l}
p_1 = x_0^4 + 3((x_1^2 + x_2^2)^2 + (x_3^2 + x_4^2)^2) \\
p_2 = \frac{1}{7}(1 + 6x_2^2 + 6(2x_0x_1^3 - 2x_1^4 - 2x_2^4 + 12x_2^3x_4 \\
\quad + x_1^2(1 - 4x_2^2 + 8x_0x_3 + 5x_3^2 + 12x_2x_4 - 3x_4^2) - (x_3^2 + x_4^2)(-1 + 2x_3(-x_0 + x_3) + 2x_4^2) \\
\quad + x_2^2(-3x_3^2 + 5x_4^2) + 2x_2x_4(-1 + 4x_0x_3 + 6x_3^2 + 6x_4^2) + 2x_1(x_3 + 8x_2x_3x_4 + x_0(x_2^2 + 4x_3^2 + 4x_2x_4))) \\
p_3 = \frac{1}{7}(1 - 12x_1^4 - 12x_2^4 - 2x_2^3(\sqrt{7}x_0 + 2\sqrt{7}x_3 + 6x_4) - 2x_1^3(x_0 + 4\sqrt{7}x_4) - 2x_2^2(-3 + 9x_3^2 + 13x_4^2) \\
\quad - 2x_1^2(-3 + 12x_2^2 + 2\sqrt{7}x_2x_3 + 13x_3^2 + 6x_2x_4 + 9x_4^2 + x_0(\sqrt{7}x_2 + 4x_3 - 4\sqrt{7}x_4)) \\
\quad - 2(x_3^2 + x_4^2)(-3 + x_0(x_3 + \sqrt{7}x_4) + 6(x_3^2 + x_4^2)) \\
\quad - 2x_1(x_3 + 8x_2x_3x_4 + 2\sqrt{7}x_3^2x_4 + \sqrt{7}x_4(-1 + 4x_2^2 + 2x_4^2) \\
\quad + x_0(x_2^2 + 4x_2(\sqrt{7}x_3 + x_4) + 4x_3(x_3 + \sqrt{7}x_4))) \\
\quad - 2x_2(4\sqrt{7}x_3^3 - x_4 + 6x_4^3 + x_3^2(-4\sqrt{7}x_0 + 6x_4) + x_3(4x_0x_4 + \sqrt{7}(-1 + 4x_4^2)))) \\
p_4 = \frac{1}{7}(1 + 2(-6x_1^4 - 6x_2^4 + x_2^3(\sqrt{7}x_0 + 2\sqrt{7}x_3 - 6x_4) - x_1^3(x_0 - 4\sqrt{7}x_4) + x_2^2(3 - 9x_3^2 - 13x_4^2) \\
\quad - (x_3^2 + x_4^2)(-3 + x_0(x_3 - \sqrt{7}x_4) + 6(x_3^2 + x_4^2)) \\
\quad - x_1(x_3 + 8x_2x_3x_4 - 2\sqrt{7}x_3^2x_4 + \sqrt{7}x_4(1 - 4x_2^2 - 2x_4^2) \\
\quad + x_0(x_2^2 + 4x_2(-\sqrt{7}x_3 + x_4) + 4x_3(x_3 - \sqrt{7}x_4))) \\
\quad + x_1^2(3 - 12x_2^2 + 2\sqrt{7}x_2x_3 - 13x_3^2 - 6x_2x_4 - 9x_4^2 + x_0(\sqrt{7}x_2 - 4(x_3 + \sqrt{7}x_4))) \\
\quad + x_2(4\sqrt{7}x_3^3 + x_4 - 6x_4^3 - 2x_3^2(2\sqrt{7}x_0 + 3x_4) + x_3(-4x_0x_4 + \sqrt{7}(-1 + 4x_4^2)))) \\
\end{array} \right. \tag{5.26}$$

Looking at the general solution for a quartic equation one realises that solving quartic equations is no easy endeavour – and solving systems of quartic equations much less so. Thus we have good reason to devise a strategy before engaging in any serious attempt at solving the system above. We note that the third and fourth polynomials are quite alike; there are many terms of shared order between the polynomials with alternating sign. Using this property while fine tuning the coefficients to eliminate as many terms as possible, and in particular the terms with root coefficients, we end up with the following polynomial system

$$\left\{ \begin{array}{l} p_1 = 4p_1 = -1 + 12(x_4^2 + x_3^2)^2 + 4x_0^4 + 12(x_1^2 + x_2^2)^2 \\ p_2 = \frac{28}{3}p_2 = -1 + 8x_3^2 + 8(-2x_4^4 - 2x_3^4 + 2x_3^3x_0 + 2x_3x_1(1 + 4x_0x_1) + 12x_4^3x_2 + x_3^2(8x_0x_1 + 5x_1^2 - 3x_2^2) \\ \quad - (x_1^2 + x_2^2)(-1 + 2x_1(-x_0 + x_1) + 2x_2^2) + x_4^2(1 + 2x_3(-2x_3 + x_0) - 3x_1^2 + 5x_2^2) \\ \quad + 2x_4x_2(-1 + 6x_3^2 + 4x_0x_1 + 6x_1^2 + 4x_3(x_0 + 2x_1) + 6x_2^2)) \\ p_3 = 14(p_3 + p_4) = -2 + 3x_4^2 + 3x_3^2 + x_0^2 + 3x_1^2 + 3x_2^2 \\ p_4 = \frac{\sqrt{7}}{4}(p_3 - p_4) = -x_4(4x_3x_0x_1 + x_4^2(x_0 + 2x_1) + x_3^2(x_0 + 2x_1) + x_1(-1 + 4x_1(-x_0 + x_1))) \\ \quad - (x_3(-1 + 4x_4^2 + 4x_3(x_3 - x_0)) + 4x_3x_0x_1 + (2x_3 + x_0)x_1^2)x_2 - 4x_4x_1x_2^2 - (2x_3 + x_0)x_2^3 \end{array} \right. \quad (5.27)$$

This equation is significantly more easy to handle. We see that the collected order of each term is even, this opens for some interesting substitutions and reveals that the polynomials are not totally general. It turns out that trying to solve this polynomial system by ordinary means, such as the brute force method of solving the polynomials one at a time, while consecutively plugging the roots into the next polynomial, does not work due to the complexity of the roots. Similarly substitutions does not do the trick, we can introduce variables $y_i = x_kx_l$ and gain a large system of quadratic equations instead, but in the end we run into the same problem. Failing to solve the system by conventional means we turn to the mathematical field of Ring Theory³ for inspiration.

5.3.1 Gröbner bases

Solving non linear multivariate systems of polynomials is no simple task and it generally requires the introduction of Gröbner⁴ bases. Given some set of polynomials a Gröbner base is another set of polynomials with the same *ideals* as the original set [31]. We will not put a lot of work into actually defining ideals, or into defining Gröbner bases for that matter, rather we will try to explain how Gröbner bases work and why they are desirable. An excellent review for the reader who wishes to know more about Gröbner bases, or who would like a more formal treatment of subject, can be found here [15].

Given some set of polynomials, P , the fundamental idea behind the Gröbner bases is to find another *simpler* set of polynomials, G , with the same roots as the original set. By “simpler” we mean that it is given on the following form

$$\left\{ \begin{array}{l} g_1(x_1) = 0 \\ g_2(x_1, x_2) = 0 \\ g_3(x_1, x_2, x_3) = 0 \\ \vdots \end{array} \right.$$

This system can be solved bottom-up by consecutively plugging the solutions for each polynomial into the next. In this way we essentially transform the multivariate system into a single variable system.

³All polynomials are formally part of the ring of polynomials in mathematics. A ring is an Abelian group under addition and a monoid under multiplication.

⁴Named after the Austrian mathematician Wolfgang Gröbner.

Constructing Gröbner bases is today mostly analogous with running the Buchberger algorithm⁵, which is an algorithm designed to find the Gröbner base for any given set of polynomials [14] 1970. The Buchberger algorithm is a generalisation of three well-known algorithms: Gaussian elimination, Euclid's algorithm for finding the greatest common divisor for polynomials and the simplex algorithm. A more formal overview of the procedure can be found here [16].

We shall briefly argue why these algorithms are relevant when solving non linear multivariate polynomial systems.

Gaussian Elimination

When solving a linear system of polynomials Gaussian elimination gives the solutions. Hence, by applying the Buchberger algorithm to a set of linear polynomials, we will by necessity retrieve Gaussian elimination. Now, think of Gaussian elimination as a procedure that rephrases sets of polynomials in easier forms; this is the desirable property of Gaussian elimination that is carried over to the Buchberger algorithm. E.g. feeding Gaussian elimination the set $\{3x+2y+2z-5, 2x-2y-5z+1\}$ will return the set $\{x-\frac{1}{5}(4+3z), y+\frac{19}{10}z-\frac{13}{10}\}$ which is a set of polynomials that contains the same combined information as the first set but in a more condensed way.

Euclid's Algorithm

Usually we think of Euclid's algorithm as an algorithm for finding the GCD of two polynomials. But, more importantly for the procedure for finding a Gröbner basis, the output polynomial of Euclid's algorithm is also a polynomial with the same roots as the common roots of the input polynomials. E.g. The GCD of the polynomials $-3+3x+7x^2+7x^3+2x^4$ and $-2-x+12x^2+5x^3$ is (x^2+2x-1) , which has the roots $x = -1 \pm \sqrt{2}$. Thus, these are the common roots of the input polynomials. In this way the new polynomial contains all information that the original system does. We can think of it as though the two input polynomials are just a clumsy way to write the output polynomial. The Buchberger algorithm for non linear equations in one variable is Euclid's algorithm.

Simplex Algorithm

The simplex algorithm is probably less known to physicists than the preceding algorithms as it is an algorithm used in linear programming. But it is nonetheless a vital part of the Buchberger algorithm. While it is intuitive that the mixture of an algorithm that solves linear multivariate systems and an algorithm that solves non linear single variable equations produces an algorithm for solving non linear multivariate systems by picking the best of the two algorithms, this is just almost true. We also need the simplex algorithm for the algorithm to run iteratively and to ensure that it always terminates. We will not outline the simplex algorithm here, it is presented in the references, but think of it as an algorithm that makes substitutions according to some predefined rules.

The Buchberger algorithm is a very powerful algorithm in that it, in principle, has a success rate of 100% [16]. Also Hilbert's Basis Theorem⁶ ensures that every polynomial system has a Gröbner base [14][15]. Calculating a Gröbner base can however be practically impossible as it requires vast amounts of computing power for complicated sets.

Even using Gröbner bases we were unable to find a solution to the polynomial system (equation 5.27).

⁵Named after the Austrian mathematician Bruno Buchberger.

⁶This is a theorem from commutative algebra about properties of rings. We will not state it here but it is given in the references.

Chapter 6

Connecting the MUSness and the SICness

In this final chapter we formulate the main result of this thesis. We more closely than before establish the link between the SICness and the MUSness of a state. Most of the results presented have been verified in prime dimensions $N \leq 23$. Note that a lot of computing power comes into deriving these results; this is further discussed in appendices A and B.

The reader already familiar with SICs and MUSs can probably read this chapter stand-alone as a review on our research on the matter. Also the results presented below and further research on the subject will be presented in a paper to appear by D. Andersson, D. M. Appleby, I. Bengtsson and H. Dang.

6.1 Preamble

In Chapter 3 we prove that all fiducial vectors are in fact MUSs (Theorem 2), why we are led to believe that there, perhaps, exists some deeper relationship between the SICness and the MUSness of a state. We have already defined the SICness of a state to be reversely proportional to the SICness function (equation 3.3). Similarly we use the following function, derived from equation 1.37, to quantify the MUSness of a state.

$$f_{MUS} = \sum_{l=1}^{N+1} \left(\sum_{k=1}^N |\langle e_l^{(k)} | \psi \rangle|^4 - \frac{2}{(N+1)} \right)^2 \quad (6.1)$$

where $e_l^{(k)}$ is the k 'th basis vector of the l 'th MUB.

Note that this function is just like the SICness function but it is constructed to be zero for MUSs instead of fiducial vectors.

A naive way of investigating this proposed relationship is to make a scatter plot of the MUSness versus the SICness for a large enough set of random states. If there exists some relation between the two, *some* structure should arise from this.

This raises the issue of how one goes about picking random quantum states. We know from Chapter 1 that all pure states sit in the complex projective $(N-1)$ -space, $\mathbb{C}\mathbb{P}^{N-1}$. Furthermore, recalling the contour plots from Chapter 4 we realise that it will not do to pick angles θ and ϕ randomly from a uniform probability distribution, because the plots become increasingly distorted as we move towards the poles. However, note that there is no change in distortion when we change the longitude but keep the latitude constant. This may, or may not, seem intuitive but it is a fundamental result from non-Euclidean geometry. This observation tells us that we must treat the generation of random θ and ϕ coordinates separately. Specifically it tells us that the ϕ coordinate actually is given by a uniform probability distribution while the probability distribution for θ must be biased to compensate for the distortion.

Guided by this reasoning we construct the general N -dimensional state vector as [12]

$$|\psi\rangle = (x_1, x_2, \dots, x_N) \quad (6.2)$$

using the permutation of $\mathbb{C}\mathbb{P}^{N-1}$

$$\begin{aligned} x_1 &= \cos \theta_1 \sin \theta_2 \cdots \sin \theta_{N-2} \sin \theta_{N-1} \\ x_2 &= \sin \theta_1 \sin \theta_2 \cdots \sin \theta_{N-2} \sin \theta_{N-1} e^{i\phi_1} \\ &\quad \vdots \\ x_{N-1} &= \cos \theta_{N-2} \sin \theta_{N-1} e^{i\phi_{N-2}} \\ x_d &= \cos \theta_{N-1} e^{i\phi_{N-1}} \end{aligned} \quad (6.3)$$

with the probability distributions

$$\phi_k \in [0, 2\pi] \quad (6.4)$$

and

$$\theta_k = \sin^{-1} \xi_k^{\frac{1}{2k}} \quad \xi_k \in [0, 1] \quad (6.5)$$

where ψ_k and ξ_k are uniformly distributed.

This concludes the preamble.

6.2 The naive approach

We are now armed with all the tools we need to address the matter at hand of making scatter plots. An example of such a plot can be seen in Figure 6.1. It turns out that the general outline of these plots is the same regardless of prime dimension, with the exception of dimension two and three; which we shall comment on later.

The procedure for making these scatter plots is quite straight forward, the algorithm runs as follows

1. Generate $N-1$ random ϕ -coordinates according to 6.4 and $N-1$ random θ -coordinates according to 6.5.
2. Calculate the resulting random vector from 6.3

3. Calculate the f_{SIC} value from 3.3
4. Calculate the f_{MUS} value from 6.1
5. Plot the result as a point with coordinates (f_{SIC}, f_{MUS})

The calculations of f_{SIC} and f_{MUS} are the most computationally heavy operations involving quaternions in dimension N . Needless to say, the time complexity¹ of this algorithm is far from linear, hence a lot of computing power is required to achieve a plot within reasonable time frames. We discuss this further in appendices A and B.

Plotting the result from having generated many random states as a scatter plot with SICness (f_{SIC}) on the x-axis and MUSness (f_{MUS}) on the y-axis, we find plots resembling the one below in Figure 6.1. This plot is also schematically presented in Figure 6.2.

Even from just a quick glance there is obvious structure to this plot, as such we conclude that our naive approach has actually revealed some connection between the SICness and the MUSness of a state. We shall dwell on some of the features of this plot to make some brief comments.

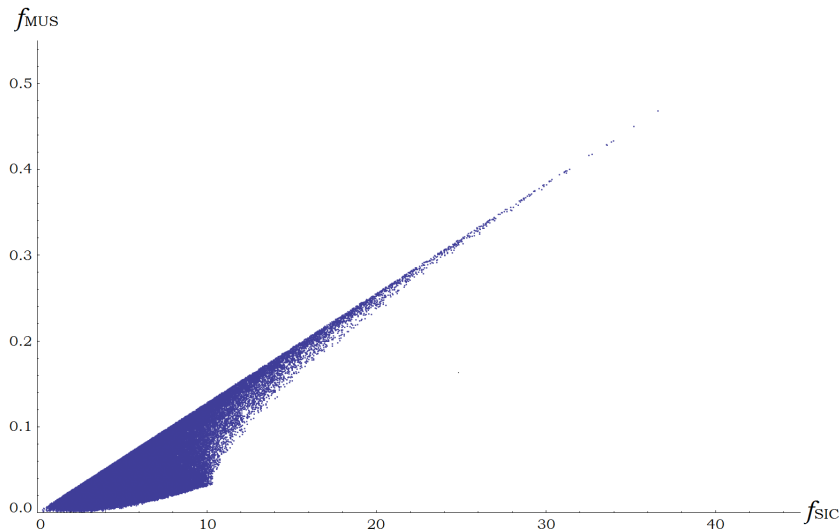


Figure 6.1: Plotting SICness versus MUSness in 5 dimensions with 10^5 points.

The bulk of points

The vast majority of points in the parameter space will end up inside the boundaries of this plot. We acknowledge that the parameter space is immense as compared to the codomain² and that only extraordinary states with fine tuned parameters will correspond to points on the boundary. This leads us to the conclusion that most configurations of parameters will not end up on the boundary, rather most configurations will correspond to about the same state. This effect will

¹Time complexity is the term used in computer science for how the evaluation time scales with increasing data set.

²The parameter space is $\mathbb{C}P^{N-1}$ which is $2(N-1)$ dimensional while the codomain is 2 dimensional, hence the dimension of the parameter space is $N-1$ times as large as the dimension of the codomain.

be stronger with increasing dimension. This is analogous to the argument used in statistical mechanics about the unlikeliness of all air molecules ending up in one corner of a box.

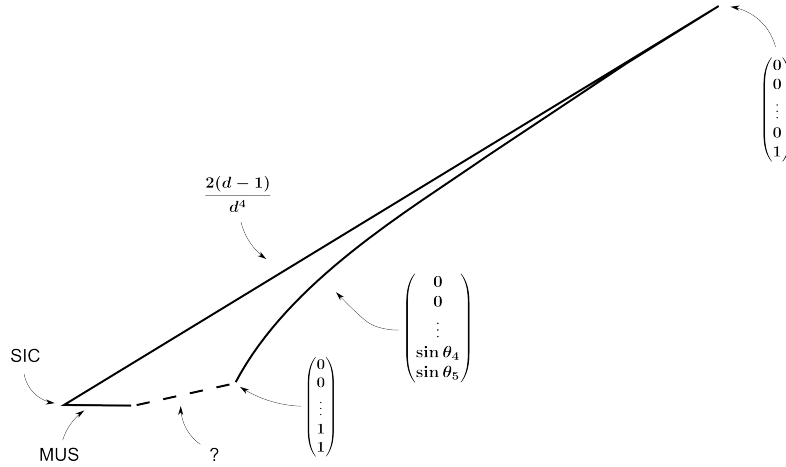


Figure 6.2: A schematic drawing of the borders of the plot. This drawing seems to be valid in all prime dimensions.

The straight line

There is no bijection between f_{SIC} and f_{MUS} , contrary, there exists many states of the same MUSness for any given SICness and vice versa. However, for any given SICness there seems to be a corresponding maximum MUSness³. We conjecture the following

Conjecture 3. *Maximum MUSness theorem*

In any prime dimension, the MUSness of a state is related to the SICness, subject to the following inequality

$$f_{MUS} \leq \frac{2(N-1)}{N^4} f_{SIC} \tag{6.6}$$

To prove analytically that this indeed the case should, in principle, be a fairly straight forward optimisation problem, though we have yet to attempt at a solution⁴. Numerically we may for instance apply *Mathematica*'s `NMaximize` to the expression $\frac{f_{MUS}}{f_{SIC}}$. However, the time complexity of the native `NMaximize` command is high and the argument is complicated, furthermore it is not parallelisable. Hence, *Mathematica* does not provide a numerical proof within a reasonable time frame for dimensions greater than 7. There is a much more efficient way of obtaining the slope of the maximum MUSness line in higher dimensions discussed further on.

The flat line

Theorem 2 states that all fiducial vectors are MUSs—but all MUSs are not fiducial vectors. Hence we expect some flat line along the f_{SIC} -axis corresponding to these MUSs. This line is

³Verified numerically in dimensions 2 ,3 ,5 ,7, 19 and 23.

⁴A footnote from the future: This has since been proven and will be presented in a paper to appear by D. Andersson, D.M. Appleby, H. Dang, I.Bengtsson and K. Blanchfield.

somewhat visible in the plot, we can see points (states) which are close to zero for the MUSness function while being no way near zeroes for the SICness function. The end points of this line are of certain interest to us. We know that at the origin of this plot sits states that are zero for both the SICness and MUSness function i.e. fiducial vectors. The other end point remains something of a mystery but we will comment on it further on.

The curved line

Using *Mathematica's* `Manipulate` command we may discern that the curved line coming from the top actually correspond to states of the form

$$|\psi\rangle = \frac{1}{\sqrt{2}} \begin{pmatrix} 0 \\ 0 \\ \vdots \\ 0 \\ \sin \theta_{N-1} \\ \cos \theta_{N-1} e^{i\phi_{N-1}} \end{pmatrix} \quad (6.7)$$

or any such similar state having all parameters but two θ_k zero. These are states being confined to a 2-dimensional plane spanned by two standard basis vectors. At the very top of the distribution we find the standard basis vectors $(1, 0, 0, \dots, 0)$, $(0, 1, 0, \dots, 0)$ etc. In fact, we may use this knowledge to calculate the slope of the maximum MUSness line in higher dimensions. Making a linear regression to this point and the origin we always seems to find a slope that concurs with Conjecture 3.

The unknown curve

Having noticed that a lot of interesting things seem to be happening at the boundary of this distribution, we naturally inquire as to the last piece of the border (dotted in Figure 6.2). However, this curve remains, as of today, something of a mystery. We know onne of the end points already from equation 6.7, this is the super position of two basis vectors

$$\frac{1}{\sqrt{2}}(|e_i\rangle + |e_j\rangle) \quad (6.8)$$

We will comment on the other end point below.

6.3 Further analysis

The above discussion has been verified for prime dimensions 5 through 23, and there seems to be no reason to believe that the pattern will break after that. As the dimension increases more points in the scatter plots will end up in the bulk, as per our previous reasoning, this is shown in Figure 6.3 where we give scatter plots for dimensions 7 and 19 using the same amount of points.

In high dimensions we do not have the economy of choosing points from the whole parameter space, rather we chose one point in the scatter plot with known parameters and study the vicinity of this point by making a sufficiently small perturbation about this point. For most points it is virtually impossible to calculate the corresponding parameter values, however, we shall soon see that some points of special interest have known parameters and we can apply this perturbation procedure to these points right away. We have already noted that the topmost point corresponds

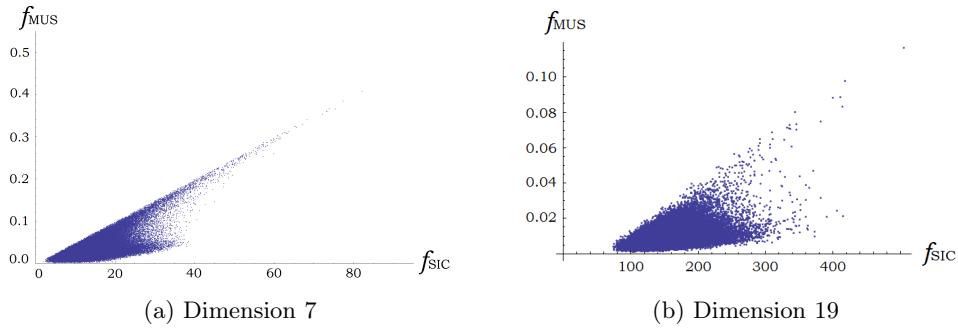


Figure 6.3: Comparison of the the scatter plots of $\frac{f_{MUS}}{f_{SIC}}$ for 100k points in dimensions 7 and 19.

to the standard basis vectors, hence we can make a perturbation about this point as a proof of concept. Regard the scatter plot in $N = 19$ as an example with 10^5 points the scatter plot reduces to a bulk of points centred as shown in Figure 6.3b. We make a perturbation about $(1, 0, 0, \dots, 0)$ we find that the boundary looks as we had anticipated, cf. figures 6.2 and 6.4.

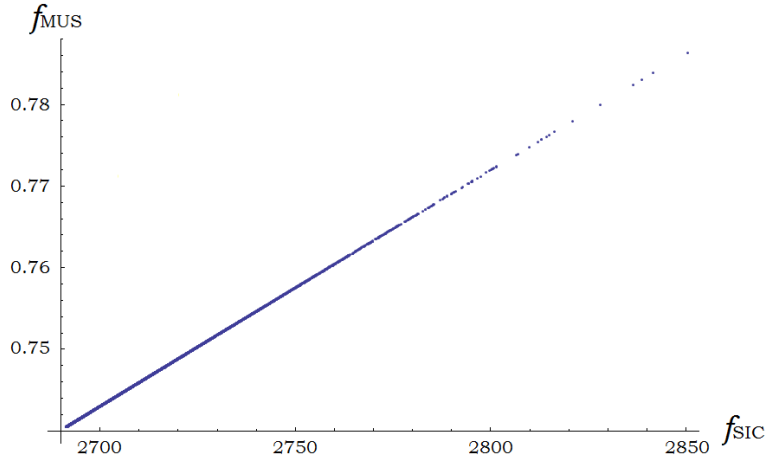


Figure 6.4: Zooming in on the region around $(1, 0, \dots, 0)$ in $N=19$.

In the spirit of curiosity and with a fair amount of by intuition, we calculate where some special points end up in dimensions five and seven. Specifically we calculate where the Alltop MUB fiducial vectors⁵ and the MUB cycling vectors⁶ sit in dimensions five and seven. The results are summarised in table 6.1 and figures 6.5a and 6.5b.

We note that the Alltop fiducial vector ends up on the straight line corresponding to the maximum MUSness for a given SICness, this is true for any choice of Alltop fiducial vector and have been verified in prime dimensions up to 19 and we may take a qualified guess that this is the case in all prime dimensions.

⁵Once again we will not formally define the Alltop MUBs, but rather just note that they are different sets of MUBs generated by some vectors called Alltop fiducial vectors. More on Alltop MUBs can be found for example here: [4] [13]

⁶As the name suggests, a vector used to cycle through MUBs. See Appleby et al [7].

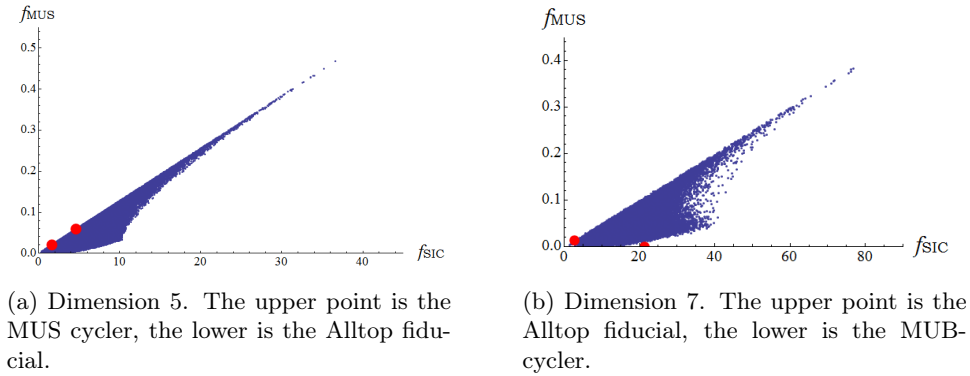


Figure 6.5: The scatter plot of $\frac{f_{MUS}}{f_{SIC}}$ with selected points marked.

N=5			N=7		
Alltop fid.	MUB-cycler	Maximum	Alltop fid.	MUB-cycler	Maximum
$(\frac{5}{3}, \frac{8}{375})$	$(\frac{8}{135}, \frac{125}{27})$	$(\frac{125}{3}, \frac{8}{15})$	$(\frac{9}{686}, \frac{21}{8})$	$(\frac{343}{16}, 0)$	$(\frac{1029}{8}, \frac{9}{14})$

Table 6.1: Coordinates in the f_{SIC} - f_{MUS} plane for chosen vectors.

The MUB-cycler is also on the maximum MUSness boundary in five dimensions, albeit a bit further up the slope. However, in 7D it sits in a rather more interesting spot; it is sitting as far out on the line of minimum uncertainty states as possible. We have proved this numerically using *Mathematica*'s `NMaximize` to maximise f_{SIC} while enforcing the constraint $f_{MUS} = 0$. Within our terminology this means that the MUB-cycler in seven dimensions is the MUS that is the least of a SIC. Further investigation shows that the MUB-cycler seems to move around in different dimensions, e.g. in $N = 13$ it sits in the bulk of points, however, doing perturbations in dimensions 19 and 23 shows some promising hints that the MUB-cycler might again be the outermost MUS.

Finally, we note that all the interesting points given in table 6.1 actually look surprisingly nice given the complexity of the functions whose quotient we are studying. One may easily construct symbolic representations of all the numbers given in terms of the dimension. This further adds to the intrigue between the SICness, and the MUSness of a state.

We have left out prime dimensions two and three up until this point. In these dimensions there is an evident bijection between the SICness and the MUSness of a state, this manifests as a straight line in the plot. The slope of this line is in agreement with previous results. The plot in three dimensions is given in Figure 6.6.

It can most certainly be analytically shown that this is bound to be a straight line, but that – ladies and gentlemen – is a story for another time.

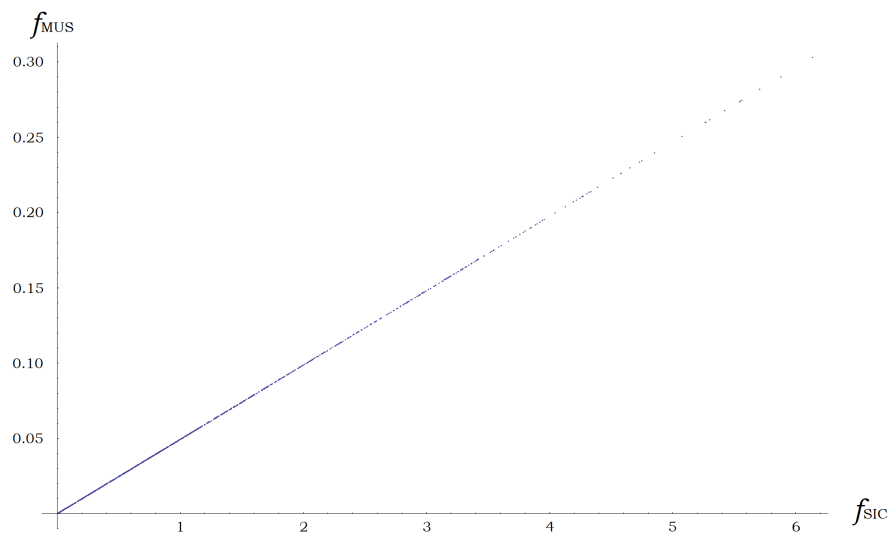


Figure 6.6: Plotting SICness versus MUSness in 3 dimensions.

Chapter 7

Epilogue

7.1 Concluding remarks

In this thesis we have explored the concept of SICs from the very beginning in their mathematical – and physical – formulation. We have also discussed the related concepts of MUBs and MUSs at some length. It is our hope that the thesis has proved rewarding for the reader new to these concepts as well as for the reader already familiar with them.

Summarising, the main contributions of this thesis are

Illustrating SICs and the SICness function in low dimensions

Chapter 4 focused on exploring the already known SICness function in a new fashion using contour plots. While this provided an illustrative description of the SICness function it also revealed something about the structure of the related quantum states. In particular we gained a complete image of the two dimensional space including MUBs, Alltop MUBs, and SICs while in four dimensions we saw that certain subspaces corresponded to a scaled version of the two dimensional plot.

An exhaustive search for MUS in the real Zauner subspace of 7D.

In chapter 5 we put a lot of work into finding all MUSs in a small portion of a Zauner subspace in 7D. In a simplified formulation we succeeded in this endeavour and all MUS were found. However, in the more general formulation we did not succeed in finding the MUS, though that told us something important about the complexity of finding MUSs.

Exploring the link between the SICness and MUSness of a state.

Finally in chapter 6 we propose and investigate the relationship between the SICness and the MUSness of a state. Among other things we conjecture an upper bound for the MUSness for any given the SICness and we examine where some interesting states sits in SICness-MUSness plane.

The proposed linkage between SICness and MUSness was formulated – and has been investigated – purely on grounds of curiosity. As such the work done on this relationship has been very exploratory in nature. Being thrilled about this unexpected relationship we have somewhat aimlessly thrown in some tests to see what comes out. The results however have been staggering and we strongly advise further investigation into this relationship, perhaps with a more systematic approach.

Apart from these results it is our hope that this thesis have advocated the use of group theory in general in physics and specifically the use of the Weyl-Heisenberg and Clifford groups for the

study of SICs. It is our firm belief that much structure found in physics can be understood through the introduction of groups.

7.2 Open questions

We leave the community with the following open questions to ponder; may anyone who feels obliged try to answer them!

- “What features of the SICness-MUSness plot is inherent to specific dimensions? Which features are found regardless of dimension?”
- “Can we prove conjecture 3?”
- “What is the meaning of a MUS being the least a SIC fiducial vector?”
- “In what dimensions is the outermost MUS a MUB cycler?”
- “What does the dashed line in figure 6.2 correspond to?”
- “Can we anticipate how the parameters vary as we move around in the plane?”
- “Is it possible to simplify the function f_{SIC}/f_{MUS} ?”

7.3 Acknowledgements

Ingemar

Först och främst vill jag tacka Ingemar för hans obevekliga stöd genom hela det här examenarbetet. Ingemar är lika mycket en briljant pedagog som en förebild och mentor. Vare sig det har varit sakkunskaper, inspiration eller stöd jag behövt har Ingemar alltid försett mig med det. Under Ingemars handledning har jag lärt mig så mycket mer än endast en liten, begränsad, del av fältet kvantinformation – jag har vuxit som fysiker.

Jag kan inte tänka mig en bättre vägvisare för studenter som söker att finna det vackra i det vi kallar naturvetenskap. Framför allt kommer jag för alltid att vara tacksam för att Ingemar fått mig lita på mina färdigheter som fysiker. Tack.

Kate and Alley

I would like to express my most sincere gratitude for all discussions about politics, cultures, news and cricket that I’ve had with Kate and Alley, with whom I have had the great opportunity to share office throughout most of the thesis. These, sometimes heated, discussions have been invaluable for keeping the spirit up; I am certain that my thesis work would not have been as ambitious if I had not been looking forward to come to the office every single day the way I did!

I would also, in particular, like to thank Kate for her guidance in quantum information theory. I have cherished our discussions and I will miss them. I feel glad for the future students who will have the benefit of Kate’s pedagogy.

Ralf and Per

When I got stuck trying to solve the general MUS equations in seven dimensions, I pulled the oldest trick in the book. Being a physicist stuck on a purely mathematical problem I phoned the maths department. Prof. Ralf Fröberg and Dr. Per Alexandersson provided material on Gröbner bases and intuition leading to the simplification of the polynomial system.

Anders

Being both a close friend and a brilliant physicist Anders' contribution to this thesis have been subtle but definitive. I am grateful that I have had the chance to try my ideas with Anders and for the support I have received when stuck on something. Above all I want to cheer for six great years as comrades as undergraduate students; the obstacles have been huge and frequent, but together we made it through!

Proofing

Thanks to everyone who had a hand in proofing this text. And in particular Yi-Hua, Alvin and Victor who were a great help in rooting out the last signs of lingering dyslexia from the text. I'm certain that you have enhanced the reading experience for anyone who takes it upon themselves to read this thesis.

Stack Exchange

This acknowledgement does not go out to anyone in particular, it goes out to all of the enthusiasts at *Stack Exchange* who with unwavering resolve answer questions, great or small, about *Mathematica*, *LaTeX*, *Inkscape*, etc. I am certain that it is enthusiasts such as these that make the modern science community go around.

Part III

Appendices

Appendix A – Supplementary Code

A lot of work throughout this Master’s thesis has been allocated to develop the *Mathematica*¹ code necessary to answer the questions we have posed. Some of the code is banal, some of it is quite clever and some of it is just downright ugly. In this appendix we will present selected parts of the codes for the reader who wishes to reproduce the results in this thesis; the reader who wishes to further investigate SICs/MUSs; or the reader who happens to be in need of similar code. This thesis is founded upon many lines of *Mathematica* code, which we, of course, can not include in this appendix, rather we will focus on bits of code which are either non-trivial, can save a lot of time or which is, by our highly subjective standards, generally nice.

Our top advices for the reader who have limited experience working with *Mathematica* is the following

- In *Mathematica* we do not rely on iterative programming where we recognise classic functions such as `for`, `do` and the likes of these. Rather we implement functional programming with functions such as `Map` and `Table`.
- Make sure you understand how to utilise pure functions ‘#’ in *Mathematica*.
- Use `Esc` where it is possible. Typing `Esc alpha Esc` in *Mathematica* results in α . We can access a variety of symbols and operators in this way, e.g. `Esc ct Esc` for complex transpose—or rather, in physics terminology, Hermitian conjugate.
- Apply short hand notation. This includes using `Esc` as suggested in the last item, but there are lots of more tricks, for example `@` will work as a pair of brackets for a command having only one argument, e.g. `Flatten@table`, `Chop@number`, etc. This way you may significantly reduce the number of brackets in an expression.
- Use the reference. *Mathematica*’s reference is thorough and well indexed. For any given command it contains summaries and in depth descriptions, basic examples and advanced examples. Hitting `F1` while marking a command will take you to the reference for that command.

But above all, the first rule of learning to write good code (this applies regardless of language and skill) is illustrated by the saying:

It is a truth universally acknowledged, that a single man in possession of good code must be in want of sharing it.

¹For the record, we are using *Mathematica* 8.0.1 and 9.0.1.

This idiom is of such paramount importance to programming that it ought to be a theorem. The point being that there are a great many places on the internet to gain inspiration for, and to ask questions about, writing good code. We list some good sources for *Mathematica* below

- An introductory course to functional programming in *Mathematica* can be found here <http://www.wolfram.com/training/courses/dev001.html>
- A more comprehensive introduction to *Mathematica* can be found here <http://library.wolfram.com/infocenter/MathSource/5216>.
- An active community of *Mathematica* coders sharing code and answering questions can be found here <http://mathematica.stackexchange.com/>.

Other than that there is of course the all-knowing *Google* to turn to for in times of need.

Calculating the unitary representation of the Weyl-Heisenberg group

This serves as a good example of how `Table` replaces `for` in *Mathematica*. Using `Table` we would write

```

1
2 (*Calculating the WH-elements using Table*)
3
4 CliffordUnitaries=
5 Table[
6   Table[tau^(i j + 2 s j) KroneckerDelta[r, Mod[s + i, n]]
7     , {r,0, n - 1}, {s, 0, n - 1}]
8 ,{i, 0, n - 1}, {j, 0, n - 1}];

```

as opposed to the more tortuous implementation using the `For`

```

1
2 (*Calculating the WH-elements using For*)
3
4 A = Array[0 &, {n, n}];
5 CliffordUnitaries = ConstantArray[0, n^2];
6 Cliffindex = 1; r = 0; s = 0;
7 For[i = 0, i <= n - 1, i++, {
8   r = 0, s = 0,
9   For[j = 0, j <= n - 1, j++, {
10    r = 0, s = 0,
11    For[k = 1, k <= n^2, k++,
12     {A[[r + 1,
13       s + 1]] = \[Tau]^(i j + 2 s j) KroneckerDelta[Mod[r, n],
14        Mod[s + i, n]],
15     If[Mod[r + 1, n] == 0, {r = 0, s++}, r++]},
16    CliffordUnitaries[[Cliffindex]] = A, Cliffindex++}}}]

```

Both codes generate the same thing; a matrix where all elements are in themselves matrices. In *Mathematica* this is the same as a table of tables—or really as nested lists. We will generally stick in a `Flatten` command to access the elements in the table of Weyl-Heisenberg group elements. Note that a very similar piece of code is used to generate the unitary representation of an element in $SL(2)$.

Simplifying Complex Numbers

Let `exp` be some complex expression which is given in polar form. Then the `FullSimplify` can be used to simplify `exp` and takes it to Cartesian form. The simplification routine in *Mathematica* roughly work in the following way:

When given an expression `FullSimplify` makes an assumption as to some possible simplification. After carrying out the suggested simplification *Mathematica* runs a decision algorithm to determine if the new expression is *simpler* than the present one. If it is simpler, the new expression is saved and the old is discarded, this protocol is then repeated until there are no more assumptions remaining.

The decision algorithm works by assigning each function in an expression a predefined complexity, it then calculates the total complexity of the expression. The transition to Cartesian form is made by defining a rule which assigns a high complexity to the exponential function e^x

```

1
2 (*Going from polar to Cartetian form*)
3
4 (*Define the rule*)
5
6 prio[e_] := 100 Count[e, _Abs, {0, Infinity}] + LeafCount[e]
7
8 (*Carry out the simplification*)
9
10 FullSimplify[exp, ComplexityFunction -> prio]

```

Specifying a Field for a Variable.

By default *Mathematica* assumes that all variables are complex. Sometimes we want to specify that some relation, for example a simplification, is to be taken over some other field, such as the real numbers. This is specified by adding the following option to the end of your command.

```

1
2 (*Simplifying in the reals*)
3
4 SomeCommand[SomeArgument, Element[{x0, x1, x2, x3, x4}, Reals]]

```

we could also write it using conventional set notation²

```

1
2 (*Simplifying in the reals*)
3
4 SomeCommand[SomeArgument, {x0, x1, x2, x3, x4} Esc e1 Esc Reals]

```

Parallelising the MUSness - SICness Plotting

The vast majority of the commands in *Mathematica* are not parallelised, which is as it should be since most commands do not require a lot of computational resources. However, many potentially

²When we write Esc we imply hitting `Esc`, in this case Esc e1 Est will result in \in in *Mathematica*.

computationally heavy commands such as `Table` and `Map` have parallelised counterparts³ [3]. There are also some commands that were developed before parallelisation were a viable option that is yet to be parallelised e.g. `Simplify`.

Below we present our code for making the plots in Chapter 6. A standard plot in Chapter 6 consists 100k points, which corresponds 100k randomly chosen vectors in \mathbb{CP}^{N-1} ; that is to say $10^5 \times N$ uniformly random numbers and $10^5 \times N$ random numbers chosen from a specific distribution. These vectors are then plugged into f_{SIC} and f_{MUS} , which are far from nice functions being sums of quartic inner products. Needless to say, making those plots are computationally heavy and we have therefore parallelised our code where it is possible.

Note that we at no point specify the number of cores to run the code on or any other machine specific options. As such it is possible to migrate this code to any machine without changing the code. Specifying what system resources is available to *Mathematica* is done by changing global parameters in the *Mathematica* host process.

```

1
2 (*Making fSIC-fMUS scatter plots*)
3
4 (*Preamble*)
5
6 n=dimension
7 samples = 10^5;
8 SICList = List [];
9 MUSList = List [];
10
11
12 (*Choosing random points*)
13
14 g[x0_, y0_] :=
15
16 Module[{x = x0, y = y0},
17 {
18   rand = ParallelTable [
19     Table[{ArcSin[RandomReal[{0, 10^(-16)}]^(1/(2 j))],
20       RandomReal[{0, 2 Pi}]}], {j, y - 1}]
21   , {i, x}];
22
23   rand = Flatten[rand, 1]
24
25 }
26 ]
27
28
29 (*Calculating the coordinates*)
30
31 randomSeeds=Flatten[g[samples, n], 1];
32
33 SIClist=ParallelTable [
34   f_SIC[Table [
35     randomSeeds [[j+(n-1)(i-1)]] [[1]] , randomSeeds [[j+(n-1)(i-1)]] [[2]] ,
36     {j, 1, n-1}]]
37   , {i, samples}];
38
39 MUSlist=ParallelTable [
40   f_MUS[Table [
41     randomSeeds [[j+(n-1)(i-1)]] [[1]] , randomSeeds [[j+(n-1)(i-1)]] [[2]] ,

```

³*Mathematica* also has a library for support of CUDA and OpenCL programming which are used to run highly parallelised computations using GPUs, but we will not digress on that here.

```

42     ,{j,1,n-1}]]
43     ,{i,samples}];

```

Spherical Plots of the SIC-function

Sometimes we want to plot a 2D function on the surface of some object rather than making a conventional plot. An example of such a plot is the f_{SIC} plots in Chapter 4, these are actually plots on the surface of a Bloch sphere, why it might be instructive to show the plots on an actual sphere. The way to realise this is to use the a combination of the options `ColorFunction` and `Hue`. Where the first command specifies that we want to colour the object according to some function and the second one specifies which function. Below we supply the code to plot f_{SIC} on a sphere.

```

1
2 (*Plotting fSIC on a sphere*)
3
4 ParametricPlot3D[{Cos[u] Sin[v], Sin[u] Sin[v], Cos[v]},
5   {u, 0, 2 Pi}, {v, 0, Pi}, PlotPoints -> 200, Mesh -> None,
6   ColorFunction -> Function[{x, y, z, u, v}, Hue[f_SIC[u, v]]],
7   ColorFunctionScaling -> True, AxesLabel -> {x, y, z}]

```

Probing a Plot Using Manipulate

When we have some function which generates a distribution of points, we sometimes want to explore which parameter values that correspond to which points. One such example is the SICness-MUSness plots in Chapter 6. This is conceived by utilising the command `Manipulate`, which is a really nice tool when we want to study the change in some system by some dynamic variable or variables. For further information and an interactive introduction see the *Mathematica* reference.

We may use the `Manipulate` command to see where different points in the parameter space ends up in the scatter plot. This is done by manipulating a function which plots a point at the coordinates ($f_{SIC}[u_1, v_1, u_2, v_2, \dots]$, $f_{MUB}[u_1, v_1, u_2, v_2, \dots]$) on the background of the $f_{SIC} - f_{MUB}$ scatter plot. Changing the values of the parameters will move the point around on the background of the scatter plot.

```

1
2 (*Probing the fSIC-fMUS plane.*)
3
4 (*In this example 'SomePlot' is a previously generated plot*)
5
6 Manipulate[
7   Show[SomePlot,
8     Graphics[{
9       Red, PointSize[0.010], Point[{fSIC[u1, v1, u2, v2, ...], fMUB[u1, v1, u2, v2 ←
10         ...}]}],
11   {ui, 0, Pi}, {vi, 0, 2 Pi}]

```

Making the θ -axis Descending

When making two dimensional plots we usually plot both axes as increasing. However, in the contour plots of Chapter 4 the ϕ -axis is decreasing, this is to compensate for the fact that we are actually looking at the surface of a sphere. The convention is to call the north pole of a sphere $\phi = 0$ and the south pole $\phi = \pi$. The following code flips the direction of the ϕ -axis while maintaining the correct values of the function.

```
1
2 (*Redefining theta*)
3
4 (*In this example theta is called v and phi is called u*)
5
6 plots = ContourPlot[fSIC[u, -v]],
7   {u, 0, 2 Pi}, {v, -Pi, 0},
8   FrameTicks -> {{0, Pi/2, Pi, 3 Pi/2, 2 Pi}, Table[{v, -v}, {v, 0, -Pi, -Pi←
9   /2}]},
   AspectRatio -> 1/2];
```

Appendix B – Computing power

For comparison, all heavy calculations are run on the following system

Component	Specification	Performance
CPU	Quad Core Intel i7-4770K Haswell	2.7/3.5/4.4 GHz ⁴
Graphics	Nvidia GTX670	1344 CUDA cores at 980 MHz / 2 GB GDDR5 at 6 GHz ⁵
RAM	Kingston	4×8 GB at 1.6 GHz
Drive	Intel SSD	180 GB, 555/520 MB/s ⁶
Motherboard	MSI Z87 MPOWER (MS-7818)	-
Operating system	Windows 7 Ultimate SP1	-

With the introduction of x64 operating systems and multi-core processors during the last ten years, there have been a paradigm shift in machine computation. The key to unlocking the full computational power of a machine has shifted from choosing the Fortran loop which is being optimally executed by the system to how good one is at parallelising code.

This stems from the fact that non-parallelised code (serial code) only runs on one CPU core whereas parallelised code runs on any chosen amount of cores. A computer today typically have 2, 4 or 8 cores, while this does not correspond to the code running twice, four or eight times as fast, it is a huge improvement in computational time⁷.

A great practical challenge in this Master's thesis has been to overcome limitations in computing resources. For future reference we will document some of the experiences we had trying to push *Mathematica* running on the above machine to the maximum. It has already been stated that the solving of the polynomial systems in the end of Chapter 5 is an example of shortage of computing resources.

Our attempted solving method was to use *Mathematica's* `Reduce` to find a solution, however, this command is not parallelisable and can not utilise the full power of the computer. Typically *Mathematica* tries to solve numerical systems of equations either by Buchberger's algorithm or by

⁴Base / Turbo / Overclocked to

⁵GPU / Graphics memory

⁶Read / Write

⁷It is not possible to give an overall estimate on how much faster a generic program will run on multiple cores, it depends on a lot of parameters such as in which language it is written and how it is written.

the Jenkins-Traub algorithm[2]. These are both iterative algorithms in nature and relies heavily on the memory available if the problem is complex. Our most ambitious attempt at solving the before mentioned system of polynomials was to let the computer run for 250 hours at which point we interrupted the computation.

When a serial algorithm in *Mathematica* encounters a hard problem it will generally occupy a lot of memory⁸. *Mathematica* allocates memory in a classical hierarchy starting with the fastest memory available according to

1. Cache
2. RAM
3. Drive

There are some point in keeping this hierarchy in mind when coding large *Mathematica* applications. The speed of these memories is roughly decreasing with about a factor of 10 with each level, provided that your drive is an SSD. Hence, make sure that you have enough RAM available before running a large computation, since it will run exceedingly slow when it starts allocate memory on the drive.

For the record, the attempted solving of the polynomial system in Chapter 5 allocated 120 GB of computer memory divided over all three levels and was showing no sign of the decreasing allocation.

Another type of computationally heavy calculations that has been handled in this thesis is the making of the scatter plots in chapter 6. As stated in appendix A this piece of code has been parallelised in order to meet the demand on computational resources. This may serve as an example of how much evaluation times might decrease when a program in parallelised. Before the parallelisation of this code making scatter plots within tolerable evaluation times was possible up to dimension seven where we experienced evaluation times of about two minutes. However, making plots in dimensions 11 and 13 was painfully slow and there was no reason to try making plots in dimensions higher than 17. After parallelisation however this code has produced plots up to dimension 31(!). The program has a run time of less than two minutes for dimensions lower than 17 and it completed 31 in about 30 minutes. During a large calculation, *Mathematica* typically allocated about 20 GB of RAM and utilised all cores at 70-95%.

When *Mathematica* is running a calculation we can not use the kernel for any other jobs for the duration of the calculation. A nice work-around for this limitation is to run several instances of *Mathematica*. For instance, if I want to make scatter plots for an hour, I of course want to be able to use *Mathematica* for other calculations meanwhile. If I then start a new instance of *Mathematica* that instance will launch its own kernels that will be free to use.

⁸This of course depends on the command used, but this is generally the case. This is certainly the case when simplifying or solving complex systems of equations. The reason for this is quite technical and at any rate not in the scope of this thesis for a degree in theoretical physics.

Appendix C – Exact Solutions to MUS in 7 Dimensions

For reference we here present all MUSs in the real subspace of 7D as defined in Chapter 5. First we give the expressions numerically, then we give the exact and fully simplified expressions. Note that the result is presented in a short hand notation using boolean algebra.

Numerical Solutions

It is strongly recommended to use the numerical representation for any practical purposes since it is a lot more straight forward than the exact representation.

$$\begin{aligned} & (x_2 == -0.295254 \wedge ((x_0 == -0.66776 \wedge x_1 == -0.0719342) \vee (x_0 == 0.66776 \wedge x_1 == 0.0719342))) \vee \\ & (x_2 == -0.270598 \wedge ((x_0 == -0.66776 \wedge x_1 == -0.138298) \vee (x_0 == 0.66776 \wedge x_1 == 0.138298))) \vee \\ & (x_2 == -0.191342 \wedge ((x_0 == -0.66776 \wedge x_1 == 0.236089) \vee (x_0 == 0.66776 \wedge x_1 == -0.236089))) \vee \\ & (x_2 == 0.191342 \wedge ((x_0 == -0.66776 \wedge x_1 == 0.236089) \vee (x_0 == 0.66776 \wedge x_1 == -0.236089))) \vee \\ & (x_2 == 0.270598 \wedge ((x_0 == -0.66776 \wedge x_1 == -0.138298) \vee (x_0 == 0.66776 \wedge x_1 == 0.138298))) \vee \\ & (x_2 == 0.295254 \wedge ((x_0 == -0.66776 \wedge x_1 == -0.0719342) \vee (x_0 == 0.66776 \wedge x_1 == 0.0719342))) \end{aligned} \tag{7.1}$$

Exact Solutions

These exact solutions are not terribly useful. They are mostly supplied as a reference and as a proof of concept. It is probably easier to calculate them from scratch using the methods supplied in this thesis than making any sense out of these.

$$\begin{aligned}
& \left[\sqrt{4 - 2\sqrt{2}} + 4x_2 == 0 \wedge \left(\left(\sqrt{28 + 42\sqrt{2}} + 14x_0 == 0 \wedge \sqrt{-84 + 70\sqrt{2}} + 28x_1 == 0 \right) \vee \right. \right. \\
& \quad \left. \left. \left(14x_0 == \sqrt{28 + 42\sqrt{2}} \wedge 28x_1 == \sqrt{-84 + 70\sqrt{2}} \right) \right) \right] \vee \\
& \left[\sqrt{28 + 42\sqrt{2}} + 14x_0 == 0 \wedge \left(\left(\sqrt{-84 + 70\sqrt{2}} + 28x_1 == 0 \wedge 4x_2 == \sqrt{4 - 2\sqrt{2}} \right) \vee \right. \right. \\
& \quad \left. \left(28x_1 == \sqrt{7(2 + 3\sqrt{2})} \wedge \left(\sqrt{2 - \sqrt{2}} + 4x_2 == 0 \vee 4x_2 == \sqrt{2 - \sqrt{2}} \right) \right) \right) \vee \\
& \quad \left(\frac{1}{\sqrt{54 + 31\sqrt{2}} + \sqrt{70(65 + 46\sqrt{2})}} + x_1 == 0 \wedge \right. \\
& \quad \left. \left(\sqrt{14(-2 - 17\sqrt{2}) + \sqrt{1030 + 740\sqrt{2}}} + 56x_2 == 0 \vee \right. \right. \\
& \quad \left. \left. 56x_2 == \sqrt{14(-2 - 17\sqrt{2}) + \sqrt{1030 + 740\sqrt{2}}} \right) \right) \right] \vee \\
& \left[14x_0 == \sqrt{28 + 42\sqrt{2}} \wedge \left(\left(28x_1 == \sqrt{-84 + 70\sqrt{2}} \wedge 4x_2 == \sqrt{4 - 2\sqrt{2}} \right) \vee \right. \right. \\
& \quad \left. \left(\sqrt{7(2 + 3\sqrt{2})} + 28x_1 == 0 \wedge \left(\sqrt{2 - \sqrt{2}} + 4x_2 == 0 \vee 4x_2 == \sqrt{2 - \sqrt{2}} \right) \right) \right) \vee \\
& \quad \left(x_1 == \frac{1}{\sqrt{54 + 31\sqrt{2}} + \sqrt{70(65 + 46\sqrt{2})}} \wedge \left(\sqrt{14(-2 - 17\sqrt{2}) + \sqrt{1030 + 740\sqrt{2}}} \right. \right. \\
& \quad \left. \left. + 56x_2 == 0 \vee 56x_2 == \sqrt{14(-2 - 17\sqrt{2}) + \sqrt{1030 + 740\sqrt{2}}} \right) \right) \right]
\end{aligned} \tag{7.2}$$

Bibliography

- [1] *Quantum Physics in Higher-Dimensional Hilbert Spaces*, 2010.
- [2] *The Wolfram Language and System Documentation Centre*. <http://reference.wolfram.com/language/tutorial/SomeNotesOnInternalImplementation.html>, 2014.
- [3] *The Wolfram Mathematica Reference*. <http://reference.wolfram.com/language/guide/ParallelComputing.html>, 2014.
- [4] W. O. Alltop. Complex sequences with low periodic correlations. *IEEE Transactions on Information Theory*, 26:350–354, 1980.
- [5] I. Amburg, R. Sharma, D. Sussman, and W. K. Wootters. States that “look the same” with respect to every basis in a mutually unbiased set. *arXiv preprint:1407.4074*, 2014.
- [6] D. M. Appleby. Symmetric informationally complete-positive operator valued measures and the extended Clifford group. *Journal of Mathematical Physics*, 2005.
- [7] D. M. Appleby, I. Bengtsson, and H. B. Dang. Galois Unitaries, Mutually Unbiased Bases, and MUB-balanced states. *arXiv preprint:1409.7987*, 2014.
- [8] D. M. Appleby, H. B. Dang, and C. A. Fuchs. Symmetric informationally-complete quantum states as analogues to orthonormal bases and minimum-uncertainty states. *Entropy*, 16(3):1484–1492, 2014.
- [9] DM Appleby, Hulya Yadsan-Appleby, and Gerhard Zauner. Galois automorphisms of a symmetric measurement. *Quantum Information & Computation*, 13(7-8):672–720, 2013.
- [10] J. J. Benedetto and M. Fickus. Finite normalized tight frames. *Advances in Computational Mathematics*, 18(2-4):357–385, 2003.
- [11] I. Bengtsson and H. Granström. The frame potential, on average. *Open Systems and Information Dynamics*, 16(145).
- [12] I. Bengtsson and K. Życzkowski. *Geometry of Quantum States: An Introduction to Quantum Entanglement*. Cambridge University Press, 2006.
- [13] K. Blanchfield. Orbits of mutually unbiased bases. *Journal of Physics A Mathematical General*, 2014.
- [14] B. Buchberger. Ein algorithmisches Kriterium für die Lösbarkeit eines algebraischen Gleichungssystems (An algorithmic criterion for the solvability of algebraic systems of equations). *Aequationes mathematicae*, 3:374–383, 1970. (english transl.: B. Buchberger, F. Winkler: Gröbner Bases and Applications, Proc. of the International Conference "33 Years

- of Gröbner Bases", 1998, RISC, Austria, London Math. Society Lecture Note Series 251, Cambridge Univ. Press, 1998, pp.535 -545).
- [15] B. Buchberger. Gröbner Bases: A short introduction for systems theorists. In *Proceedings of EUROCAST 2001 (8th International Conference on Computer Aided Systems Theory - Formal Methods and Tools for Computer Science)*, Lecture Notes in Computer Science 2178, pages 1–19. Copyright: Springer - Verlag Berlin, 2001.
- [16] B. Buchberger and M. Kauers. Buchberger's Algorithm. *Scholarpedia*, 6(10):7764–7764, 2011.
- [17] N. J. Cerf, M. Bourennane, A. Karlsson, and N. Gisin. Security of quantum key distribution using d-level systems. *Physical Review Letters*, 88(12):127902, 2002.
- [18] C. Cormick, E. F. Galvao, D. Gottesman, J. P. Paz, and A. O. Pittenger. Classicality in discrete Wigner functions. *Physical Review A*, 73(1):012301, 2006.
- [19] Hoan Bui Dang, Kate Blanchfield, Ingemar Bengtsson, and DM Appleby. Linear dependencies in weyl–heisenberg orbits. *Quantum information processing*, 12(11):3449–3475, 2013.
- [20] P. A. M. Dirac. *The Principles of Quantum Mechanics*. International series of monographs on physics (Oxford, England). 1930.
- [21] Å. Ericsson. *Exploring the Set of Quantum States*. PhD thesis, Stockholm University, Department of Physics, 2007.
- [22] J. B. Fraleigh. *A First Course in Abstract Algebra*. Pearson Education, 2003.
- [23] C. A. Fuchs. Quantum mechanics as quantum information (and only a little more). *arXiv preprint quant-ph/0205039*, 2002.
- [24] C. A. Fuchs and B. C. Stacey. Some negative remarks on operational approaches to quantum theory. *ArXiv e-prints*, January 2014.
- [25] Stuart G Hoggar. 64 lines from a quaternionic polytope. *Geometriae Dedicata*, 69(3):287–289, 1998.
- [26] I. D. Ivanovic. Geometrical description of quantal state determination. *Journal of Physics A: Mathematical and General*, 14(12):3241, 1981.
- [27] S. Lang. *Algebra*. Graduate Texts in Mathematics. Springer New York, 2002.
- [28] Roger Penrose. *The emperor's new mind: concerning computers, minds, and the laws of physics*. Oxford University Press, 1999.
- [29] J. J. J. Sakurai and J. Napolitano. *Modern Quantum Mechanics*. Addison Wesley Publishing Company Incorporated, 2010.
- [30] A. J. Scott and M. Grassl. Symmetric informationally complete positive-operator-valued measures: A new computer study. *Journal of Mathematical Physics*, 51(4):042203, 2010.
- [31] B. Sturmfels. What is a Gröbner basis? *Notices Amer. Math. Soc*, 52(10):1199–1200, 2005.
- [32] V. Veitch, S. A. H. Mousavian, D. Gottesman, and J. Emerson. The resource theory of stabilizer quantum computation. *New Journal of Physics*, 16(1):013009, 2014.

-
- [33] J. von Neumann. *Mathematische Grundlagen der Quantenmechanik (Mathematical Foundations of Quantum Mechanics)*. Grundlehren der mathematischen Wissenschaften in Einzeldarstellungen mit besonderer Berücksichtigung der Anwendungsgebiete. Springer-Verlag, 1932.
- [34] W. K. Wootters and B. D. Fields. Optimal state-determination by mutually unbiased measurements. *Annals of Physics*, 191(2):363–381, 1989.
- [35] G. Zauner. Quantum designs—foundations of a non-commutative theory of designs. *Ph. D. thesis, University of Vienna*, 1999.